MIMO Systems with Multifunctional Reconfigurable Antennas

Uzma Afsheen

A thesis presented for the degree of
Doctor of Philosophy
in
Electrical and Computer Engineering
at the
University of Canterbury,
Christchurch, New Zealand.

2019

ABSTRACT

This work presents a novel class of space time trellis codes based on super quasi-orthogonal space time codes for a reconfigurable multi-input multi-output antenna system. We call them space time state trellis codes (STSTCs). The motivation is to design a code that has all the good properties of the super orthogonal space time trellis codes, but can also extract the additional diversity gain offered by reconfigurable antennas. It is shown through simulations that the proposed code outperforms the existing super orthogonal space time trellis code, which fails to achieve full diversity in a reconfigurable antenna system. The proposed code is essentially a three dimensional trellis code, allowing us to code across space, time and reconfigurable antenna states. STSTCs achieve the diversity order expected of four transmit antennas while using only two reconfigurable transmit antennas. These codes have been designed for two and four trellis states and for two and four branch trellis structures for BPSK and QPSK constellations. The proposed STSTCs exploit the additional degrees of diversity offered by reconfigurable antennas and changing propagation states, achieving full rate, full diversity and high coding gain. This work also gives pairwise error probability performance analysis for the proposed STSTCs in a quasi-static Rayleigh fading channel. It is also shown through the analysis and simulations, that traditional minimum coding gain distance (CGD) is not adequate criteria for code design and that additional gains can be achieved by considering the minimum CGD of minimum return path (MRP). This work also gives a code design criteria which is based not only on minimum CGD of the parallel path, but also on the minimum CGD MRP, and have also given rank of the partial valid path and the performance factor. This provides additional gains without requiring the complete distance spectrum to be evaluated.

This work also presents a reconfigurable antenna codebook feedback scheme to reduce precoding codebook loss without increasing the number of feedback bits. The reconfigurable antenna codebook feedback MIMO system proposed aims to achieve the performance of large codebook size (N_C) with the benefits of small N_C. With limited codebook cardinality, it is impossible to find a codebook entry at zero distance from the corresponding channel values and a loss is incurred. Increasing the number of possible channel conditions instead of increasing the codebook size and hence the number of feedback bits, is the basis of our underlying approach towards minimizing the loss due to codebook mismatch. Increasing the number of possible channel conditions while having limited codebook cardinality, gives new degrees of freedom, such as reduced codebook or quantization loss and overall improvement in SNR due to increased channel power if the channel states are carefully selected. Analysis and simulations show that increasing the number of receive antenna states (S) has the same effect as codebook size expansion when the codeword and state selection is based on minimizing the distance between channel and codeword. In addition, an optimal selection approach (OA) is proposed. It maximizes both the channel power and the direction by carefully selecting the channel state and the codeword. This work also considers two more selection approaches called Channel Direction (CD) and Channel Power (CP), to investigate the source of the gains achieved in OA . The SNR and rates achieved with perfect feedback in a traditional non-reconfigurable antenna system, can be exceeded with only $S = 2$, using the proposed OA selection. We also find that doubling S gives approximately 40 % SNR gain as compared to $S = 1$, using the proposed OA selection. The effects of imperfect CSI are also considered.

Dedicated to my parents

and

my lovely daughters

ACKNOWLEDGEMENTS

First and foremost, praises and thanks to Almighty Allah for bestowing His blessings upon me and giving me the strength and courage to carry out and complete this work.

I would like to express my deepest and most sincere gratitude to my research supervisors, Prof. Philippa Martin, Dean of Engineering, University of Canterbury and Prof. Peter Smith, Victoria University of Wellington, for their persistent motivation, patience, and guidance, throughout my doctoral work. Their invaluable insight, feedback and advice have made this research a success.

My appreciation also goes to the University of Canterbury for their scholarship to pursue my PhD. I am grateful to Prof. Philippa Martin and University of Canterbury for providing me the opportunity to attend the VTC 2013 in LasVegas, USA and AusCTW 2014, in Sydney, Australia. I would also like to thank former members of the Communications research group for valuable discussions and support, enriching my research experience. I am also very grateful to my respected teachers and my friends, for their sincere guidance, love and for believing in me.

I would like to give my special thanks to my beloved family, specially my parents, Shireen and Qaseem, my brother Waqas, and both my lovely sisters, Sarah and Irsah, for their prayers, sacrifices, encouragement and moral support through every step in this endeavor. Last but not least, I will always value the love from my daughters, Faleha and Fariha, as a huge source of encouragement and motivation to complete my thesis.

CONTENTS

LIST OF TABLES

LIST OF FIGURES

ABBREVIATIONS

APSK	amplitude phase shift keying.
AWGN	additive white Guassian noise.
B	number of blocks in a frame.
BER	bit error rate.
BPSK	binary phase shift keying.
$\mathbb{CB}$	codebook matrix.
$\mathbf{C}$	codeword.
$\mathbf{C}_p$	precoding channel matrix.
CB	codebook.
CD	channel direction.
CD1	channel direction is maximized over all CPSs and codewords $\mathbf{C}_p$, simultaneously.
CD2	channel direction is maximized over all CPSs first and then the best codeword is selected based on the best sum rate.
cdf	cumulative distribution function.
CGD	coding gain distance. It is equal to the det($\mathbf{D^H D}$). where H denotes the Hermitian transpose and D is the difference matrix.
CP	channel power.

CPS	channel propagation state.
CSn	STSTC codeword for the n^{th} trellis state.
CSI	channel state information.
$\mathbf{D}$	difference matrix.
D	comparitive diversity.
$\mathbf{E}[.]$	expectation.
F	frame length.
FB	feedback.
FER	frame error rate.
γ	mean transmit signal power to mean receive noise power.
$\mathbf{H}_s$	channel matrix for the s^{th} CPS due to the reconfigurable antennas.
i.i.d	independent and identically distributed.
Λ_s	instantaneous channel power.
K	number of multipaths present in the frequency selective channel.
L	number of symbol periods.
	number of transmission streams in chapter 5.
λ_i	for $(i = 1, 2, ..., min(N_r, N_t))$ are the eigenvalues of $\mathbf{H}_s^{\dagger}\mathbf{H}_s$.
LTE	Long-Term Evolution.
min CGD	minimum coding gain distance.
MIMO	multi-input multi-output.
MISO	multi-input single-output.
MGF	moment generating function.

ML	maximum likelihood.
MRP	minimum return path.
m	column number in a codeword.
n	number of trellis state.
nc	total number of codes considered for exhaustive search.
N	total number of trellis states.
N_b	number of branches diverging from or merging into a trellis state.
N_C	size of the codebook.
$\tilde{N_C}$	expanded codebook size.
N_t	number of transmit antennas.
N_r	number of receive antennas.
NRA	non reconfigurable antenna.
OA	optimal selection approach.
OSTBCs	orthogonal space time block codes.
$\mathcal{P}$	number of paths out of 12 valid paths, having minimum CGD MRP $<$ 10,000.
p	total number of parallel paths in each branch of trellis.
p^*	selected codeword index.
pdf	probability density function.
PEP	pairwise error probability.
PF	performance factor.
PFB	perfect feedback.
PP	parallel path.

ϕ_1	angle with which symbols x_1 and x_2 are rotated in our STSTC codeword.
ϕ_2	angle with which symbols x_3 and x_4 are rotated in our STSTC codeword.
q	total number of thetas.
QOSTBCs	quasi-orthogonal space time block codes.
QPSK	quadrature phase shift keying.
r	rate.
$\mathbf{R}$	received matrix.
R	number of reconfigurable receive antenna states.
RA	reconfigurable antenna.
RF	radio frequency.
RPVP	rank of the partial valid path.
RVQ	Random vector Quantization.
Γ	received signal to noise ratio.
SER	symbol error rate.
SINR	signal-to-interference noise ratio.
SNR	signal-to-noise ratio.
S	number of reconfigurable transmit antenna states in chapter 3 and 4.
	total number of CPSs due to reconfigurable receive antenna states in chapter 5.
s^*	selected channel propagation state.
s	antenna state in chapter 3, channel propagation state in chapter 5.
SOSTTCs	super orthogonal space time trellis codes.
SQOSTTCs	super quasi-orthogonal space time trellis codes.

SF	space frequency.
ST	space time.
STBC	space time block code.
STC	space time code.
STF	space time frequency.
STSBC	space time state block code.
STSTC	space time state trellis code.
STTC	space time trellis code.
$\mathcal{SR}$	sum rate.
θ_m	angle with which the m^{th} column of the STSTC codeword is rotated.
θ_m^n	θ_m for the n^{th} TS.
t	time or number of the transition in the trellis.
T	length of the error event.
TS	trellis state.
TS_n	n^{th} trellis state.
v	total number of valid paths.
$\mathbf{v}_s$	normalized channel direction.
$\tilde{x_i}$	i^{th} symbol x rotated by ϕ_z, $z = 1$ for $i = 1, 2$, $z = 2$ for $i = 3, 4$.
α_m	difference of θ_m from the transmitted and non transmitted possible codewords.
β_z	difference of ϕ_z from the transmitted and non transmitted possible codewords.

Chapter 1

INTRODUCTION

1.1 OVERVIEW OF THE RECONFIGURABLE ANTENNA MIMO SYSTEM

Reconfigurable antenna multi input multi output (MIMO) systems has a lot of potential to improve the communications. MIMO communication systems employ multiple transmit and receive antennas to achieve diversity, throughput and/or coding gains. It can be hard to fit a large number of transmit antennas on small hand held devices. In addition, each antenna requires its own RF chain increasing harware and consuming power. One way to work around this is to employ reconfigurable antennas [2–5] which is a promising solution. Reconfigurable antennas are strong candidates for 5G and beyond technologies, where a single device is needed to support multiple radio access technologies with diverse operational requirements [6]. They can be reconfigured in a predefined or adaptive manner, to operate with different polarizations and radiation patterns and also at various frequency bands at the same time [7], [8], [9]. In addition to the above mentioned capabilities, it offers an additional degree of freedom by changing the propagation channel dynamically and deliberately, thus enhancing diversity gain.

1.2 PROBLEM STATEMENTS AND FOCUS

Our focus is increasing diversity gain in a MIMO system, making use of the additional degrees of freedom provided by the use of reconfigurable antennas. Diversity gains in a

multiple input and single output system can be obtained by using space time codes or through intelligent use of channel state information at the transmitter employing transmit beamforming and codebook feedback [10].

First we look at the space time coding techniques and identify the gap in the literature in this context. It is seen that orthogonal space time block codes (OSTBCs) [11, 12] provide full diversity and simple maximum likelihood decoding, but achieve little or no coding gain. Space time trellis codes (STTCs) [11] achieve full diversity and provide coding gain but at the cost of increased complexity. Super orthogonal space time trellis codes (SOSTTCs) [13] use an OSTBC as a kernel within the trellis code. They combine the set partitioning principle in [14] and a super set of OSTBC methodically, to provide full diversity, simple decoding and improved coding gain over the earlier space time trellis code schemes [15]. However, full rate OSTBCs do not exist for more than two transmit antennas with linear receivers [12]. To overcome this problem, quasi-orthogonal space time block codes (QOSTBCs) were proposed in the literature to provide full rate [16,17]. Later, rotated QOSTBCs [18,19] were proposed to provide full diversity and full rate. In [20,21], a super quasi-orthogonal space time trellis code (SQOSTTC) was presented for four transmit antennas. It combines the constellation rotation of SOSTTC with that of QOSTBCs methodically to obtain space time codes giving full rate, full diversity and high coding gain for four transmit antennas. However, both SOSTTCs [13] and SQOSTTCs [20, 21] provide high coding gain and are full rate but we show that that they fail to achieve the diversity gains possible in a reconfigurable antenna system [22]. Space time state block codes (STSBC) were proposed by Jafarkhani and Fazel for reconfigurable antenna systems in [23]. They showed that the maximum achievable diversity order of a MIMO communication system employing reconfigurable antennas at the transmitter is given by the product of the number of transmit antennas, N_t, and receive antennas, N_r, as well as the number of radiation states, S and R, of the reconfigurable transmit and receive antennas, respectively. The maximum diversity offered by SOSTTC [13] is $< N_t N_r SR$ in a reconfigurable antenna system.

This motivated us to design a code that has all the good properties of the SOSTTC, but can also extract the additional diversity gain offered by reconfigurable antennas, by using a STSBC as the kernel within a SOSTTC. Our aim is to give essentially a three dimensional trellis code, allowing us to code across space, time and reconfigurable antenna states that are available as a resource due to the deployment of reconfigurable antennas, providing better gains than the existing block and trellis codes in a Rayleigh fading channel.

Our focus is not hardware complexity reduction rather a three dimentional code to take advantage of the additional degrees of diversity offered by multi-functional reconfigurable antennas MIMO communication system. A code that has all the good properties of SOSTTC but can also provide full diversity, is required.

Secondly, we looked at the intelligent use of the channel employing transmit beam forming. A significant amount of research had been focussed on limited feedback precoding systems [24], [25] and codebook transmit beamforming is now a part of LTE standards [26] and is of great interest in next generation systems due to its well researched benefits [25]. In a code book precoding system, it is assumed that the receiver has correct channel state information (CSI), but instead of feeding back the entire CSI to the transmitter, it compares the normalized reconfigurable channel with the entries in a codebook and feeds back just the index of the nearest codebook entry. With limited codebook cardinality, it is impossible to find a codebook entry at zero distance from the corresponding channel values and a loss is incurred [27]. It is desirable to choose N_C large to obtain a good approximation of the channel. On the other hand, minimizing the number of feedback bits motivates choosing a small N_C. The trade-off between performance and the amount of feedback has been extensively researched [24], [25]. The codebook size, N_C, naturally has an impact on the performance of a quantized beamforming system and is also related to system diversity [10]. It has been shown in [10] that in order to achieve full diversity the codebook size should be greater than or equal to the number of transmit antennas. Reducing this codebook loss is the aim with the focus on not increasing the codebook size. And also to achieve full diversity while using a codebook of smaller size. We tried to address

this issue by proposing and investigating a codebook feedback MIMO system employing reconfigurable antennas. A solution which is required to achieve the performance of large N_C with the benefits of small N_C, i.e fewer feedback bits is given. Increasing the number of possible channel conditions instead of increasing the codebook size and hence the number of feedback bits, is the basis of our underlying approach towards minimizing the loss due to codebook mismatch. Increasing the number of possible channel conditions while having limited codebook cardinality, gives new degrees of freedom, such as reduced codebook or quantization loss and overall improvement in SNR due to increased channel power if the channel states are carefully selected.

We considered quasi-static Rayleigh fading channel, with the assumptiom that the reconfigurable channel is constant for one antenna state. codebooks used are LTE, Grassmanian codebooks [10] and Random vector Quantization (RVQ) codebooks [28].

1.3 THESIS OUTLINE AND CONTRIBUTIONS

The organization and contributions of the thesis are as follows:

Chapter 2 gives the necessary literature review and focuses on the basic concepts of wireless communication challenges of fading and inter symbol interference including the types of fading channels and the MIMO communication system. The various diversity techniques are presented along with the discussions on space time coding, transmit beamforming using codebooks and reconfigurable antennas.

Chapter 3 emphasizes the need for our proposed space time state trellis codes (STSTC) and presents the code design for two trellis states and four trellis states. It starts with a 2 branch trellis and extends it to 4 branch trellis. Pairwise error probability performance analysis for the proposed STSTCs in a quasi-static Rayleigh fading channel is also given. Simulation results are presented and discussed using BPSK and QPSK for our proposed STSTCs.

Chapter 4 is focused on the application and suitability of our proposed STSTCs with various switching and selection techniques. We consider a fully reconfigurable open loop and closed loop MIMO communication system. Diversity comparison and SNR gains are presented and discussed for different scenarios.

Chapter 5 presents our work on reducing codebook loss by using reconfigurable receive antennas. In this chapter, first we consider a limited feedback multi-input single-output precoding system equipped with reconfigurable antennas and later extend it to reconfigurable multi-input multi-output limited feedback precoding system. It gives the three codeword and reconfigurable antenna selection techniques and presents the analytical forms of the expected SNRs for the selection approaches. We also consider the effect of imperfect CSI. The reconfigurable antenna codebook feedback system proposed achieve the performance of large codebook size N_C with the benefits of small N_C, i.e fewer feedback bits.

Chapter 6 summarizes the contributions followed by several directions of interest for future extensions.

1.4 PUBLICATIONS

The following papers were published as a result of this PhD research.

1. U. Afsheen, P. A. Martin and P. J. Smith, "Space Time State Trellis Codes for Reconfigurable Antenna Systems," 2013 IEEE 78th Vehicular Technology Conference (VTC Fall), Las Vegas, NV, 2013, pp. 1-5.

In this paper we proposed a novel class of space time trellis codes based on super quasi-orthogonal space time codes for a reconfigurable antenna system. We called them Space Time State Trellis Codes (STSTCs). The proposed codes are capable of taking advantage of the additional degrees of diversity offered by reconfigurable antennas and changing propagation states. They achieved full rate, full diversity and high coding gain. Simulation results demonstrated their good performance. STSTCs presented achieve the diversity

order expected for four transmit antennas while using only two reconfigurable transmit antennas. Our code out performed the existing super orthogonal space time trellis code, which failed to achieve full diversity in a reconfigurable antenna system.

2. U. Afsheen, P. A. Martin and P. J. Smith, "Space Time State Trellis Codes for MIMO Systems Using Reconfigurable Antennas," in IEEE Transactions on Communications, vol. 63, no. 10, pp. 3660-3670, Oct. 2015.

In this paper we extended our work in [18] to design 4 TS STSTCs for BPSK and QPSK using different trellis structures. We provided pairwise error probability performance analysis for the proposed STSTCs in a quasi-static Rayleigh fading channel. This analysis, showed that the traditional approach of maximizing minimum coding gain distance of the parallel path is not a sufficient criterion for code design and that additional gains can be achieved by also maximizing the minimum coding gain distance of the minimum return path. We also gave the rank of the partial valid path and the performance factor as quick design criteria to get additional gains without evaluating the complete distance spectrum.

3. U. Afsheen, P. J. Smith and P. A. Martin, "Reducing codebook loss by using reconfigurable receive antennas in limited feedback precoded MIMO systems," 2014 Australian Communications Theory Workshop (AusCTW), Sydney, NSW, 2014, pp. 62-67.

It is known that the performance of limited feedback precoding systems depends on the size of the codebook, determined by the number of feedback bits. Increasing the number of feedback bits improves performance. However, this in turn requires a significant increase in the control channel bandwidth. The goal of the proposed reconfigurable antenna codebook scheme was to improve the closed-loop precoding gain without increasing the number of feedback bits. We employed reconfigurable antennas at the receiver resulting in multiple possible channel conditions. We had shown through simulations that increasing the number of receive antenna states had the same effect as a bigger codebook in terms of received signal to noise ratio gain, improved symbol error rate and sum rate gain. Different codeword and reconfigurable antenna state selection methods were considered

for both single and multi-layer transmissions and different system sizes, using LTE and Grassmannian codebooks with MMSE and SVD receivers.

4. U. Afsheen, P. J. Smith and P. A. Martin, "Reducing codebook loss with reconfigurable receive antennas," in IET Communications, vol. 10, no. 8, pp. 955-961, 19 5 2016.

In this study, a reconfigurable antenna codebook feedback scheme was investigated to reduce precoding codebook loss without increasing the number of feedback bits. Analysis and simulations showed that increasing the number of receive antenna states (S) has the same effect as codebook size expansion when the codeword and state selection is based on minimising the distance between channel and codeword. In addition, the authors proposed an optimum selection approach. The signal to noise ratio and rates achieved with perfect feedback in a traditional non-reconfigurable antenna system, can be exceeded with only $S = 2$, using the proposed optimum selection. In fact doubling S gives an approximate SNR gain of 40 compared with $S = 1$. The authors also consider the effects of channel estimation errors and correlated antenna states.

Chapter 2

LITERATURE REVIEW

This chapter is focused on background needed for this research. We cover basic concepts of wireless communication challenges of fading channels and inter-symbol interference (ISI), types of fading channels and the multi-input multi-output (MIMO) wireless communication system. Various diversity techniques are presented. Space time codes are introduced, with the focus on space time block codes (STBC), space time trellis codes (STTC), and super orthogonal space time codes concatenating the above two, followed by the comparision of STBCs and STTCs. It then gives the disadvantages of space time codes and gives the introduction to space frequency codes and space time frequency codes. Reconfigurable antennas' basics and their various types are introduced. Existing work on reconfigurable antenna MIMO communication system and coding is presented and space time state block codes are introduced. Antenna state switching and selection is discussed with respect to reconfigurable antennas MIMO system. Finally it introduces transmit beamforming using codebooks and reconfigurable antennas.

2.1 FADING CHANNELS

A fading channel is a wireless communication channel that experiences variation of the attenuation of a signal with many different variables. The presence of reflectors in the environment surrounding a transmitter and receiver create multiple paths that a transmitted signal can traverse. As a result, the receiver sees the superposition of multiple copies of

the transmitted signal, each traversing a different path. Each signal copy will experience differences in attenuation, delay and phase shift while travelling from the source to the receiver. This can result in either constructive or destructive interference, amplifying or attenuating the signal power seen at the receiver. Fading channels can be classified as flat or frequency selective based on multipath time delay and can also be classified as slow or fast based on Doppler spread. Coherence time is a parameter used to describe the channels time varying nature. It denotes the time duration over which the channel exhibits a time invariant nature [29]. It is a measure of the minimum time required for the magnitude change or phase change of the channel to become uncorrelated from its previous value. The coherence time of the channel is related to a quantity known as the Doppler spread of the channel. When a user or reflectors in its environment is moving, the user's velocity causes a shift in the frequency of the signal transmitted along each signal path. This phenomenon is known as the Doppler shift. Signals traveling along different paths can have different Doppler shifts, corresponding to different rates of change in phase. The difference in Doppler shifts between different signal components contributing to a signal fading channel tap is known as the Doppler spread. Channels with a large Doppler spread have signal components that are each changing independently in phase over time. Since fading depends on whether signal components add constructively or destructively, such channels have a very short coherence time. Doppler spread and coherence time are parameters that describe the frequency-dispersion nature of the mobile channel. Their values with respect to the transmitted signal bandwidths and the symbol duration (period) can help determine if the channel is experiencing fast fading or slow fading. The Doppler spread is a linear functions of the signal frequency. The variation of Doppler spread with frequency is important when the operating frequency bands are different for two systems. For instance, a system operating at 2 GHz has a Doppler spread twice that of a 1 GHz system, and thus resulting in a coherence time half as large. This gives rise to fading faster, with shorter fade duration, and channel measurements that become outdated twice as fast. Coherence Bandwidth is a parameter that is used to describe the channels time dispersive nature. More specifically it denotes the range of frequencies over which the channel exhibits an

equal gain and linear phase or flat behaviour [29].

As a result, there are four categories of fading channels [30]:

1. Flat/ frequency non-selective slow fading channel: When the bandwidth of the signal is less than the coherence bandwidth of the channel and the signal duration is much shorter than the coherence time of the channel, frequency non-selective slow fading channel appears.

2. Flat/ frequency non-selective fast fading channel:When the bandwidth of the signal is less than the coherence bandwidth of the channel and the signal duration is much larger than the coherence time of the channel, frequency non-selective fast fading channel appears.

3. Frequency selective slow fading channel: When the bandwidth of the signal is larger than the coherence bandwidth of the channel and the signal duration is much shorter than the coherence time of the channel, frequency selective slow fading channel appears.

4. Frequency selective fast fading channel: When the bandwidth of the signal is larger than the coherence bandwidth of the channel and the signal duration is much larger than the coherence time of the channel, frequency selective fast fading channel appears.

In the case of flat fading, the impulse response of the channel can be approximated by one delta function and in the case of frequency selective fading, multiple delta functions are used. The amplitude of these delta functions are random, due to the inherent nature of the multipath and random location of the objects in the surrounding [30], [31], [32]. To examine the behaviour of the amplitude and power of the signals, statistical models are needed. The fading channel models commonly used are

- Rayleigh fading model [32], [31], [30].

- Ricean fading model [32], [31], [30].

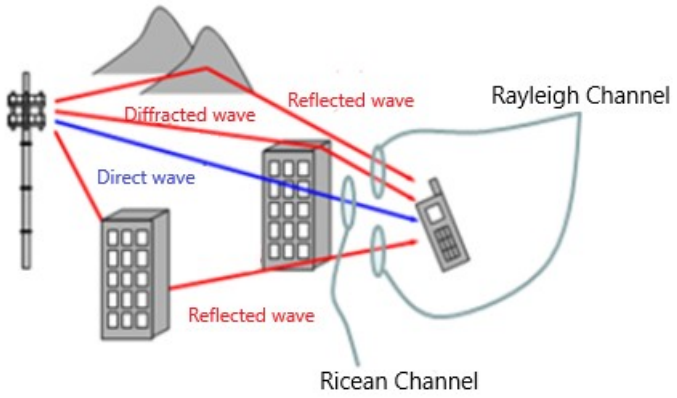

Figure 2.1 Multipath propagation resulting in different fading channels.

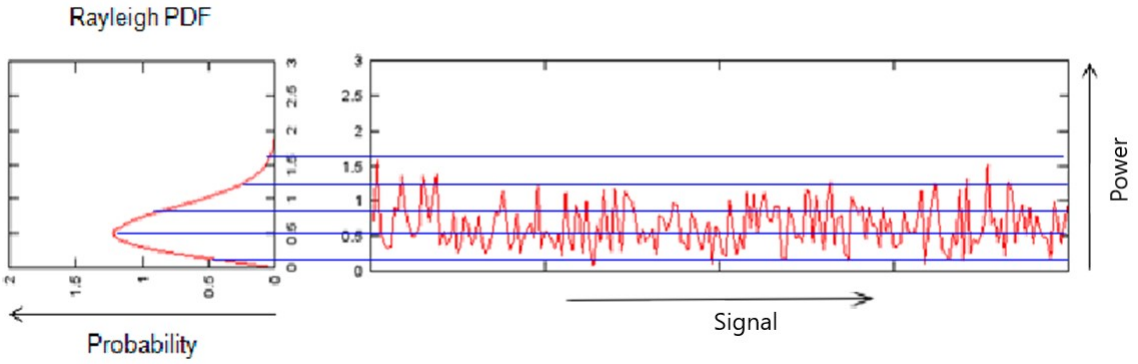

Figure 2.2 Rayleigh pdf.

As shown in Fig. 2.1, for line of sight between the transmitter and receiver Ricean fading model is used. When there is no line of sight between the transmitter and the receiver and many buildings and other objects attenuate, reflect, refract and diffract the signal, the channel follows Rayleigh Probability Density Function as shown in Fig. 2.2, and it is called a Rayleigh fading channel. Within transmission blocks it may be constant also referred to as flat or varying also referred to as selective. If the channel does not change for

a block of transmission and it changes independently within the blocks of transmission, it is called quasi-static Rayleigh fading channel [33]. These constants may be different for each block and their value is the result of combined channel's flat gain and consistent phase values. The quasi-static channel model belongs to the general class of composite channels [33] also known as mixed channels [34].

2.2 TECHNICAL CHALLENGES OF WIRELESS COMMUNICATIONS

Data sent using wireless communication typically experiences multipath propagation. This is due to the fact that the transmit signal can reach the receiver via different paths each of which has a distinct amplitude, delay, direction of departure from the transmitter and direction of arrival at the receiver [32]. If the arriving signal has a longer duration than the transmitted signal, then in the time domain the impulse response of the channel is not a delta function and in the frequency domain the transfer function of the channel varies over the bandwidth of interest. This results in delay dispersion and inter-symbol interference (ISI) [32], [31]. The multipath fading channel results in the received power varying with time/place due to constructive and destructive interference. However, multipath can be used to our advantage if we can combine the multiple received copies intelligently [32].

Wireless communications employing multiple antennas are focused here. The impacts of fading due to multipath can be seen in the time, frequency and spatial domains. The ISI resulting from multipath leads to errors that cannot be eliminated by simply increasing the transmit power [32]. In a single antenna system it cannot be used to our advantage. Multiple antenna systems employing codes such as space-time (ST), space-frequency(SF), space-time-frequency (STF) codes [30] achieve diversity gains on multipath channels by exploiting the different sub channels offered, to achieve better error performance.

Spectrum limitations, energy limitations and user mobility are the other problems associated with sending data over a wireless channel.

Hence, simply put the communication goals generally are

- high data rates-multiplexing gain;
- reliable data/lower error rates-diversity gain and coding gains;
- low SINR-antenna gain;

The available resources are

- space
- time
- frequency
- antenna polarization
- antenna radiation pattern
- multipaths
- Angle of arrival (AoA)

These characteristics make the wireless channel propagation states. This research is focused on reliable data with improved SNR and diversity gains.

2.3 MIMO WIRELESS COMMUNICATION SYSTEM

Due to the ever increasing demand for faster data transmission speed, multiple antenna systems have been actively investigated [35], [36] for recent and future telecommunication systems. The channel capacity of a multiple antenna system with N_t transmit and N_r receive antennas can be increased by a factor of min (N_t , N_r), without using additional spectral bandwidth or transmit power. Fig. 2.3 presents a MIMO system model with N_t transmit and N_r receive antennas. The great potential of using multiple antennas for wireless communication has been apparent during the last decade [30], [37]. The

performance of a MIMO system can be measured by the capacity of the system [38]. It is given by

$$C = \log_2 \det(\mathbf{I}_{N_r} + \frac{\gamma}{N_t}\mathbf{H}\mathbf{H}^*)\ bps/Hz, \tag{2.1}$$

where N_r is the number of receiving antennas, N_t is the number of transmitting antennas, $\mathbf{I}_{N_r}$ is the $N_r \times N_r$ identity matrix, γ is the average receiver signal-to-noise ratio (SNR), $\mathbf{H}$ is the normalized channel matrix, and $\{.\}^*$ denotes the conjugate transpose, provided the transmitter has no knowledge of the channel and the power is equally distributed to each transmitting antenna [34].

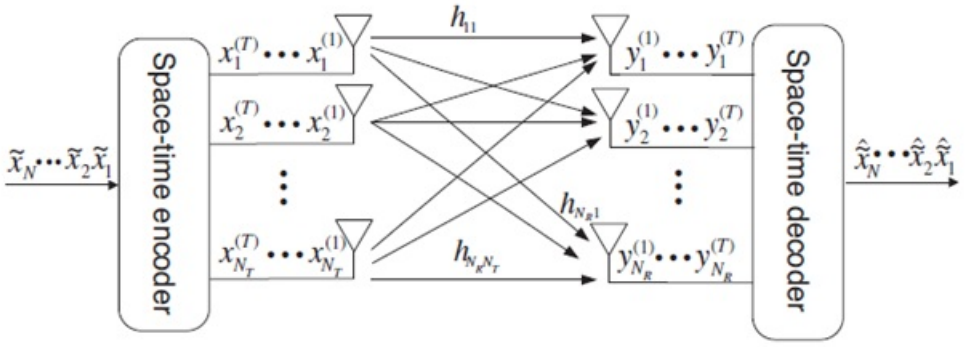

Figure 2.3 MIMO system model.

Considering the properties of the propagation channel as variables not in our control, there are two approaches to raise the capacity of a MIMO system:

1. Increase the diversity of the system.

2. Increase the amount of signal power received.

Note that diversity will boost if the rank of the MIMO channel HH* is increased. The diversity and SNR can be manipulated through the preference of antennas to be used in the system [34]. The capability of antenna diversity to boost system capacity has been widely researched [39] showing that spatial [40], [41], polarization [41], [42] and angle diversity

schemes [43], [44], [45] are all capable of increasing capacity. The results of [46] mark the increase in diversity as a result of antenna reconfiguration and not as a consequence of antenna gain which typically increases capacity [38].

Polarization diversity [point 2 in Section 2.4] improves symbol error rate, and permitted by the channel can provide a gain of up to an order of magnitude if the space-time modulation technique used is spatial multiplexing [47]. Using polarization diversity, principally, usually gives performance degradation for transmit diversity schemes for example Alamouti's transmit diversity scheme [47]. Where a trade-off between diversity and data rate is needed, switching between spatial multiplexing and transmit diversity, respectively, is established. The performance of spatial multiplexing and transmit diversity differ greatly depending on the channel conditions. A switching between spatial multiplexing and transmit diversity based on the instantaneous channel state information has also been proposed in [48]. [49] presents an adaptive MIMO system that adjusts the space-time modulation (that is spatial multiplexing and transmit diversity) technique, and the antenna resources (for example polarization) according to the channel. Interchange between reconfigurable antenna and adaptive signaling feedback to each other, has a lot of potential in broadband MIMO system design methodology [49].

2.4 DIVERSITY

The probability that all statistically independent fading channels simultaneously experience deep fading is very low. This concept is used to provide diversity in data transmission [50], [51]. Diversity techniques are used essentially to convert a time varying wireless channel into an AWGN like channel without major instantaneous fading, thus steepening the BER versus SNR curve [31].

The following techniques realizes diversity gain:

1. Spatial diversity uses N_t sufficiently separated antennas to create N_t independent

wireless channels. Spatial diversity, also known as antenna diversity, is the oldest and simplest diversity technique [29], [32], [52]. Spatial diversity can be achieved by transmitting the same signal to several antenna elements so that multiple copies of the transmitted signal are received at different antennas [32], [52]. In order to ensure that the fading amplitudes corresponding to each antenna are approximately independent, the antennas need to be spaced by at least half a wavelength [53], [29]. Spatial diversity can be categorized as transmit and receive diversity, depending on whether the diversity is realized at the transmitter or receiver [52]. It can also be classified as macroscopic and microscopic diversity. Large-scale or macroscopic diversity is linked with shadowing effects which are due to big obstacles like walls or large buildings, between the transmitter and receiver. It is available when there are different transmit or receive antennas, that are separated in space on a large scale. Then the chances that all links are obstructed together by a major object is smaller than that for a specific link. Small scale or microscopic diversity occurs in dense scattering environments with multi path fading and can be achieved using different co-located antennas. As the number of antennas increases the error performance due to fading improves. [54] presents a thorough study emphasizing the importance of spatial diversity for wireless communication systems. The concept of using large-scale diversity in wireless communication systems was rooted in the 1970's [55]. Also, since the 1950's [56], the idea of using multiple receive antennas for achieving small-scale diversity has been acknowledged. By 1990's the transmit diversity techniques were matured [57].

2. Polarization diversity occurs when independent channels are established using the fact that vertically and horizontally polarized paths are independent. Polarization diversity can be achieved without any requirement for minimum distance between antenna elements. Theoretically it doubles the antenna diversity order [58].

3. Time diversity/delay diversity occurs when the same information replicas are transmitted at adequately separated time instances (more than the coherence time).

4. Frequency diversity occurs when the same information is replicated and simultaneously transmitted at sufficiently separated frequency bands (more than the coherence bandwidth).

5. Angle diversity/ pattern diversity occurs when multiple receive antennas with different directivity are used to receive the same signal at different angles.

6. Multipath diversity is available when frequency selectivity is present, which is the typical situation for broadband wireless channels [59].

Although an early beginning of transmit diversity schemes was made with two papers that independently proposed a simple technique called delay diversity [60], [61], [62]. Its value was recognized in 1998, when Alamouti proposed a simple technique for two transmit antennas [57]. In the same year, Tarokh, Seshadri, and Calderbank presented their space-time trellis codes (STTCs) [63], which are two-dimensional coding schemes for systems with multiple transmit antennas. Delay diversity and Alamouti's transmit diversity scheme provide solely a diversity gain that is full diversity with regard to the number of transmit and receive antennas, STTCs gives both a diversity gain and an additional coding gain.

2.5 SPACE TIME CODES

Space time coding is a transmit diversity technique exploiting the spatial domain in MIMO technology as shown in Fig. 2.4. Any space time code can be analyzed in terms of coding gain and diversity gain. The coding and diversity advantage influence the performance curve in different ways. The diversity gain affects the slope of the BER and FER versus SNR curves. The greater the diversity, the more steeper the slope. Coding gain has an advantage to shift the BER and FER versus SNR curves to the left.

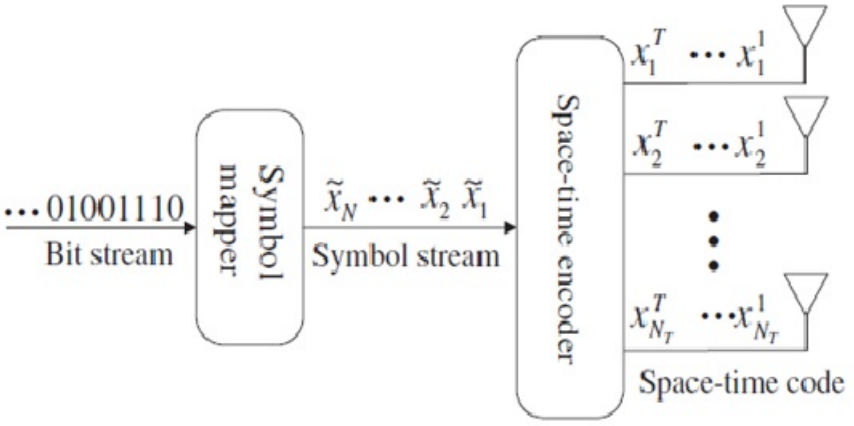

Figure 2.4 Space time coded MIMO system.

2.5.1 Space Time Block Codes

Orthogonal space-time block codes (OSTBCs) [57], [63] are coded modulation schemes designed for quasi-static flat fading channels. The main advantage of OSTBCs is that a maximum diversity gain can be achieved with relatively simple linear-processing at the receiver [63], [57], [64]. The orthogonality conditions and simple decoding capability of OSTBCs can be relaxed in exchange for a higher rate for $N_t > 2$ by using the quasi-orthogonal space time block code (QOSTBC) structures introduced in [65] and [66]. Later on, improved QOSTBCs were proposed using constellation rotation [67], [68], [69], [70] [71]. A rotated QOSTBC gives both rate one and full diversity and outperforms OSTBC. The cost is higher decoding complexity.

2.5.2 Space Time Trellis Code

Space-time trellis codes (STTCs) are another type of ST codes. They are a signalling scheme that is developed considering a joint design of error control coding, modulation and transmit diversity. STTCs were first introduced in [51] by Taroakh, Seshardi and Calderbank. Their performance on flat fading channels, in terms of coding gain, diversity gain and spectral efficiency, was investigated in [72], [73], [74]. The coding gain is achieved

through the inherent nature of the STTC itself. STTCs operate on one input symbol at a time producing a sequence of vector symbols whose length represents the number of transmit antennas [51], [75], [76], [77], [78].

For the decoding of the space time trellis coded systems, the Viterbi algorithm can be used. In the Viterbi algorithm, the branch metric is given by

$$\sum_{t=1}^{T}\sum_{j=1}^{N_r}\left|y_t^j - \sum_{i=1}^{N_t} h_{j,i}x_t^i\right|^2, \tag{2.2}$$

where y_t^j is the received signal at the j^{th} receive antenna during t^{th} symbol period, and $h_{j,i}$ is the channel gain between the i^{th} transmit antenna and j^{th} receive antenna. Using the branch metric in (2.2), a path with the minimum Euclidean distance is chosen for the detection of the symbols received.

The design objective is to construct the code with full diversity advantage and the maximum possible coding advantage. A number of manual codes with full diversity advantage have been given in [51]. Codes with larger coding gain than those in [51] along with full diversity are delivered in [76] and [77]. These codes are constructed through exhaustive computer searches. A number of new code designs and a more organized method of code development ensuring full diversity is provided in [78]. Codes presented in [79] are obtained by best distance spectrum properties search among all codes.

In [80] generation of STTC via coset partitioning has been presented to generate quickly and easily the 2^{nv}-state 2^n-PSK STTCs without the time consuming exhaustive and systematic search. With an exhaustive search, 4 billion STTCs for 4 state 4 PSK and 4 transmit antennas must be analyzed. The number of codes increases drastically with the number of states 2^{nv}, the modulation level 2^n and the number of transmit antennas N_t.

The 4 and 8 state STTCs of [79] have the same coding gain as the STTCs of [76], however they outperform the STTCs of [76] due to superior distance spectrum properties [79]. The STTCs of [76] outperform the STTCs of [51] as given in [77], [79].

2.5.3 Super Orthogonal Space Time Trellis Code

In order to provide enhanced coding advantage over earlier STTCs along with full rate and full spatial diversity, Super-Orthogonal Space-Time Trellis Codes (SOSTTCs) were proposed by Jafarkhani and Seshadri [81]. These codes were constructed for quasi-static fading channels and are based on the rank and determinant criteria. The error performance of SOSTTCs decays when they are used in wideband or frequency selective fading channels due to the large number of parallel transitions in the given trellis structure. To achieve multipath diversity with the SOSTTC, parallel transitions could be prevented by expanding the number of trellis states. In order to avoid parallel transitions in a full-rate SOSTTC with QPSK, a trellis structure with at least 16-states is needed [82].

2.5.4 Space Time Block Codes versus Space Time Trellis Codes

The key feature of STBCs is that it provides full diversity along with significantly low encoder and decoder complexity. However, typically, they do not contribute coding gain. STTCs not only provide full diversity gain but their key advantage over STBCs is the contribution of coding gain. Their disadvantage is that they are more difficult to design and require a computationally intensive encoder and decoder (expensive ML decoding). Efforts have been made to bring the advantages of both the codes together by concatenating them in various ways and thus enabling higher coding gains along with the diversity [83], [84], [85], [86]. With the same number of trellis states, concatenated STBC outperforms STTC at signal to noise ratios of interest for 1 and 2 receive antennas, however with increasing number of antennas and trellis states, the STTC starts to exceed the performance of concatenated STBC [83] due to the inherent nature of STBC's poor performance and losing capacity with increasing number of antennas [87]. Thus STTC remains the more powerful codes for higher numbers of antennas, which is a requirement for 5G and beyond technologies.

2.5.5 Disadvantages of Space Time Codes

Space time codes typically assume the channel to be constant for N_t symbol periods. Early work is involved in the constructions of various block orthogonal, trellis and turbo codes to be used along with space diversity scheme [51], [63]. However, large delay spread in frequency selective fading channels destroys the orthogonality of the signal received [88] and makes detection of the system more difficult. The use of space diversity in the context of OFDM transforms frequency selective fading of a single carrier system into multiple flat fading channels, and the effects of large delay spread can be mitigated using OFDM cyclic prefix. Some guard band could also be introduced in between carriers to avoid intercarrier interference among the many adjacent subcarriers in the OFDM system.

2.6 SPACE FREQUENCY CODES

Space-frequency (SF) codes were introduced in [89], [90] in relation to OFDM and MIMO, to fully attain frequency and spatial diversity that would address both fast fading and frequency-selective fading for broadband channels. Space/antenna and the frequency/sub-carriers are the two dimensions used by SF codes to code. The first few proposed SF coding schemes [91], [92], [93], [94] reused ST codes as SF codes by simply replacing the time axis by the frequency axis, and the full diversity offered by the channel is not exploited. Later the code design criteria for SF coding were derived [95], [95], [96]. It has been shown that a MIMO-OFDM system can attain a maximum diversity gain equal to the product of the receive antennas, the number of transmit antennas and the number of multipaths present in the frequency selective channel (K), $N_t N_r K$, provided the channel correlation matrix is full rank [91], [92], [93].

The codes proposed in [97], [98], [96], [99] give full-diversity, but their rate is at most equal to one complex symbol per channel use . Also, the authors of [97], [98] expect that the multipaths coincide with the receiver sampling instants, which is not always the case. The codes proposed in [100] have rate N_t complex symbols per channel use, but

their attainment of full-diversity is not proven. They only claim that exhaustive computer search has shown these codes to be of full-diversity when $N_t = 2$ and BPSK/QPSK signal sets are employed. The SF codes proposed in [101] achieve both full-diversity as well as rate N_t, but again they are limited by the assumption of that the number of OFDM tones to be equal to $N_t K$ and also that the multipath delays coincide with receiver sampling instants.

2.7 SPACE TIME FREQUENCY CODES

Space time frequency (STF) codes, codes across space, frequency and time, and hence are capable of achieving an additional temporal diversity advantage on top of space and multipath diversity gains offered by the MIMO-OFDM channel [93]. Authors in [102] and [103] proved that these code can achieve a diversity order that is equal to the product of the number of transmit and receive antennas, the number of independent channel taps and the rank of the channel temporal correlation matrix.

These codes were proposed for frequency selective channels or MIMO OFDM [104] and diversity was proven to increase from $N_t N_r$ to $N_t N_r K$ [105]. The approach of space-frequency coding is to disseminate the channel symbols over various transmit antennas and OFDM subcarriers within one OFDM block. If higher decoding complexity and long delays are acceptable, then coding over several OFDM block periods, results in STF codes [106], [103]. At very high SNR, STF codes are unstable and SF codes perform better [107].

Super-orthogonal space-time-frequency trellis codes (SOSTFTCs) have been proposed in [108], which provide full rate, full diversity (multipath and spatial) in MIMO OFDM systems.It was shown in [108] that the 16-state 3D SOSTFTC improves the error performance compared to the corresponding full-rate 4-state SOSTTC given by Jafarkhani and Seshadri [81] and 16-state 2D STTC given by Agrawal et al. [109], in a frequency selective environment.

In [110] extended-SOSTFTCs are proposed in which parallel transitions are avoided to

enhance their performance in multipath channels. Another class of STF trellis codes with good performance, low decoding complexity and low number of trellis states is Quasi-Orthogonal Space-Time-Frequency Trellis Codes (QOSTFTCs). It methodically combines a quasi-orthogonal space time frequency block code (QOSTFBC) [111] with a trellis code for a frequency selective channel with two taps. The block code from [111] exploits the full diversity available in the MIMO-OFDM channel, but it fails to give additional coding gain beyond that achieved from the trellis code. The QOSTFBC is related to the QOSTBC designed using four transmit antennas [69], with the difference that the QOSTFBC is implemented as a block diagonal quasi-orthogonal structure to take advantage of coding across the three dimensions (space, frequency and time) such that both the coding gain and multipath diversity can be simultaneously achieved. Unlike previous STF trellis codes designed by computer search or manually these are designed methodically and outperform the other available STFTCs [110].

2.8 RECONFIGURABLE ANTENNAS

Reconfigurable antennas [112], [113], [114] are based on the principle that by altering the antenna's physical configuration, the current density on the antenna may be controlled in a desirable manner and therefore its radiation pattern/polarization/frequency can be changed dynamically. Based on the requirement on the reconfiguration property of the antenna, there are four major types of reconfiguration techniques: electrical, optical, mechanical and material. To change the antenna's physical configuration, one can use Micro-electromechanical Systems (MEMS) switches [112], [115], [116], [117], [118], [119] or active devices such as diodes or field-effect transistors (FETs).

Each different way a reconfigurable antenna can radiate is termed as a radiation state. If distinct radiation states are created by exciting different operational frequencies, the antenna is referred to as a frequency-reconfigurable antenna [9], [120], [121]. In other cases, the radiation states are associated with distinct radiation patterns [122], [123], [124], [125],

[120], [126], or polarizations [112], [127], [128], [129], [130], [131]. A hybrid reconfiguration can also be acheived by simultaneously changing several antenna parameters [7], [8].

The Octagonal Reconfigurable Isolated Orthogonal Element (ORIOL) antenna has special interest for its use in low consumption, compact and cheap handheld devices [112]. The ORIOL antenna is a 2 port microstrip feed planar radiating structure based on an octagonal patch. The two ports are orthogonal to each other and each port is connected through a reconfigurable feeding network to two distinct points in adjacent sides of the octagonal patch, with MEM switches. The ORIOL antenna uses four MEMS switches and it can operate in two different states. The PIXEL antennacan be described as a microstrip radiator composed of an $M \times M$ square matrix of metallic pixels interconnected through MEMS switches [132]. The basic principle of operation of the PIXEL antenna is that by interconnecting specific sets of pixels within this matrix, several radiating structures can be mapped. These distinct mapped patches ultimately radiate through distinct operating frequencies.

ORIOL [112] and PIXEL [133], [132] antennas have been used for simulations of reconfigurable MIMO systems. The propagation scenario of 2 partially correlated channel can be created by ORIOL antenna [112], while the propagation scenario of upto 5 uncorrelated channel can be achieved by PIXEL antennas [121] that as a result produce higher diversity gains. With the use of reconfigurable antennas the way the propagation channel is accessed can be changed dynamically and intentionally and thus there is added scope for further exploiting the gains of MIMO communication systems.

In [133], [132], [134], it is shown that the diversity order of a reconfigurable MIMO system is given by the product of transmit and receive antennas along with the number of reconfigurable radiation states, with the use of proper codification and power allocation. These gains do not require more bandwidth, transmitted power, coding complexity, or number of transmit and receive antenna ports, but are achieved as a result of a more efficient use of the propagation channel.

When the reconfigurable antennas at the transmitter and receiver periodically switch their radiation states, its called state-switching, which creates a block fading channel model [135]. The space time state block codes (STSBCs) in section 2.9, are applied over state-switching in an open-loop configuration with reconfigurable antennas at the transmitter. STSBCs have been proved to be capable of giving a diversity gain equal to the product of the total number of propagation states offered by the reconfigurable system and the number of transmit and receive antennas [135].

State-switching is still applicable, when the reconfigurable antennas are working at the receiver, a state selection scheme to give enhanced performance gains in terms of average received Signal to Noise Ratio (SNR) has been proposed in [114]. This scheme [114] has a decoding delay which increases linearly with the number of channel propagation states and decoding complexity that increases exponentially. Therefore, there is a tradeoff between the decoding complexity and decoding delay of the system versus the level of diversity that can be obtained . Prior to data transmission using the Alamouti code, a simple state selection scheme has also been proposed in [115], where the authors have proposed choice of the best channel state, i.e. the one producing the largest received SNR. In addition to attaining full diversity, state selection can also produce a selection gain over state

State-switching is still applicable, when reconfigurable antennas are employed at the receiver, however, a state selection scheme to provide enhanced performance gains in terms of average received Signal to Noise Ratio (SNR) has been proposed in [132]. This scheme [132] has a decoding complexity which rises exponentially and a decoding delay that rises linearly with the number of channel propagation states. Therefore, there is a tradeoff between decoding complexity and decoding delay of the system versus the level of diversity one can obtain. A simple state selection scheme has also been proposed in [134], which emphasizes choosing the channel state prior to data transmission, that gives the largest received SNR. The state selection in addition to obtaining full diversity can also produce a selection gain over state switching [136].

2.9 SPACE TIME STATE CODES

For any number of channel propagation states, based on a generalized block-diagonal quasi-orthogonal space-time block code [67], [68], [69], [70], [71], [111], a general coding scheme has been proposed, referred to as STSBCs. It may be referred to as a 3-dimensional code, because it considers additionally the radiation state diversity offered by using reconfigurable antennas along with time and space dimensions exploitation.

In [112], the capability of the ORIOL antenna to create 2 partially correlated channel propagation states has been united with an appropriate coding of the transmitted signal, so that the diversity order of MIMO communication systems may be improved. This has been done using a state-switching scheme in which the transmit and receive reconfigurable antennas switch their radiation states methodically, establishing a block fading channel model. In [132] the use of PIXEL antennas [121], which are capable of generating up to 5 uncorrelated channel propagation states, had been proved to offer higher diversity gains.

For a reconfigurable system with Ψ channel propagation states the STSBCs codeword of period Ψ is denoted by STS-Ψ and is given by [136] as

$$\mathbf{C}_{STS-\Psi} = \frac{1}{\sqrt{2\Psi}} \begin{bmatrix} \mathbf{A}(S_1, S_2) & \underline{0} & \cdots & \underline{0} \\ \underline{0} & \mathbf{A}(S_3, S_4) & \cdots & \underline{0} \\ \vdots & \vdots & \ddots & \vdots \\ \underline{0} & \underline{0} & \cdots & \mathbf{A}(S_{2\Psi-1}, S_{2\Psi}) \end{bmatrix}, \tag{2.3}$$

where $\mathbf{C}_\psi = \mathbf{A}(S_{2\psi-1}, S_{2\psi})$ for $\psi \in \{1, 2, ..., \Psi\}$ and

$$\mathbf{A}(x_1, x_2) = \begin{bmatrix} x_1 & x_2 \\ -x_2^* & x_1^* \end{bmatrix}. \tag{2.4}$$

Each diagonal block represents a codeword transmitted at a particular state of the antennas and within each block the columns represent the time and rows represent the antennas.

Also,

$$[S_1 S_3 ... S_{2\Psi-1}]^T = \Theta[s_1 s_3 ... s_{2\Psi-1}]^T \tag{2.5}$$

and

$$[S_2 S_4 ... S_{2\Psi}]^T = \Theta[s_2 s_4 ... s_{2\Psi}]^T, \tag{2.6}$$

where $\Theta = \mathbf{U}\times$ diag$\left\{1, e^{j\theta_1}, ..., e^{j\theta_{\Psi-1}}\right\}$ and $\mathbf{U}$ is a $\Psi \times \Psi$ matrix which is a Hadamard matrix (in case it is present) or is constructed by eliminating the entries of entire columns and rows from a Hadamard matrix. The optimal rotation angles, θ_i's, are chosen to maximize the coding gain, generally by means of exhaustive search.

[132] proposes a scheme for reconfigurable receive antennas, in which STSBCs are used jointly with selection at the receiver. Simulation results in [132] exhibit the dominance of coding gain at low SNR, and dominance of selection gain at high SNR.

2.10 CODEBOOK TRANSMIT BEAMFORMING

Diversity gains in a multiple input and single output (MISO) system can be obtained by using space time codes or through intelligent use of channel state information (CSI) at the transmitter employing transmit beamforming and codebook feedback [10]. It has been shown in [10] that in order to achieve full diversity the codebook size should be greater than or equal to the number of transmit antennas.

A significant amount of research had been focussed on limited feedback precoding systems [24], [25] and codebook transmit beamforming is now a part of LTE standards [26] and is of great interest in next generation systems due to its well researched benefits [25]. Some popular codebooks are Grassmanian codebooks [10] and Random vector Quantization (RVQ) codebooks [28].

The codebook size, impacts the quantized beamforming system's efficiency and is also related to system diversity [10]. It is desirable to choose codebook size large to obtain

a good approximation of the channel. On the other hand, minimizing the number of feedback bits motivates choosing a small codebook size.

2.11 SUMMARY

In this chapter the relevant literature is reviewed starting with the types of fading channels and the need for diversity in order to increase reliability and channel capacity. Then 2D ST codes with particular emphasis on STTCs having higher inherent coding gains due to its coding stucture are presented. The short falls of 2D ST codes on frequency selective channels are discussed which creates a need for 2D SF and 3D STF codes used with MIMO OFDM. To increase the diversity in a more realistic channel scenario which is frequency selective and fast fading, more suitable 3D STF codes are discussed which encode along the three dimensions of the channel. Then the advancements in reconfigurable antennas and STS codes are discussed which explore the added dimension of channel propagation state due to changing antenna state and thus increase diversity. In the end, codebook transmit beamforming is discussed.

Chapter 3

SPACE TIME STATE TRELLIS CODES

3.1 INTRODUCTION AND BACKGROUND

Multiple Input Multiple Output (MIMO) communication systems employ multiple transmit and receive antennas to achieve diversity, throughput and/or coding gains. It can be difficult to fit a large number of transmit antennas on small hand held devices. In addition, each antenna requires its own RF chain. One way to work around this is to employ reconfigurable antennas [2–5], which have the ability to change their radiation pattern, frequency of operation or polarization in a pre-defined or adaptive manner. This allows the propagation channel to be altered dynamically and deliberately, resulting in additional degrees of freedom. This can be used to improve performance [137]. Orthogonal space time block codes (OSTBCs) [11, 12] provide full diversity and simple maximum likelihood (ML) decoding, but achieve little or no coding gain. Space time trellis codes (STTCs) [11] achieve full diversity and provide coding gain but at the cost of increased complexity. Super orthogonal space time trellis codes (SOSTTCs) [13] use an OSTBC as a kernel within the trellis code. They combine the set partitioning principle in [14] and a super set of OSTBC methodically, to provide full diversity, simple decoding and improved coding gain over the earlier space time trellis code (STTC) schemes [15]. However, full rate OSTBCs do not exist for more than two transmit antennas [12]. To overcome this problem, quasi-orthogonal space time block codes (QOSTBCs) were proposed in the literature to provide full rate [16, 17]. Later, rotated QOSTBCs [18, 19] were proposed to provide full diversity

and full rate. In [20,21], a super quasi-orthogonal space time trellis code (SQOSTTC) was introduced for four transmit antennas. It combines the constellation rotation of SOSTTC with that of QOSTBCs in an organized way to obtain a class of space time codes that provide full rate, full diversity and high coding gain for four transmit antennas.

SOSTTCs [13] and SQOSTTCs [20, 21] provide high coding gain and are full rate but it has been shown that they fail to achieve the diversity gains possible in a reconfigurable antenna system [22]. Space time state block codes (STSBC) were proposed by Jafarkhani and Fazel for reconfigurable antenna systems in [23]. They showed that the maximum achievable diversity order of a MIMO communication system employing reconfigurable antennas at the transmitter is given by the product of the number of transmit antennas, N_t, and receive antennas, N_r, as well as the number of radiation states, S and R, of the reconfigurable transmit and receive antennas, respectively. This motivated us to design a code that has all the good properties of the SOSTTC, but can also extract the additional diversity gain offered by reconfigurable antennas, by using a STSBC as the kernel within a SOSTTC. Our code is essentially a three dimensional trellis code, allowing us to code across space, time and reconfigurable antenna states. It is a concatenation of SOSTTC [13] and STSBC [23]. We call it a space time state trellis code (STSTC). It is straight forward to show that the proposed STSTCs are full rate and achieve full diversity N_tN_rSR. The maximum diversity offered by SOSTTC [13] is $< N_tN_rSR$ in a reconfigurable antenna system.

It is shown in this chapter that full diversity is not possible in a reconfigurable transmit antenna system with $N_t = 2, S = 2$, while using SOSTTC. And hence we propose 2 TS STSTC. We then provide 4 TS STSTCs for BPSK and QPSK using different trellis structures and give pairwise error probability (PEP) performance analysis for the proposed STSTCs in a quasi-static Rayleigh fading channel. In the analysis we have shown that considering only minimum coding gain distance (CGD) is a lacking criteria for best code design and that additional gains can be achieved by considering the minimum CGD of minimum return path (MRP). We also give a new code design criteria which is based not

only on minimum CGD of the parallel path (PP), but also on the minimum CGD MRP and have also given rank of the partial valid path and the performance factor as a quick design criteria to get additional gains without evaluating the complete distance spectrum.

This chapter is organized as follows. First, we describe our reconfigurable antenna system model. Then, we present the structure of the proposed STSTC. We give the design criteria for 2 trellis state STSTCs and the various 4 trellis state STSTCs. We also give the STSTC PEP analysis using BPSK and the 4 trellis state 2 branch trellis structure. Finally, simulation results are presented and conclusions drawn.

3.2 SYSTEM MODEL

The system model consists of a MIMO system with N_t transmit and N_r receive antennas. Each transmit and receive antenna is equipped with a reconfigurable antenna that has S and R uncorrelated channel propagation states (CPS), respectively. This results in SR possible new channel matrices. The channel matrix during the sr^{th} CPS, is defined as

$$\mathbf{H}_{sr} = \begin{bmatrix} h_{11}^{sr} & \cdots & h_{k1}^{sr} \\ \vdots & \ddots & \vdots \\ h_{1l}^{sr} & \cdots & h_{kl}^{sr} \end{bmatrix}, \tag{3.1}$$

where h_{kl}^{sr} denotes the channel coefficient between the k^{th} transmit and l^{th} receive antenna. Also, $s \epsilon S$ and $r \epsilon R$. We assume a frequency flat quasi-static Rayleigh fading channel, where each h_{kl}^{sr} is a zero mean complex Gaussian random variable with variance of 1. We assume perfect channel state information (CSI) at the receiver, but none at the transmitter. We assume $R = 1$ (non reconfigurable receive antenna) and that the transmit antennas change their states every two time slots and the fading channels are constant over a frame of length F. The $L \times N_r$ received matrix is given by

$$\mathbf{R} = \mathbf{CH} + \mathbf{N}, \tag{3.2}$$

where $\mathbf{C}$ is the $L \times N_t$ codeword matrix, $\mathbf{H}$ is the $N_t \times N_r$ overall channel matrix $[\mathbf{H}_1, \mathbf{H}_2, ..., \mathbf{H}_S]$, where each $\mathbf{H}_s$ is independent, $\mathbf{N}$ is the $L \times N_r$ AWGN matrix and L is the number of symbol periods in $\mathbf{C}$. At any time t, the received signal at the l^{th} receive antenna is given by

$$r_t^l = \sum_{k=1}^{Nt} h_{kl}^s c_t^k + n_t^l \tag{3.3}$$

where c_t^k is the symbol transmitted from the k^{th} antenna at time t and n_t^l is the AWGN noise at the l^{th} receive antenna at time t.

3.3 CODE DESIGN

The Alamouti OSTBC has full rate and full diversity [12]. It transmits the $L \times N_t$ codeword matrix

$$\begin{bmatrix} x_1 & x_2 \\ -x_2^* & x_1^* \end{bmatrix}, \tag{3.4}$$

using $N_t = 2$ antennas (columns) and $L = 2$ symbol periods (rows). The $N_t = 2$ transmit antenna SOSTTC of [13] can be formed by rotating the first column of the Alamouti code in (3.4), by θ to give

$$\begin{bmatrix} x_1 e^{j\theta} & x_2 \\ -x_2^* e^{j\theta} & x_1^* \end{bmatrix}. \tag{3.5}$$

The matrix subsets are constructed using the classical set partitioning method with the goal of maximizing the minimum coding gain distance (CGD) [13] instead of the Euclidean distance. The codewords in (3.5) are assigned to each state of the trellis and every branch in the trellis corresponds to a block of two symbols for transmission over two time slots.

The SQOSTTC of [69] for four transmit antennas ($S = 1$), has the structure given by the

$L \times N_t$ matrix

$$\begin{bmatrix} (x_1 e^{j\phi_1})e^{j\theta_1} & (x_2 e^{j\phi_1})e^{j\theta_2} & (x_3 e^{-j\phi_2}) & (x_4 e^{j\phi_2}) \\ -(x_2^* e^{-j\phi_1})e^{j\theta_1} & (x_1^* e^{-j\phi_1})e^{j\theta_2} & -(x_4^* e^{-j\phi_2}) & (x_3^* e^{-j\phi_2}) \\ (x_3 e^{-j\phi_2})e^{j\theta_1} & (x_4 e^{j\phi_2})e^{j\theta_2} & (x_1 e^{j\phi_1}) & (x_2 e^{j\phi_1}) \\ -(x_4^* e^{-j\phi_2})e^{j\theta_1} & (x_3^* e^{-j\phi_2})e^{j\theta_2} & -(x_2^* e^{-j\phi_1}) & (x_1^* e^{-j\phi_1}) \end{bmatrix}. \tag{3.6}$$

It uses a rotated QOSTBC as its kernel in a SOSTTC. This code provides full diversity and has rate one.

Our STSTC uses a modified STSBC [133] or block diagonal rotated QOSTBC [68] as the kernel within a SOSTTCs instead of an OSTBC. The block codes require modification to ensure full rate and full diversity. The STSBC of [133] can be written as

$$\begin{bmatrix} x_1 + x_3 e^{j\phi} & x_2 + x_4 e^{j\phi} & 0 & 0 \\ -x_2^* - x_4^* e^{-j\phi} & x_1^* + x_3^* e^{-j\phi} & 0 & 0 \\ 0 & 0 & x_1 - x_3 e^{j\phi} & x_2 - x_4 e^{j\phi} \\ 0 & 0 & -x_2^* + x_4^* e^{-j\phi} & x_1^* - x_3^* e^{-j\phi} \end{bmatrix}, \tag{3.7}$$

where symbols x_3 and x_4 are taken from a rotated constellation (x_1 and x_2 can be rotated instead due to symmetry). In our work, we allow all four symbols to be rotated. Thus, the kernel used in the trellis to form our STSTC for $N_t = 2$ reconfigurable transmit antennas with $S = 2$ can be written as

$$\begin{bmatrix} (v_1 + v_3) & (v_2 + v_4) & 0 & 0 \\ -(v_2^* + v_4^*) & (v_1^* + v_3^*) & 0 & 0 \\ 0 & 0 & (v_1 - v_3) & (v_2 - v_4) \\ 0 & 0 & -(v_2^* - v_4^*) & (v_1^* - v_3^*) \end{bmatrix}, \tag{3.8}$$

where $v_1 = x_1 e^{j\phi_1}$, $v_2 = x_2 e^{j\phi_1}$, $v_3 = x_3 e^{j\phi_2}$, $v_4 = x_4 e^{j\phi_2}$. As in the design of SQOSTTC [69], we rotate the m^{th} column of (3.8) by $e^{j\theta_m}$, where θ_m belongs to $0 \rightarrow 2\pi$. Using the four rotations possible and considering also the rotation of x_1 and x_2, along with x_3

and x_4, gives new degrees of freedom and is sufficient to provide additional constellation matrices to design a full diversity and full rate trellis code with high coding gain.

$CSn(x_1, x_2, x_3, x_4, \phi_1^n, \phi_2^n, \theta_1^n, \theta_2^n, \theta_3^n, \theta_4^n) =$

$$\begin{bmatrix} (x_1 e^{j\phi_1^n} + x_3 e^{j\phi_2^n}) e^{j\theta_1^n} & (x_2 e^{j\phi_1^n} + x_4 e^{j\phi_2^n}) e^{j\theta_2^n} & 0 & 0 \\ -(x_2^* e^{-j\phi_1^n} + x_4^* e^{-j\phi_2^n}) e^{j\theta_1^n} & (x_1^* e^{-j\phi_1^n} + x_3^* e^{-j\phi_2^n}) e^{j\theta_2^n} & 0 & 0 \\ 0 & 0 & (x_1 e^{j\phi_1^n} - x_3 e^{j\phi_2^n}) e^{j\theta_3^n} & (x_2 e^{j\phi_1^n} - x_4 e^{j\phi_2^n} e^{j\theta_4^n}) \\ 0 & 0 & -(x_2^* e^{-j\phi_1^n} - x_4^* e^{-j\phi_2^n}) e^{j\theta_3^n} & (x_1^* e^{-j\phi_1^n} - x_3^* e^{-j\phi_2^n} e^{j\theta_4^n}) \end{bmatrix}. \tag{3.9}$$

The transmission matrix for the proposed STSTC for two reconfigurable transmit antennas and $S = 2$ CPS can be written as in (3.9). The rows represent time and columns represent transmit antennas, such that column one and three represent the transmissions from antenna 1 and column two and four represent the transmissions from antenna 2. The first two columns correspond to the two antennas in the $s = 1$ state and the last two columns corresponds to the two antennas in the $s = 2$ state and n corresponds to the number of the trellis state (TS). We assume that the switching of the reconfigurable antennas is very fast compared to the symbol duration; therefore the switching time is negligible.

The symbols x_1, x_2, x_3, x_4, which are selected by input bits are from an MPSK constellation, and are rotated using ϕ and θ resulting in a constellation very similar to APSK. The specific rotation set of ϕ_1, ϕ_2, θ_1 θ_2 θ_3 θ_4 used, differs in the codewords for each state of the trellis. The codewords diverging from a state and merging to a state are chosen from the different sets as shown in Fig. 3.1 for BPSK and Fig. 3.2 for QPSK. We used the optimum set partitioning from [13]. This is based on Ungerboek's set partitioning method in [14], and is designed to maximize the minimum CGD. Bits 0 and 1 corresponds to 1 and -1 constellation points for BPSK and for QPSK, symbol indices 0,1,2,3 correspond to constellation points $1 + j, -1 + j, -1 - j$ and $1 - j$, respectively. The codewords from (3.9) are assigned to each state of the trellis. Every branch in the trellis corresponds to a block of four symbols given by (3.9) for transmission over four time slots. The Viterbi algorithm is used for the ML decoding of STSTCs. At each step the best branch among all parallel

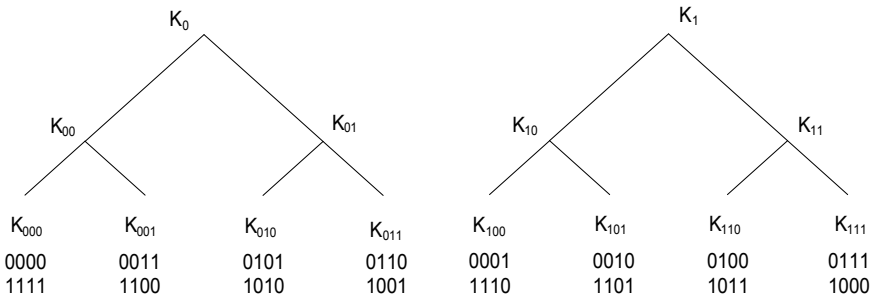

Figure 3.1 Set partitioning for BPSK for two reconfigurable transmit antennas using STSTC.

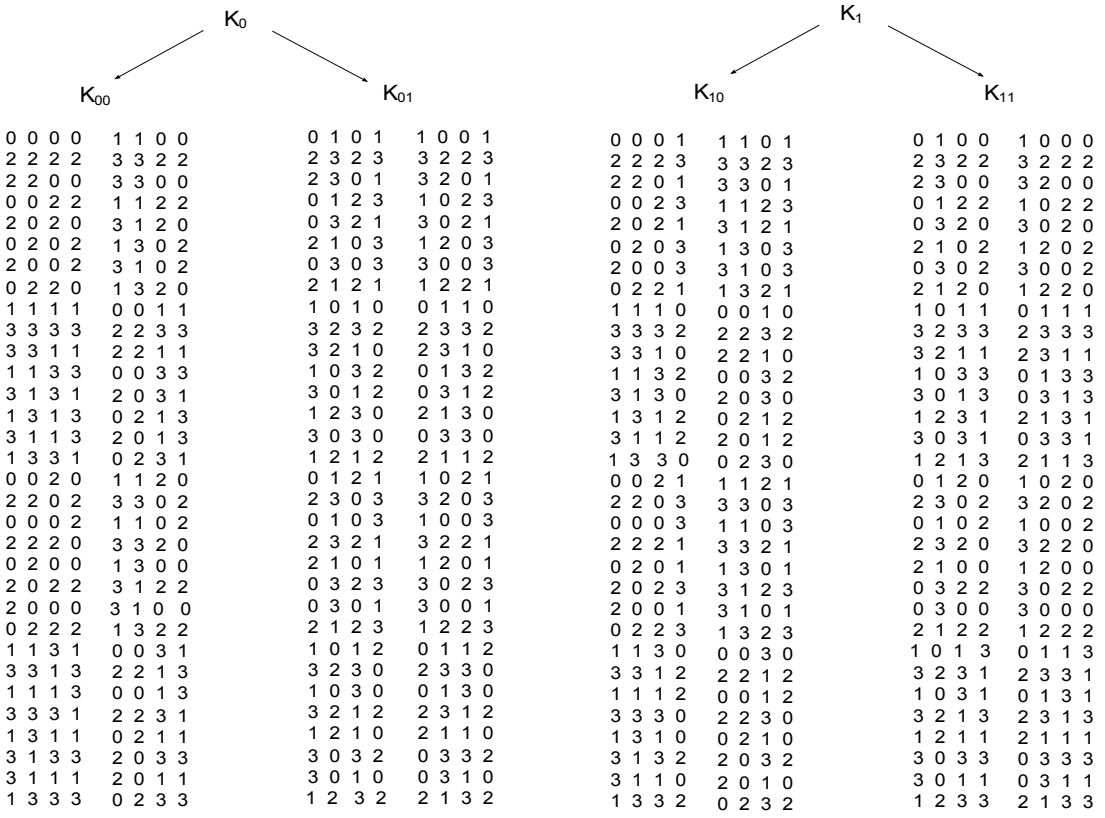

Figure 3.2 Set partitioning for QPSK for two reconfigurable transmit antennas using STSTC.

branches is first evaluated using the branch metric presented in [22]. This best parallel branch is then used to calculate the path metrics in the Viterbi algorithm which is equal to the sum of the branch metrics forming the valid paths. The most likely path is the one with minimum path gain. The STSTCs are designed for $N_t = 2$ transmit antennas, with $S = 2$ reconfigurable states per antenna, however extension to $S > 2$ is straightforward.

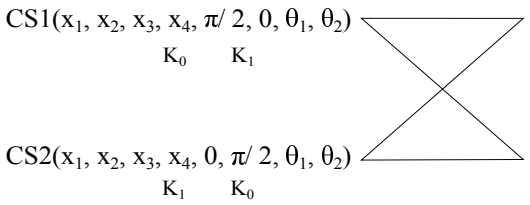

Figure 3.3 A two trellis state STSTC $r = 1$ bit/s/Hz using BPSK for two transmit antennas.

Table 3.1 Constellation rotations in (3.9) for the 2 TS 2 branch trellis in Fig. 3.3 for BPSK STSTC.

	BPSK $r = 1$bits/s/Hz		
n	ϕ_1	ϕ_2	$\theta^n_{m=1,2,3,4}$
1	0	$\pi/2$	0
2	$\pi/2$	0	0

3.3.1 2TS BPSK STSTC

The code is designed in 2 steps:

1. First the minimum parallel path CGD (min CGD PP) is increased by set partitioning and then ϕ is selected to maximize it.

2. Second the minimum CGD of the minimum return path (min CGD MRP) is maximized by carefully selecting the rotation angles in a particular trellis structure for each state. The selection of the values of ϕ and θ, given in Table 3.1, is based on maximizing the minimum rank of the difference of transmission matrix and maximizing the CGD for T=1 transitions (parallel paths) and T=2 transitions (minimum return path) simultaneously. As shown in Fig. 3.4 for BPSK, the difference of $\phi = \pi/2$ gives maximum parallel path CGD, then the set $[\theta_1^1\theta_2^1\theta_3^1\theta_4^1, \theta_1^2\theta_2^2\theta_3^2\theta_4^2]$, is selected based on the minimum return path CGD from the figure, such that the sets that give constant CGD are rejected, then the one with maximum CGD value at the selected difference of ϕ is taken. It is obvious that as minimum CGD MRP increases the FER degrades. Another important design parameter in two state codes is the minimum rank of the non valid path. If this is zero then the code is rejected. Note that θ is not unique.

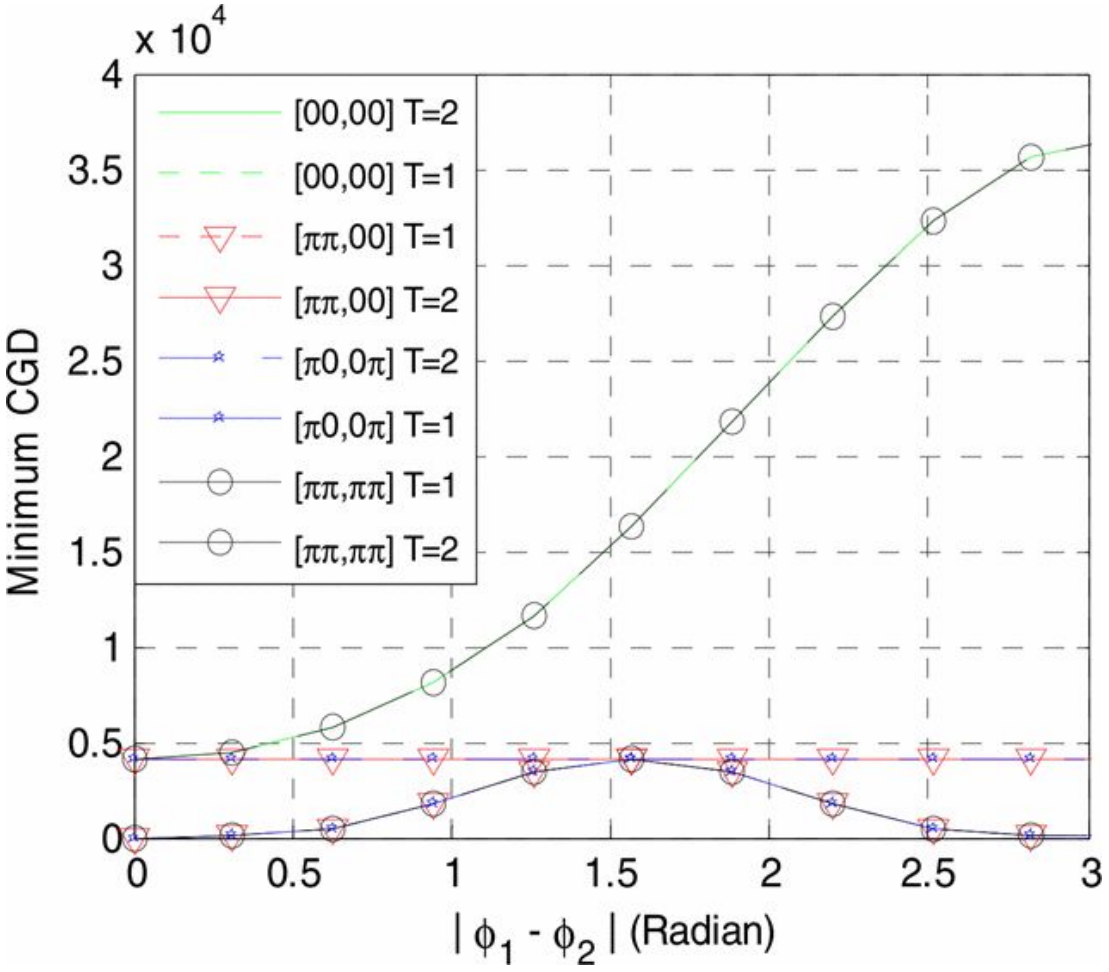

Figure 3.4 Minimum CGD for various rotations $[\theta_1^1\theta_2^1\theta_3^1\theta_4^1, \theta_1^2\theta_2^2\theta_3^2\theta_4^2]$, for two trellis state, two branch trellis using BPSK. Here $\theta_3^1\theta_4^1, \theta_3^2\theta_4^2$ are zero.

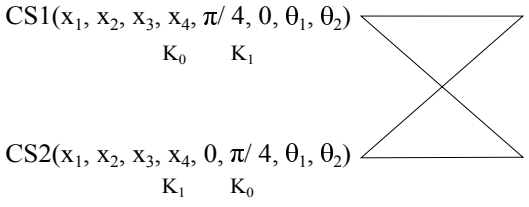

Figure 3.5 A two trellis state STSTC $r = 2$ bit/s/Hz using QPSK for two transmit antennas.

Table 3.2 Constellation rotations in (3.9) for the 2 TS 2 branch trellis in Fig. 3.5 for QPSK STSTC.

TS	QPSK $r = 2$bits/s/Hz		
n	ϕ_1	ϕ_2	$\theta^n_{m=1,2,3,4}$
1	0	$\pi/4$	0
2	$\pi/4$	0	0

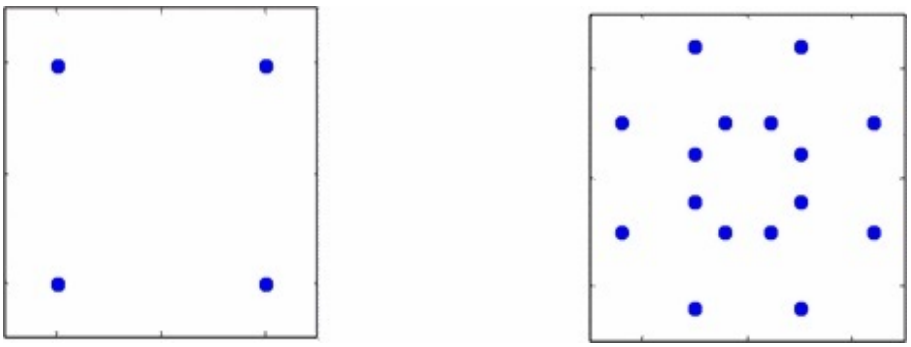

Figure 3.6 STSTC resulting constellation for BPSK (left) and QPSK (right).

3.3.2 2TS QPSK STSTC

Table 3.1 gives the values of ϕ_1, ϕ_2, θ_m^n for the 2 state trellis in Fig. 3.3 for rate $r = 1$ bits/s/Hz and Table 3.2 gives the values of ϕ_1, ϕ_2, θ_m^n for the 2 state trellis in Fig. 3.5 for $r = 2$ bits/s/Hz, where θ_m^n represents θ_m for the n^{th} TS. The STSTCs are designed for $N_t = 2$ transmit antennas, with $S = 2$ reconfigurable states per antenna, however, extension to $S > 2$ is straightforward. Also note that θ is not required for a 2 TS STSTC, as $\theta_{m=1,2,3,4}^{n=1,2} = 0$ provides good performance. Note here that the structure of our code in (9) has a kernel that is similar to the STSBC of [16], with the exception that ϕ_1 is not always zero and ϕ_2 is not always $\pi/2$ as in the STSBC for $S = 2$ CPS and a BPSK constellation. This is done to achieve full rate. In our code, symbols x_1 and x_2 are rotated with the angle ϕ_1 and symbols x_3 and x_4 are rotated with the angle ϕ_2. For BPSK, ϕ_1 and ϕ_2 belong to $\{0, \pi/2\}$ and for QPSK, ϕ_1 and ϕ_2 belong to $\{0, \pi/4\}$ to achieve full diversity and maximum gain. The resulting constellations of our scheme for 2 TS STSTCs are very similar to APSK and are shown in Fig. 3.6 for BPSK and QPSK.

3.3.3 4 TS BPSK STSTC - 2 branch trellis

According to Ungerboeks rule [14], $TS_1 = TS_3$ and $TS_2 = TS_4$ for the 4 TS 2 branch trellis shown in Fig. 3.7. Following this rule and considering two thetas, there are 16 possible codes which can further be divided into 3 categories, A, B and C as follows.
Case A: $\theta_1^n \theta_2^n$ for $n = 1$ and 2 are equal (4 possible codes).

Case B: $\theta_1^n \theta_2^n$ for $n = 1$ and 2 are partially opposite (8 possible codes).

Case C: $\theta_1^n \theta_2^n$ for $n = 1$ and 2 are opposite (4 possible codes).

We now look at the CGD of 4 TS STSTCs given in Fig. 3.7 and Table 3.3, for $r = 1$ bits/s/Hz using BPSK. These codes require at least 3 transitions to remerge to the same state. All possible error paths with T=3 transitions are considered and the corresponding CGD MRP is calculated. The CGD PP of the parallel paths with T=1, in each branch of the trellis is then calculated. CGD is equal to the $\det(\mathbf{D}^H \mathbf{D})$ for each branch, where H denotes the Hermitian transpose and $\mathbf{D}$ is the difference matrix. The total number of parallel paths (p) in each branch is equal to $\frac{M^{N_t S}}{N_b} = 8$, where N_b is the number of branches diverging from or merging into each TS.

It is found that the maximum min CGD PP = 4096 for all codes and the maximum min CGD MRP is $4096, 12288, 36864$ for C, B and A codes, respectively. Examples of codes A, B and C are shown in table 3.3 and their FER are plotted in Fig 3.17. The code A with the highest min CGD MRP performs the best inspite of all the three codes having same min CGD PP = 4096.

It is also found that for STSTCs codeword to work best with 4 TS 2 branch trellis, the θ for TS_1 and TS_2 needs to be equal and ϕ opposite. This rule along with the Ungerboek's rule makes $\theta_1^n \theta_2^n$ equal for all states. One such case could be $\theta_1^n \theta_2^n = 0$ for $n = 1, 2, 3, 4$. Thus, we can say that θ is not required for STSTC for this particular trellis structure. Note that even with θ equal to zero, it is still a trellis code and has a coding gain over STSBC. Also, note here that the structure of our code has a kernel that is similar to the STSBC of [16], with the exception that ϕ_1 is not always zero and ϕ_2 is not always $\pi/2$ as in the STSBC for $S = 2$ CPS and a BPSK constellation. This is done to achieve full rate. In our code, symbols x_1 and x_2 are rotated with the angle ϕ_1 and symbols x_3 and x_4 are rotated with the angle ϕ_2. For BPSK, ϕ_1 and ϕ_2 belong to $\{0, \pi/2\}$ to achieve full diversity and maximum gain.

Table 3.3 Constellation rotations in (3.9) for the 4 state 2 branch trellis in Fig.3.7 for BPSK STSTC.

TS	CASE A BPSK $r = 1$ bits/s/Hz				
n	ϕ_1	ϕ_2	θ_1^n	θ_2^n	$\theta_{m=3,4}^n$
1	0	$\pi/2$	0	0	0
2	$\pi/2$	0	0	0	0
3	0	$\pi/2$	0	0	0
4	$\pi/2$	0	0	0	0
TS	CASE B BPSK $r = 1$ bits/s/Hz				
n	ϕ_1	ϕ_2	θ_1^n	θ_2^n	$\theta_{m=3,4}^n$
1	0	$\pi/2$	0	π	0
2	$\pi/2$	0	0	0	0
3	0	$\pi/2$	0	π	0
4	$\pi/2$	0	0	0	0
TS	CASE C BPSK $r = 1$ bits/s/Hz				
n	ϕ_1	ϕ_2	θ_1^n	θ_2^n	$\theta_{m=3,4}^n$
1	0	$\pi/2$	0	π	0
2	$\pi/2$	0	π	0	0
3	0	$\pi/2$	0	π	0
4	$\pi/2$	0	π	0	0

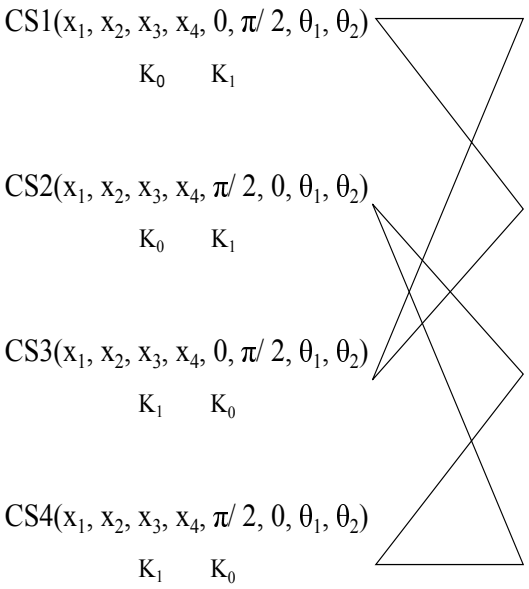

Figure 3.7 A four trellis state STSTC $r = 1$ bit/s/Hz using BPSK for two transmit antennas.

3.3.4 4 TS BPSK STSTC - 4 branch trellis

For the 4 TS 4 branch trellis structure shown in Fig. 3.8, we define a performance factor (PF), minimum rank of the partial valid path (RPVP) and the minimum CGD MRP as the design criteria for STSTCs. Several other parameters are also explored but the above mentioned parameters have the biggest impact on the performance and they contributed in a pattern, hence, PF, RPVP and minimum CGD MRP are chosen to design good codes. The number of codes considered are equal to $nc = w^{q \times N}$, where q = number of thetas, w = number of values each theta can take, N = total number of TS. PF is defined as

$$PF = \frac{1}{v \times p^T} \sum_{i=1}^{v} \sum_{j=1}^{p^T} CGDMRP, \tag{3.10}$$

where v = total number of valid paths = 12, p = the total number of parallel paths in each branch = 4 and T = the length of error event for the MRP = 2. PF should be greater than 8×10^4 for good performance. Also the PF criteria is only valid if RPVP is non zero and the total number (out of 12 valid paths) of minimum CGD MRP $<$ 10,000, ($\mathcal{P}$), should not be more than 6. RPVP is defined as the minimum rank of the difference matrix of the individual branches in a valid path (for this trellis there are 2 branches and 12 valid paths). For example let the two paths in Fig. 3.8 be from TS0 to TS0 to TS0 (correct path) and from TS0 to TS1 to TS0 (incorrect but valid path). Then the two partial valid paths in it will be TS0 to TS1 and TS1 to TS0. In this particular trellis for each possible error event there will be $v = 12$ valid paths and hence $2 \times v = 24$ partial valid paths. On each of the 24 partial valid paths there are 64 possible difference matrices according to the set partitioning. For this case $\theta^n_{m=1,2}$ belong to $(0, \pi/4, \pi/2, 3\pi/4, \pi)$ and $\theta^n_{m=3,4} = 0$. Then, $nc = 5^8$ codes are considered and some of the interesting sample codes are presented in Table 3.4 and their FERs are plotted later in the results section. These are based on exhaustive search. The maximum min CGP PP= 4096 and maximum min CGD MRP=6400. We have shown through simulation results in section 3.5 that the STSTCs with same min CGD PP and min CGD MRP can have different FER performance based

Table 3.4 Constellation rotations in (3.9) for the 4 state 4 branch trellis in Fig.3.8 for BPSK STSTC ($\theta^n_{m=3,4} = 0$)

n	ϕ_1	ϕ_2	θ^n_1	θ^n_2	PF	$\mathcal{P}$	RPVP
TS	CASE I min CGD MRP=6400						
1	0	$\pi/2$	$3\pi/4$	$3\pi/4$	8.4	3	2
2	$\pi/2$	0	0	0	$\times 10^4$		
3	0	$\pi/2$	0	0			
4	$\pi/2$	0	π	π			
TS	CASE J min CGD MRP=6400						
1	0	$\pi/2$	π	π	6.9	3	1
2	$\pi/2$	0	0	π	$\times 10^4$		
3	0	$\pi/2$	$\pi/4$	0			
4	$\pi/2$	0	π	0			
TS	CASE K min CGD MRP=6400						
1	0	$\pi/2$	0	π	7.9	5	0
2	$\pi/2$	0	0	π	$\times 10^4$		
3	0	$\pi/2$	$3\pi/4$	$\pi/4$			
4	$\pi/2$	0	π	0			
TS	CASE L min CGD MRP=4096						
1	0	$\pi/2$	$\pi/2$	$\pi/2$	9.8	6	2
2	$\pi/2$	0	π	0	$\times 10^4$		
3	0	$\pi/2$	$\pi/2$	$\pi/2$			
4	$\pi/2$	0	$\pi/4$	$3\pi/4$			
TS	CASE M min CGD MRP=4096						
1	0	$\pi/2$	0	0	9.8	9	1
2	$\pi/2$	0	π	$3\pi/4$	$\times 10^4$		
3	0	$\pi/2$	0	0			
4	$\pi/2$	0	0	0			

on maximizing the PF.

In order to design a good STSTC, first discard all codes with zero RPVP. Then maximize the minimum CGD MRP, $\mathcal{P}$ and PF such that $\mathcal{P} \leq 6$ and PF $> 8 \times 10^{-4}$. This is achieved through exhaustive search. The codes designed are optimal for five θs that are considered. By considering the above quick criteria on top of minimum CGD of the code, additional performance gains are achieved without going into the intensive calculation of the complete distance spectrum which is very complex and time consuming.

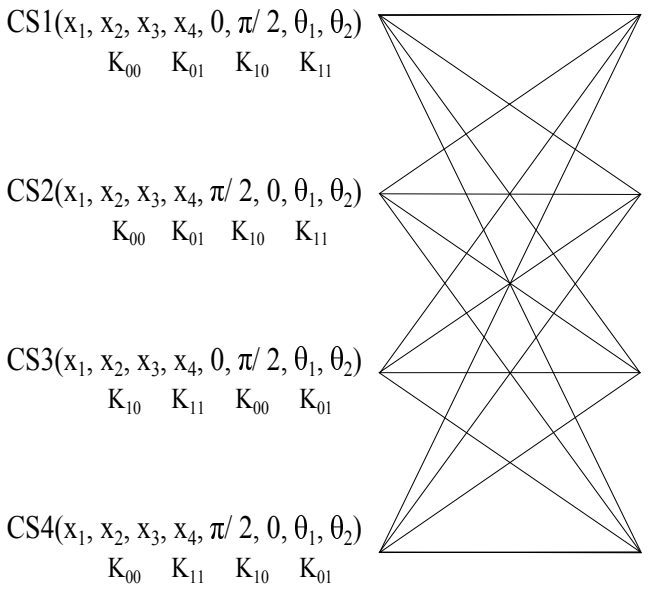

Figure 3.8 A modified four trellis state STSTC r=1 bit/s/Hz using BPSK for two transmit antennas.

3.3.5 4 TS QPSK STSTC - 2 branch trellis

Similar to 4 TS BPSK STSTC and following the Ungerboeks rule [14], the $TS_1 = TS_3$ and $TS_2 = TS_4$ for the 4 TS 2 branch trellis shown in Fig.3.9. Then following this rule and also considering angle selections, there are 16 possible codes which are further divided into 3 categories, A, B and C as follows.

Case A: $\theta_1^n \theta_2^n$ for $n = 1$ and 2 are equal (4 possible codes).

Case B: $\theta_1^n \theta_2^n$ for $n = 1$ and 2 are partially opposite (8 possible codes).

Case C: $\theta_1^n \theta_2^n$ for $n = 1$ and 2 are opposite (4 possible codes).

We look at the CGD of 4 TS STSTCs given in Fig. 3.9 and Table 3.5, for $r = 2$ bits/s/Hz using QPSK. These codes require at least 3 transitions to remerge to the same state. All possible error paths with T=3 transitions are considered and the corresponding CGD MRP is calculated. The CGD PP of the parallel paths with T=1, in each branch of the trellis is also calculated which is equal to the $det(\mathbf{D}^H\mathbf{D})$ for each branch, where H denotes the Hermitian transpose and $\mathbf{D}$ is the difference matrix. The number of parallel paths in each branch is equal to $p = \dfrac{M^{N_t S}}{N_b} = 128$, where N_b is the number of branches diverging from or merging into each TS.

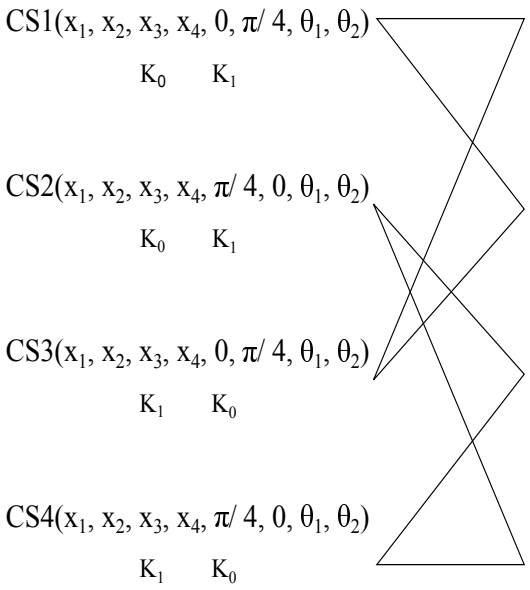

Figure 3.9 A four trellis state STSTC $r = 2$ bit/s/Hz using QPSK for two transmit antennas.

It is found that the maximum min CGD PP = 64 for all codes and the maximum min CGD MRP is $256, 432$ and 728 for C, B and A codes, respectively. Examples of codes A, B and C are shown in Table 3.5 and their FERs are plotted in Fig. 3.18. The code A with the highest min CGD MRP performs the best inspite of all the three codes having the same min CGD PP = 64.

It is also found that for STSTCs codeword to work best with 4 TS 2 branch trellis, the θ for TS_1 and TS_2 need to be equal and ϕ opposite. This rule along with the Ungerboek's rule makes $\theta_1^n \theta_2^n$ equal for all states. One of such case is $\theta_1^n \theta_2^n = 0$ for $n = 1, 2, 3, 4$. Thus we can say that θ is not required for this particular STSTC trellis structure.

3.3.6 4 TS QPSK STSTC - 4 branch trellis

4 TS 4 branch STSTC using 2 theta as given in Table 3.6, Fig. 3.10 and Fig. 3.11 is based on exhaustive search for maximizing CGD MRP and the number of codes considered

Table 3.5 Constellation rotations in (3.9) for the 4 state 2 branch trellis in Fig.3.9 for QPSK STSTC.

TS	CASE A QPSK $r = 2$ bits/s/Hz				
n	ϕ_1	ϕ_2	θ_1^n	θ_2^n	$\theta_{m=3,4}^n$
1	0	$\pi/4$	0	0	0
2	$\pi/4$	0	0	0	0
3	0	$\pi/4$	0	0	0
4	$\pi/4$	0	0	0	0
TS	CASE B QPSK $r = 2$ bits/s/Hz				
n	ϕ_1	ϕ_2	θ_1^n	θ_2^n	$\theta_{m=3,4}^n$
1	0	$\pi/4$	0	π	0
2	$\pi/4$	0	0	0	0
3	0	$\pi/4$	0	π	0
4	$\pi/4$	0	0	0	0
TS	CASE C QPSK $r = 2$ bits/s/Hz				
n	ϕ_1	ϕ_2	θ_1^n	θ_2^n	$\theta_{m=3,4}^n$
1	0	$\pi/4$	0	π	0
2	$\pi/4$	0	π	0	0
3	0	$\pi/4$	0	π	0
4	$\pi/4$	0	π	0	0

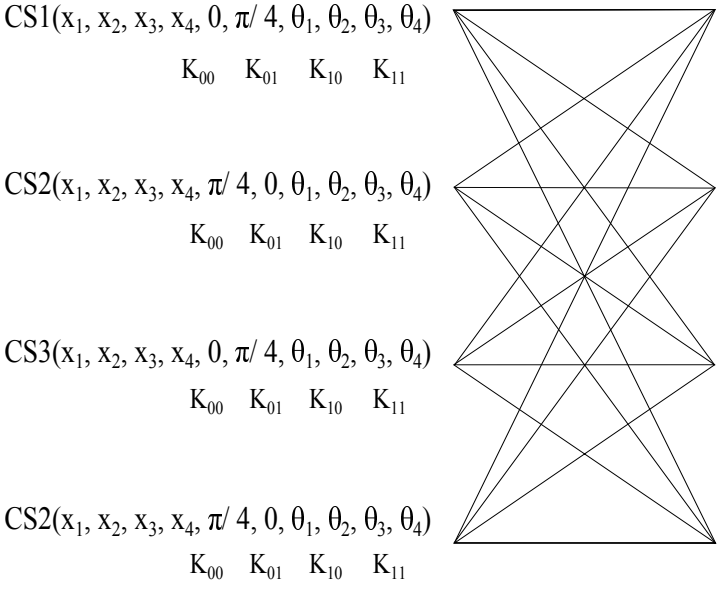

Figure 3.10 A four trellis state STSTC r=2 bit/s/Hz using QPSK for two transmit antennas.

are equal to $nc = 5^8$. The angles considered are $(0, \pi/4, \pi/2, 3\pi/4, \pi)$. In 4 TS 4 branch STSTCs using 2 θ only, the performance is limited by the CGD of MRP which is maximum

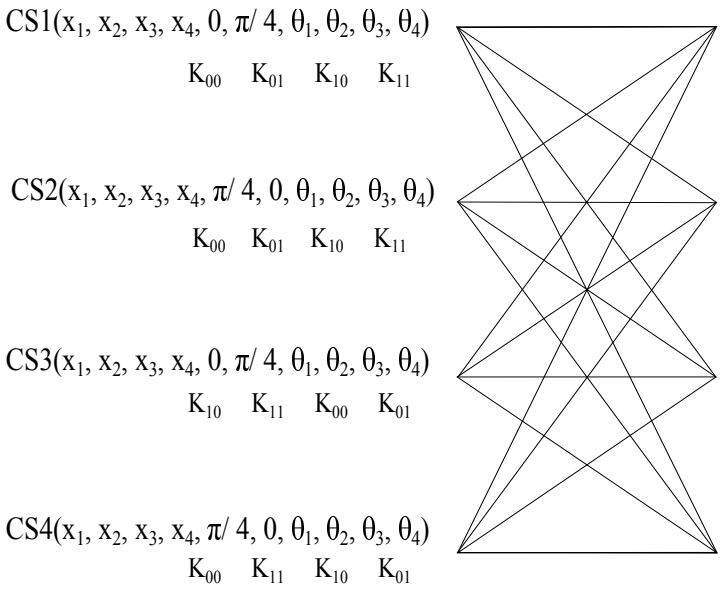

Figure 3.11 A modified four trellis state STSTC r=2 bit/s/Hz using QPSK for two transmit antennas.

equal to 90 while the CGD of PP is 256. The performance of 4 TS 4 branch 2 theta STSTCs will still be better than the 4 TS 2 branch STSTCs whose performance is limited by PP CGD equal to 64. In order to increase the minimum CGD MRP, more angles need to be introduced to maintain full rank and thus higher CGD. Due to block diagonal nature of our code only two θ are not enough to maintain full rank at higher modulations as already the 6 entries out of 16 are null. For example, in a 4 TS 4 branch trellis, the probability to get null difference matrices or non full rank difference matrices is high if angles are not carefully chosen.

Here we introduce 4 TS 4 branch STSTCs with 4 θ to get the benefits of the higher PP CGD equal to 256 and increased MRP CGD so the performance can be enhanced. The STSTC presented in Table 3.7 gives good results and can be further optimized based on exhaustive search, however, it is not performed here to choose the best CGD MRP, as it involves considering $nc = 5^{16}$ codes, which will be very time consuming.

Also we modify the trellis in the last two states to get a better performance by about 1 dB. The modified 4 TS 4 branch 4 θ STSTC is given in Fig. 3.11 and Table 3.7. For

Table 3.6 Constellation rotations in (3.9) for the original/modified 4 TS 4 branch 2 θ STSTC in Fig. 3.10 for QPSK STSTC.

TS	QPSK $r = 2$ bits/s/Hz					
n	ϕ_1	ϕ_2	θ_1^n	θ_2^n	θ_3^n	θ_4^n
1	0	$\pi/4$	$\pi/2$	0	0	0
2	$\pi/4$	0	$\pi/4$	π	0	0
3	0	$\pi/4$	π	$3\pi/4$	0	0
4	$\pi/4$	0	$\pi/2$	0	0	0

Table 3.7 Constellation rotations in (3.9) for the original/modified 4 TS 4 branch 4 θ STSTC in Fig. 3.10 and Fig. 3.11 for QPSK STSTC.

TS	QPSK $r = 2$ bits/s/Hz					
n	ϕ_1	ϕ_2	θ_1^n	θ_2^n	θ_3^n	θ_4^n
1	0	$\pi/4$	0	0	$\pi/4$	$\pi/4$
2	$\pi/4$	0	$\pi/2$	$\pi/2$	0	0
3	0	$\pi/4$	π	π	$\pi/2$	$\pi/2$
4	$\pi/4$	0	$\pi/4$	$\pi/4$	$\pi/2$	$\pi/2$

the original trellis shown in Fig. 3.10, the minimum CGD PP of the code is 256 and the minimum CGD MRP is 221. For the modified trellis shown in Fig. 3.11, the minimum CGD PP of the code is 256 and the minimum CGD MRP is 272. Note that the modified trellis performs better due to the higher CGD MRP.

3.4 SIMULATION RESULTS FOR 2TS STSTCS

In this section we provide simulation results for the proposed STSTCs. First we consider $N_t = 2, N_r = 1$ and BPSK. Both the transmit antennas are reconfigurable with $S = 2$ independent states each and both change states at the same time. Thus giving a reconfigurable antenna system that has two independent channel matrices H_s for $s = 1, 2$. In all simulations, a frame consists of $F = 132L$ symbol periods and $B = F/4 = 33$ block intervals of duration $4L$, L denotes a symbol period and the proposed STSTCs with two trellis states from Fig. 3.3 are considered. Performance is evaluated using frame error rate (FER) versus the signal to noise ratio (SNR) curves.

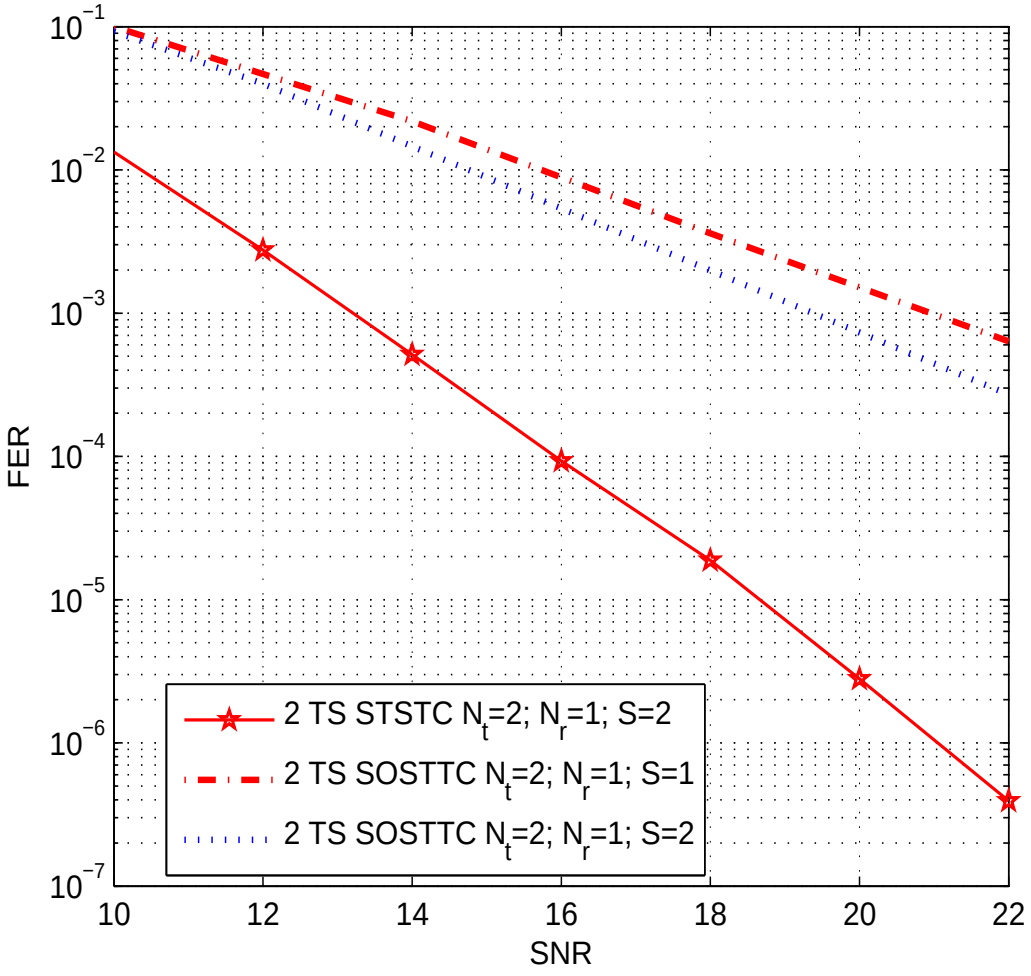

Figure 3.12 FER of the proposed STSTC for Nt = 2, S = 2 and Nr = 1 and comparison with SOSTTC with Nt = 2, S = 1, 2 and Nr = 1, using BPSK ; r = 1 bits/s/Hz.

We now compare both reconfigurable and non-reconfigurable system performances using the proposed STSTC. A 2 TS SOSTTC with $S = 1$ CPS and $S = 2$ CPS is considered for comparison purposes. The FER is shown in Fig. 3.12. When SOSTTC is used in an $S = 2$ reconfigurable antenna system, the gain is about 1 dB over $S = 1$ with only a slight increase in diversity. In contrast, the proposed STSTC with $S = 2$ CPS, achieves the full diversity of $2N_tN_r = 4N_r$. It can be seen in Fig. 3.12, at a FER of 10^{-3}, proposed STSTC is more than 6 dB better than the corresponding SOSTTC [13], in the same reconfigurable scenario.

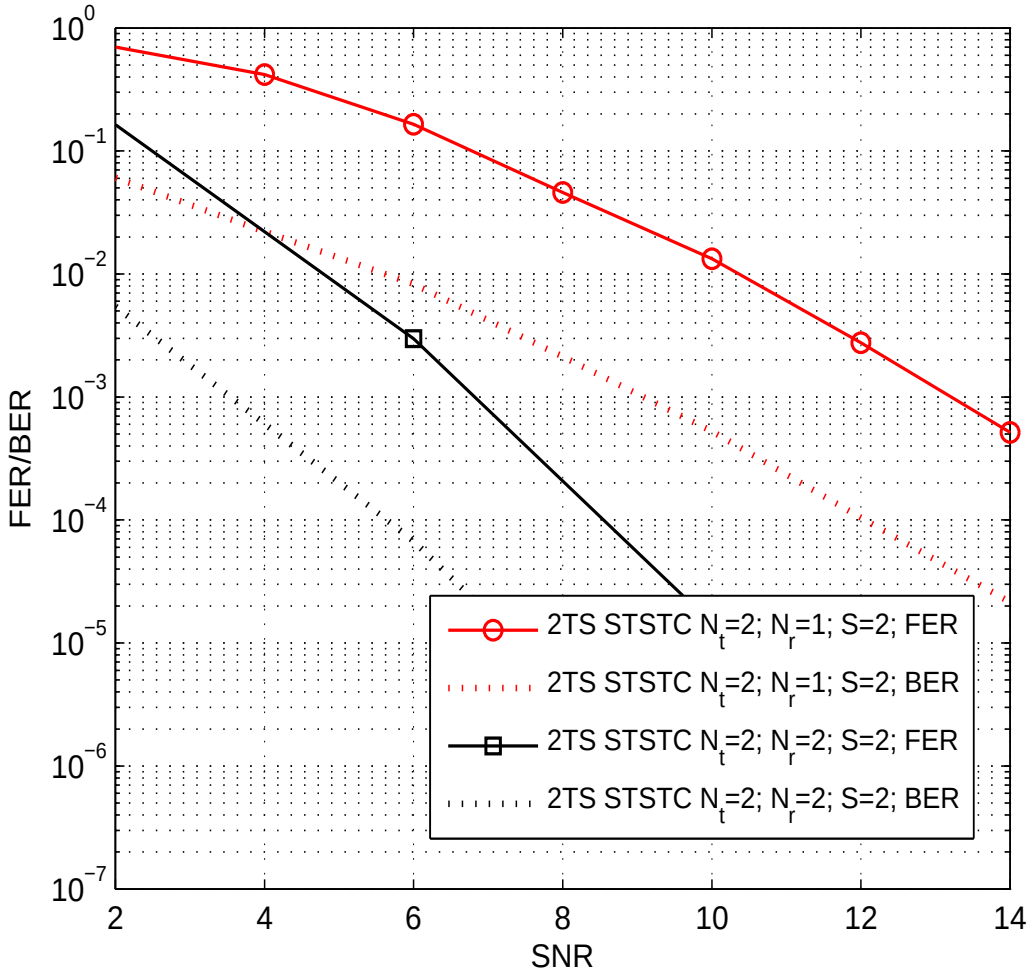

Figure 3.13 FER and BER of the proposed STSTC for Nt = 2 and Nr = 1, 2, using BPSK ; r = 1 bits/s/Hz.

We now consider $N_t = 2$ and $N_r = 2$. Fig. 3.13 gives the BER and FER performance results of the proposed STSTC with 2 TS and $S = 2$ CPS. The dotted lines show the simulation results using $N_r = 1$ non-reconfigurable receive antenna and the solid lines show the simulation results using $N_r = 2$ non- reconfigurable receive antennas. Both these results are simulated for rate $r = 1$ bits/s/Hz using BPSK. At a FER of 10^{-3} a gain of 6.4 dB is achieved by using $N_r = 2$ instead of $N_r = 1$.

We now present simulation results of the proposed STSTC for $r = 2$ bits/s/Hz using QPSK. Fig. 3.14 gives the FER performance curves for $N_t = 2$ reconfigurable transmit

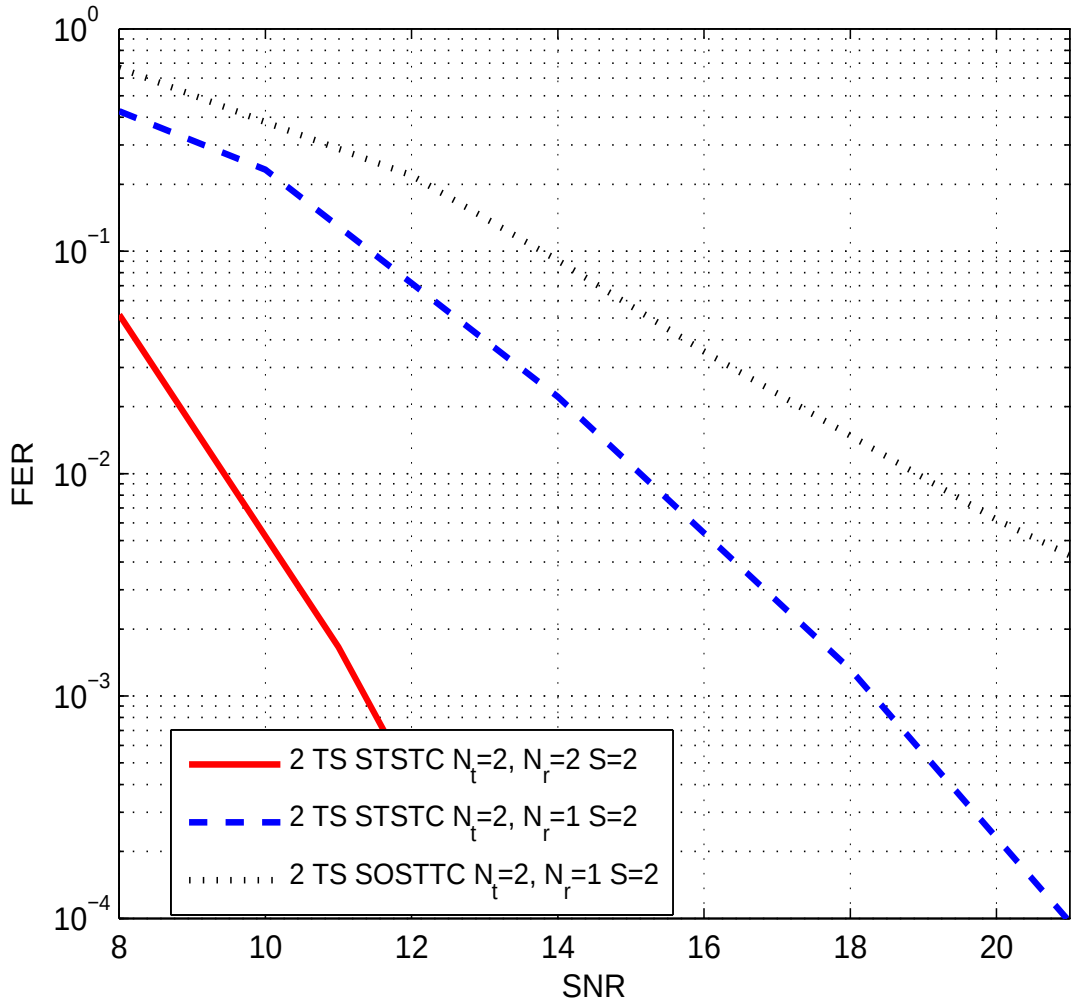

Figure 3.14 FER of the proposed STSTC for Nt = 2, Nr = 1, 2 and comparison with SOSTTC with Nt = 2, S = 2 and Nr = 1, using QPSK ; r = 2 bits/s/Hz.

antennas with $S = 2$ CPS and $N_r = 1$ (dotted line), $N_r = 2$ (solid line) non-reconfigurable receive antennas. At a FER of 10^{-2} a gain of 5.7 dB is achieved when two receive antennas are used. We have also shown results from a 2 TS SOSTTC using $N_t = 2$ reconfigurable antennas with $S = 2$ CPS and $N_r = 1$, for comparison. It can be seen, at a FER of 10^{-2}, the proposed STSTC is 3.8 dB better than the corresponding SOSTTC, in the same reconfigurable scenario due to achieving full diversity.

In Fig. 3.15 the results from our STSTCs using $N_t = 2$, $S = 2$ and $N_r = 1$ are compared with SOSTTCs and SQOSTTC using $N_t = 4, S = 1$ (non-reconfigurable transmit

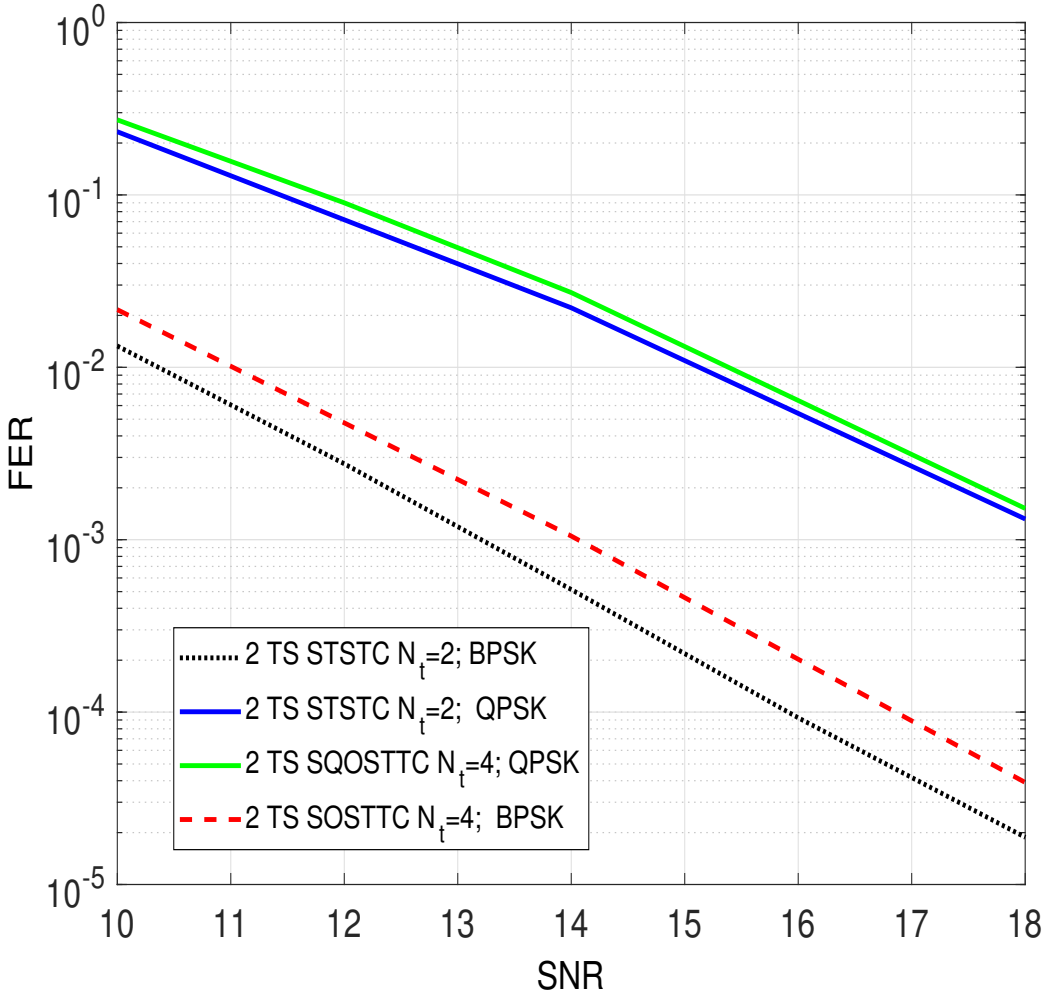

Figure 3.15 Slope comparison of SOSTTC using Nt = 4 and the proposed STSTC using Nt = 2 for r = 1bits/s/Hz using BPSK and SQOSTTC using Nt = 4 and the proposed STSTC using Nt = 2 for r = 2bits/s/Hz using QPSK.

antennas) and $N_r = 1$ for $r = 1$ bits/s/Hz using BPSK and $r = 2$ bits/s/Hz using QPSK, respectively. Here only the slopes of the FER curves are compared and not the gains to emphasize the diversity offered by the system. It is noteworthy that the FER curves in each case follow the same slope. Thus by using our proposed codes with only two reconfigurable transmit antennas, a diversity equivalent to 4 transmit antennas can be achieved. Fig. 3.16 gives the BER performance curves of STSBCs, and the proposed STSTCs. With only two TSs the proposed STSTC is 3.4 dB better, at a BER of 10^{-5}.

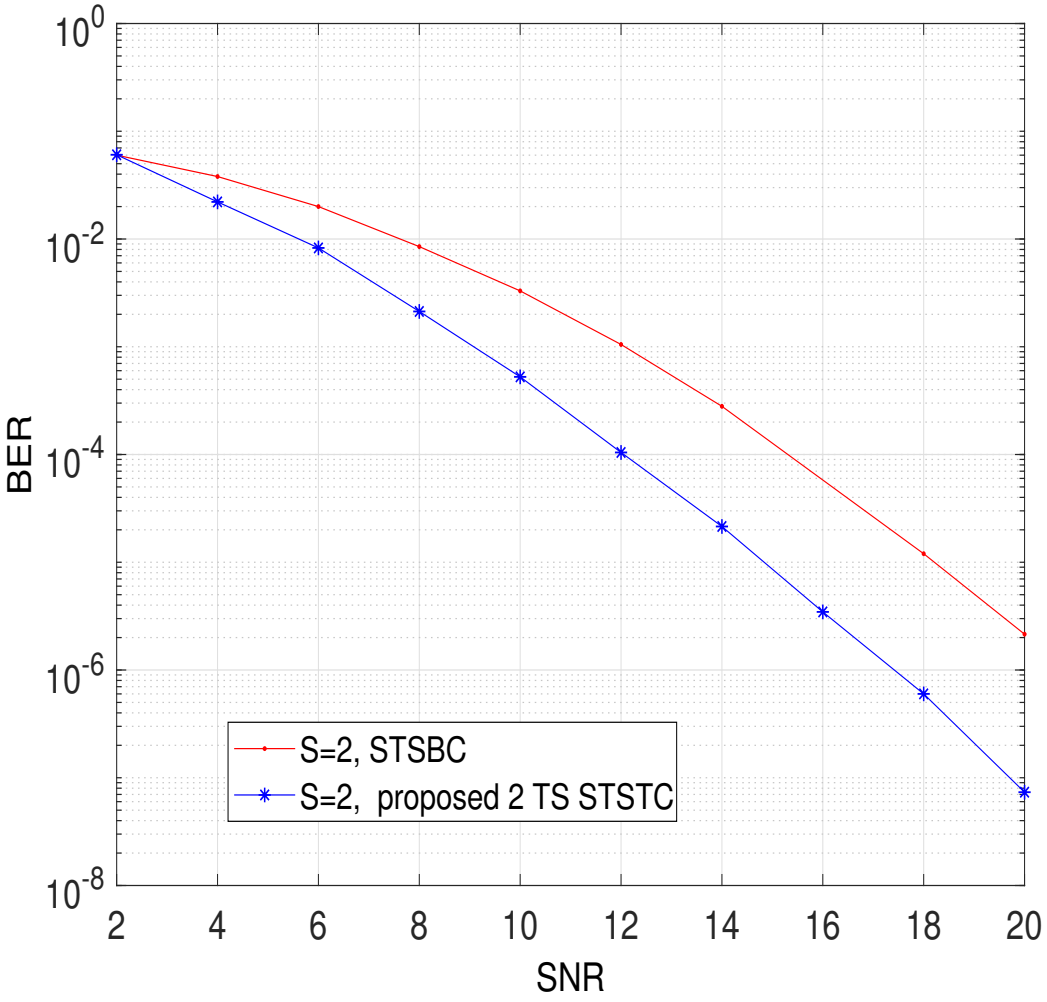

Figure 3.16 BER comparison of STSBC and the proposed STSTC in a reconfigurable transmit antenna MIMO system; Nt = 2, S = 2 and Nr = 1; r = 1 bits/s/Hz using BPSK.

3.5 SIMULATION RESULTS FOR 4TS STSTCS

In this section we provide the simulation results for the proposed 4 TS STSTCs. First we consider two transmit antennas, $N_t = 2$, one non reconfigurable receive antenna, $N_r = 1$. Both the transmit antennas are reconfigurable, with two independent states each and both change states at the same time. Thus giving a reconfigurable antenna system that has two independent channel matrices H_s for $S = 1, 2$. In all simulations, a frame consists of $F = 132$ symbol periods. Performance is evaluated using frame error rate versus the transmit signal to noise ratio curves.

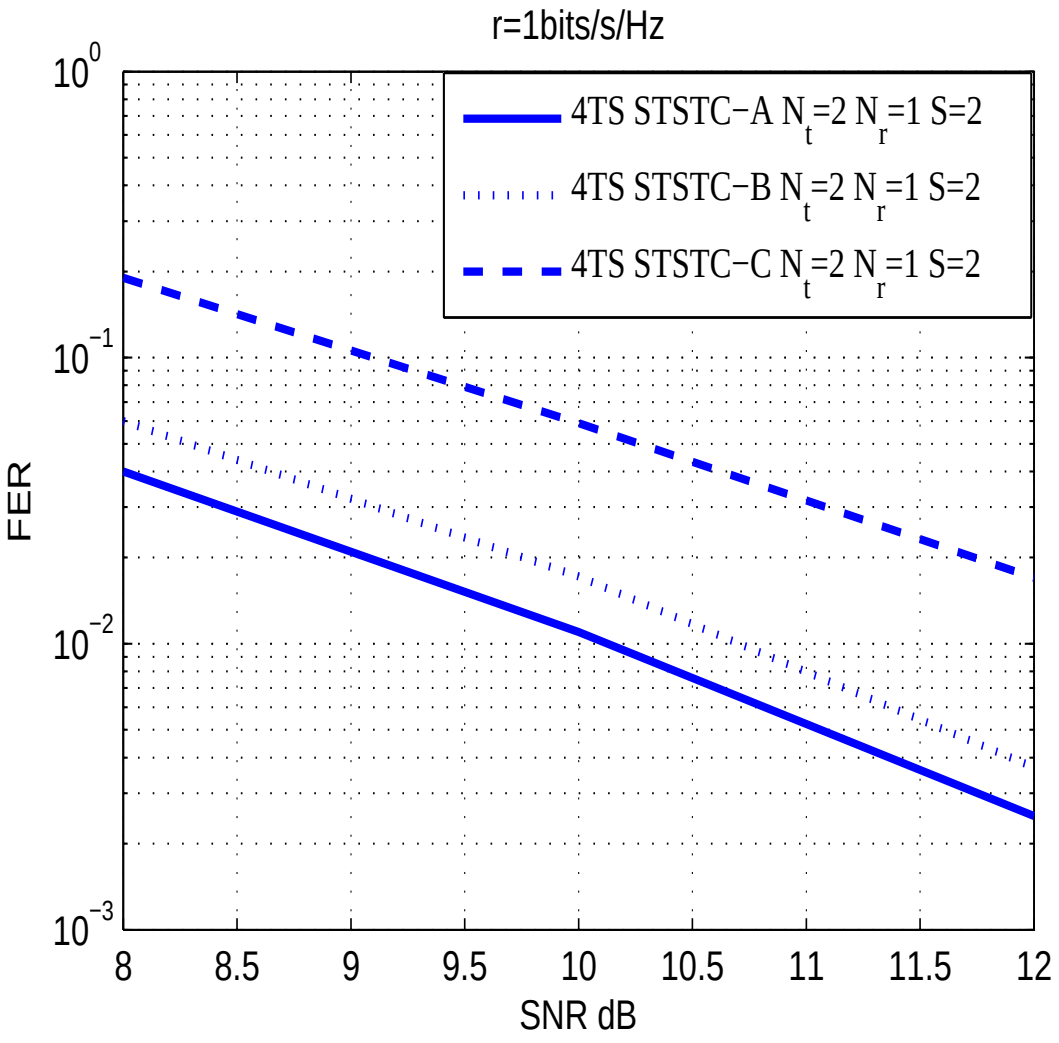

Figure 3.17 FER performance of 4 TS STSTC $r = 1$ bit/s/Hz using BPSK given in Fig.3.7 and Table 3.3 for two transmit antennas.

Fig. 3.17 gives the FER performance of 4 TS STSTC given in Fig. 3.7 and Table 3.3 for $r = 1$ bit/s/Hz using BPSK and shows that the STSTC A performs 0.5 dB better than STSTC B and about 2.5 dB better than STSTC C at an FER of 10^{-2}. Also note that all the three codes have the same diversity and same minimum CGD PP, however the coding gain varies due to the minimum MRP CGD which are 36864, 12288 and 4096 for STSTC A, B and C, respectively.

Fig. 3.18 gives the FER performance of 4 TS STSTC given in Fig. 3.9 and Table 3.5 for $r = 2$ bit/s/Hz using QPSK, and shows that the STSTC A performs 0.3 dB better than

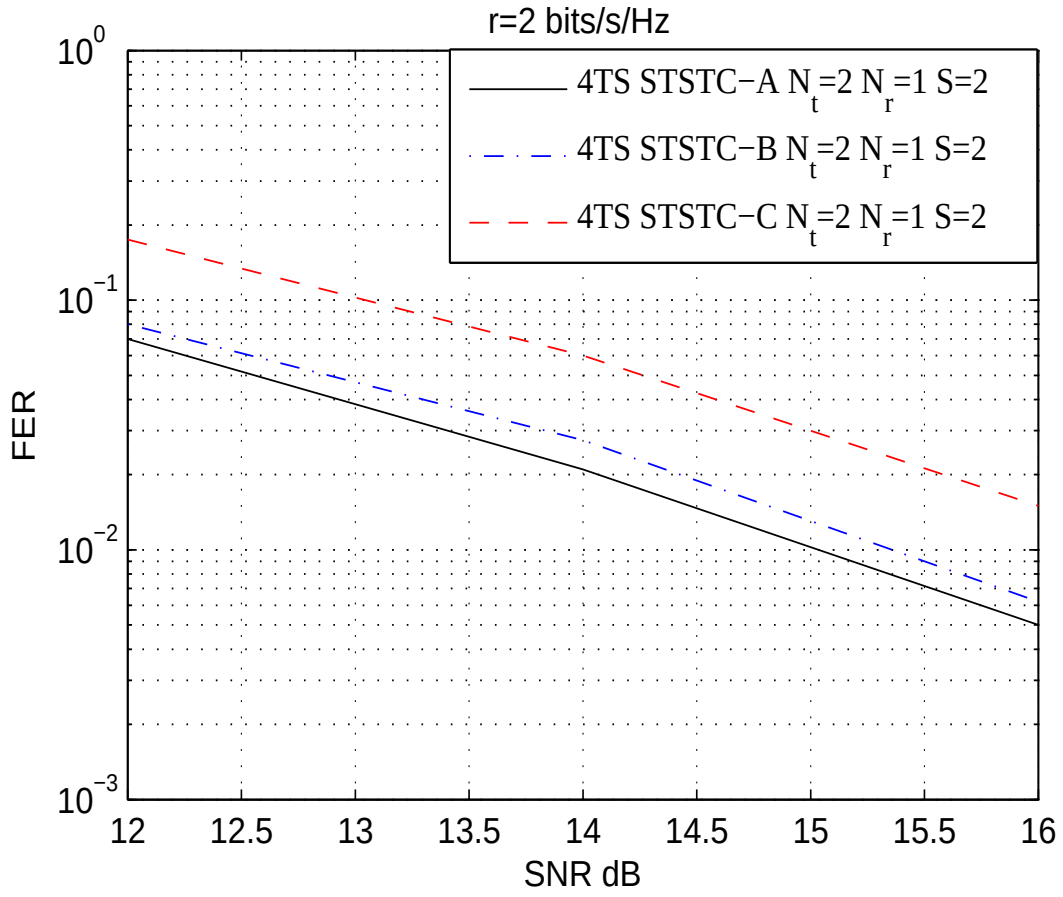

Figure 3.18 FER performance for four trellis state 2 branch STSTC given in Fig.3.9 and Table.3.5 for $r = 2$ bit/s/Hz using QPSK for two transmit antennas.

STSTC B and about 1.5 dB better than STSTC C at an FER of 10^{-2}. Also note that all the three codes have the same diversity and same minimum CGD = 64, however the coding gain varies due to the CGD MRP which are 728, 432 and 256 for STSTC A, B and C, respectively.

Fig. 3.19 gives the FER performance of the 4 TS STSTCs given in Table 3.4 for BPSK. It can be seen that the FER performance of cases I, J, K, inspite of the same CGD PP and CGD MRP varies based on the PF and RPVP. Although Case K has a better PF, it performs worst because of zero RPVP (PF is only valid if RPVP is non zero and $\mathcal{P} \leq 6$). At an FER 10^{-3} CASE I having a PF of 8.4 performs about 0.5 dB better than CASE J which has a PF of 6.9 and is about 1.7 dB better than CASE K at an FER of 10^{-2}.

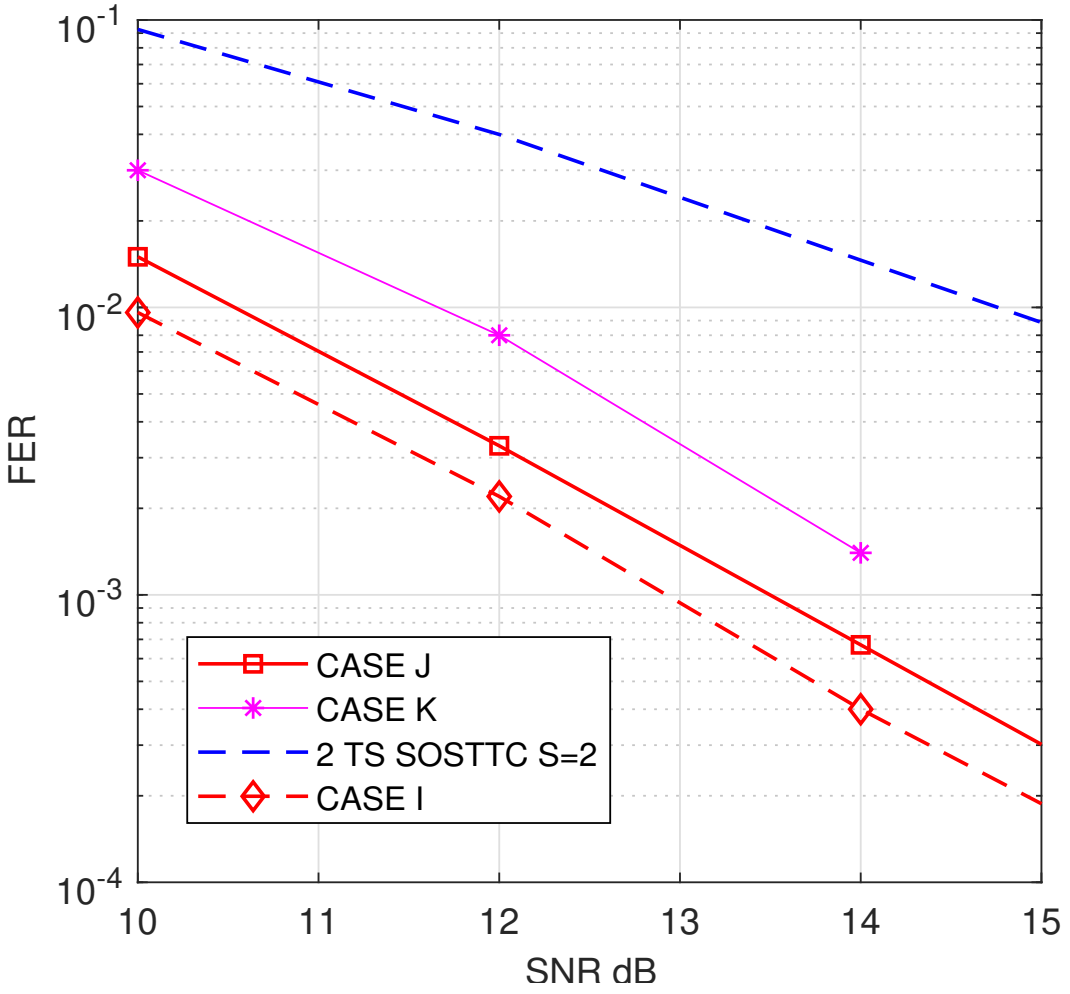

Figure 3.19 FER performance for 4 TS 4 branch STSTC given in Fig. 3.8 and Table. 3.4 for $r = 1$ bit/s/Hz using BPSK with $N_t = 2, S = 2, N_r = 1$.

However, all the STSTCs show full diversity for $S = 2$ and are 4.6 dB, 4.1 dB and 3 dB better than the same system using SOSTTC with $S = 2$. In Fig. 3.20 we emphasize the importance of $\mathcal{P} \leq 6$ using CASE L and M while keeping all other parameters fixed. Both the cases have same PF, CGD MRP and a non zero RPVP. However, CASE L performs about 0.35 dB better than CASE M at an FER of 10^{-2} as $\mathcal{P} = 6$ for the former and $\mathcal{P} = 9$ for the latter. Also both these cases perform inferior to CASE K inspite of better PF due to lower CGD MRP and worse $\mathcal{P}$. So, all these parameters need to be optimized simultaneously for the best code and are capable of adding gains.

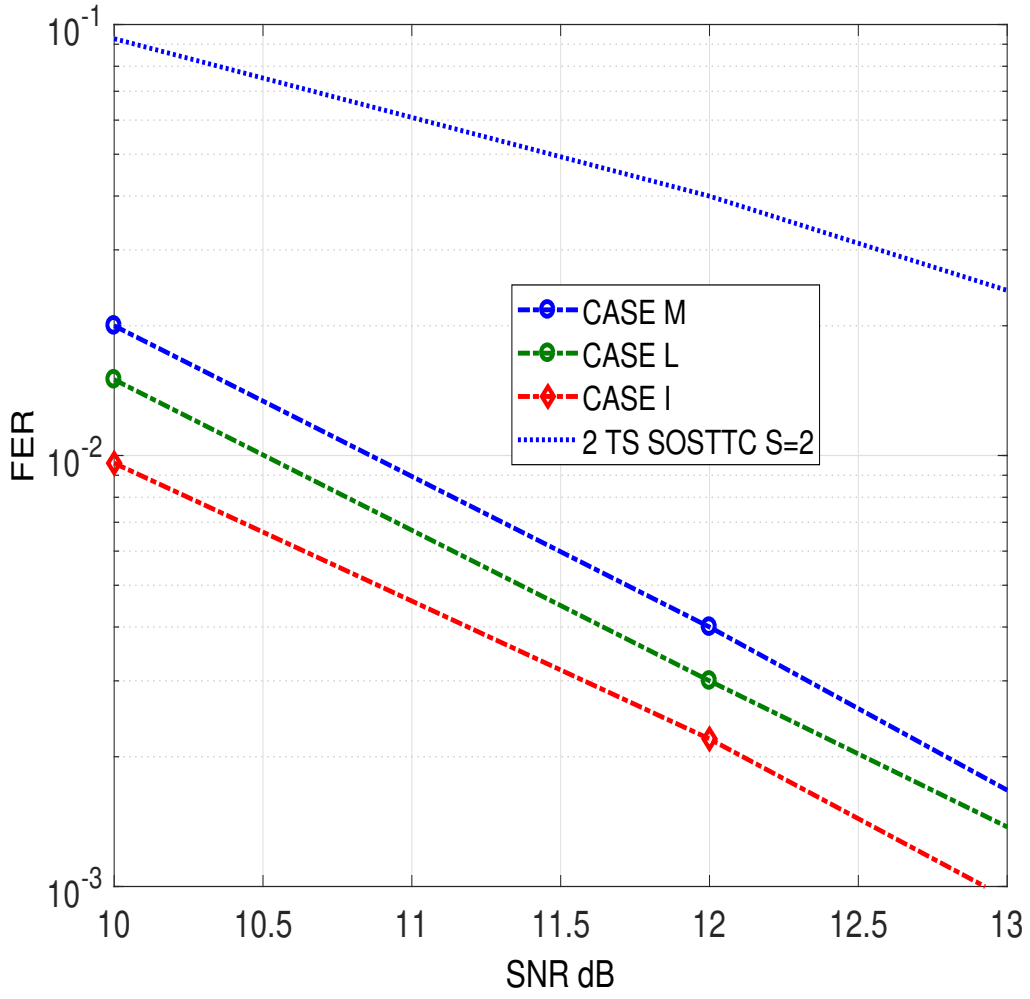

Figure 3.20 FER performance for 4 TS 4 branch STSTC given in Fig. 3.8 and Table.3.4 for $r = 1$ bit/s/Hz using BPSK with $N_t = 2, S = 2, N_r = 1$.

The FER performance of the 4 TS 4 branch original and modified trellis STSTCs is given in Fig. 3.21 for $r = 2$ bits/s/Hz using QPSK. A gain of about 0.4 dB in SNR can be seen at an FER of 10^{-3} by using the modified trellis.

Fig. 3.22 shows the FER performance of the best 4 TS 2 branch trellis STSTC, given in Fig. 3.9, Table 3.5 and its comparison with the best 4 TS 4 branch 2 theta STSTC given in Fig. 3.10, Table 3.6 and 4 TS 4 branch 4 theta STSTC using modified trellis given in Fig. 3.11, Table 3.7. It can be seen that the 4 TS 4 branch 4 theta modified trellis performs best. It has an improvement of about 0.5 dB and 0.4 dB over the other two STSTCs at

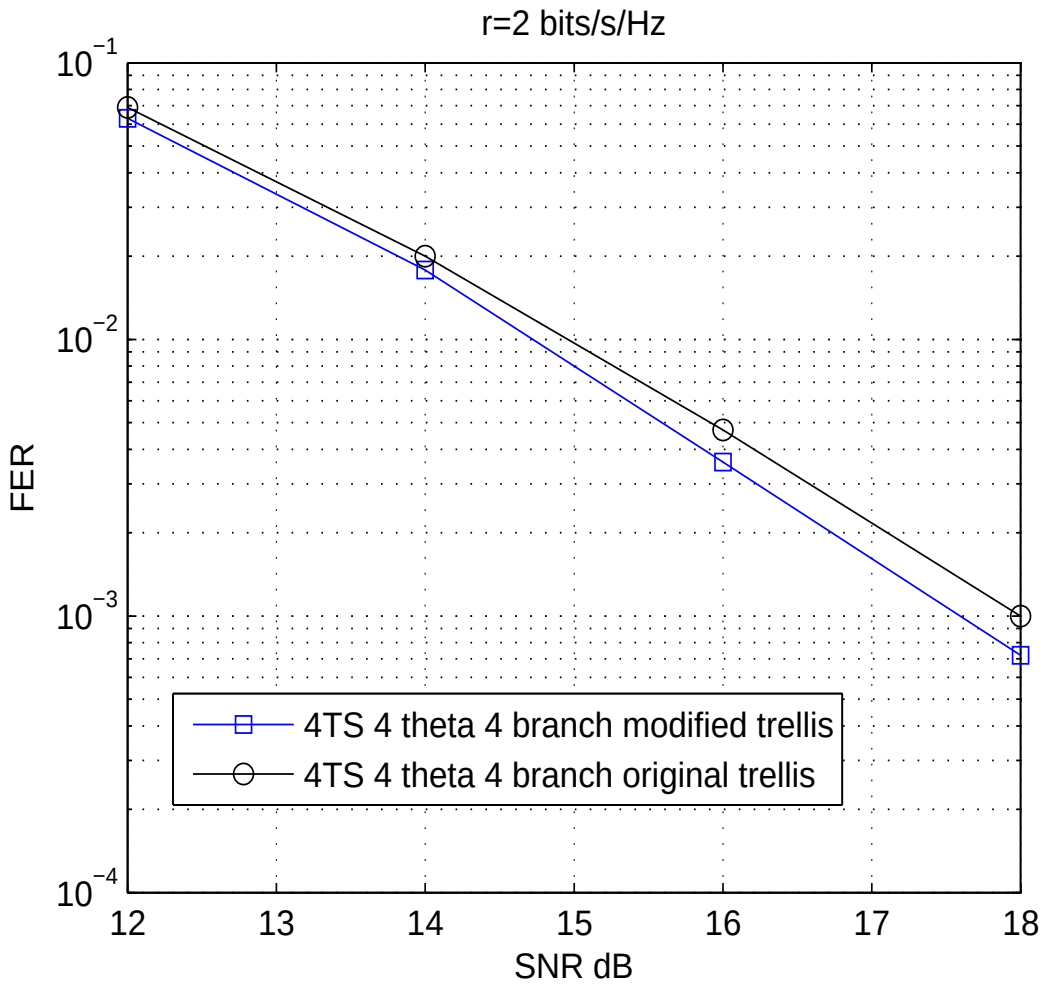

Figure 3.21 FER Performance of 4 TS 4 branch 4 theta STSTC in Fig. 3.10 and 3.11 for r=2 bits/s/Hz using QPSK and $N_t = 2$, $S = 2$ and $N_r = 1$.

an FER of 10^{-3}.

3.6 PEP ANALYSIS

In this section we present the PEP of the STSTCs considering the 4 TS 2 branch trellis in Fig. 3.7. We use this analysis to show the importance of minimum CGD MRP by evaluating the PEP of the STSTCs A, B and C given in Table 3.3 using $r = 1$ bits/s/Hz and BPSK.

Let $\tilde{x}_i = x_i e^{j\phi_z}$ and $\dot{\tilde{x}}_i = \tilde{x}_i e^{j\alpha_m}$, where, $\theta_m - \acute{\theta_m} = \alpha_m$, $\phi_z - \acute{\phi_z} = \beta_z$, $z = 1$ for $i = 1, 2$,

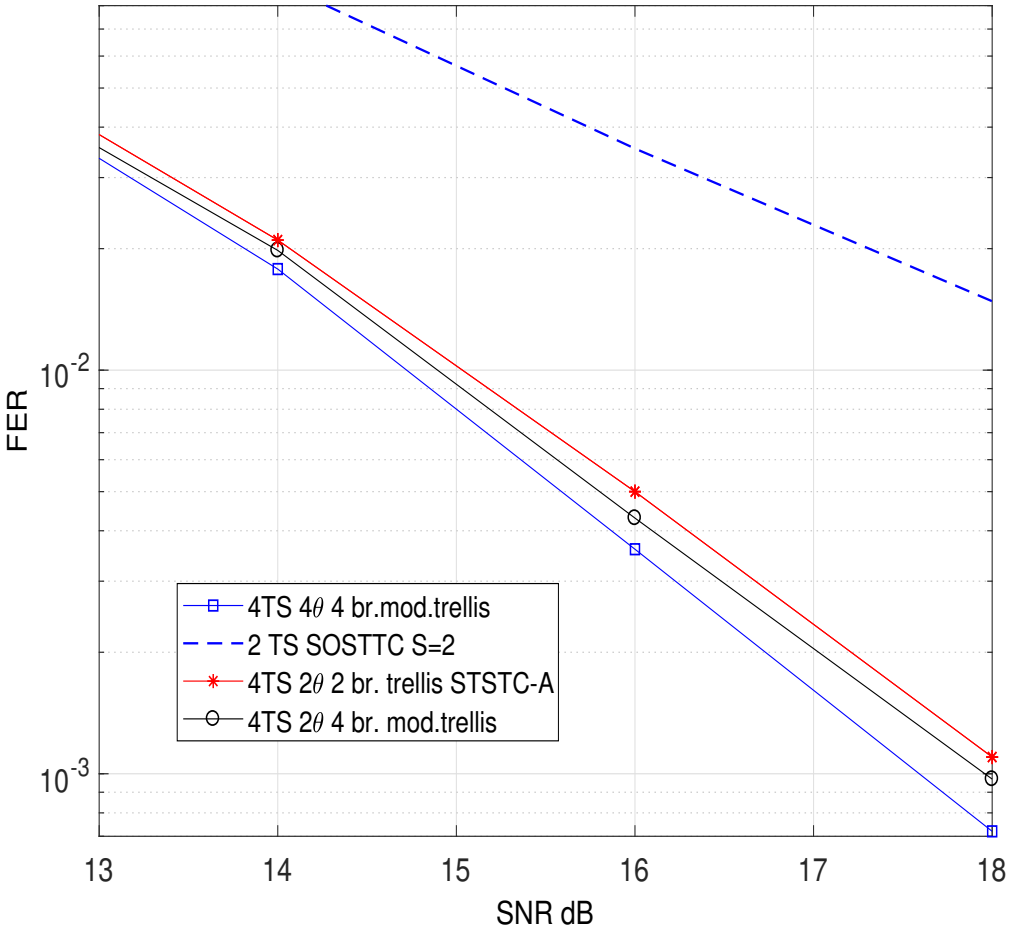

Figure 3.22 FER Performance of 4 TS STSTCs for r=2 bits/s/Hz using QPSK with $N_t = 2$, $S = 2$ and $N_r = 1$. (br.=branch, mod.=modified).

$z = 2$ for $i = 3, 4$ and $m \in \{1, 2, 3, 4\}$. Here θ and ϕ have the same meaning as in (3.9). Let the difference matrix be $\mathbf{D}_t \triangleq CSn^t - C\acute{S}n^t$, where CSn^t is from (3.9) and refers to the codeword in the t^{th} transmission interval and the dash notation represents a non-transmitted possible codeword. Then we have for each time t,

$$\mathbf{D}_t^H \mathbf{D}_t = \begin{bmatrix} E_1^t + E_2^t & 0 & 0 & 0 \\ 0 & E_1^t + E_2^t & 0 & 0 \\ 0 & 0 & G_1^t + G_2^t & 0 \\ 0 & 0 & 0 & G_1^t + G_2^t \end{bmatrix}, \tag{3.11}$$

where

$$E_1^t + E_2^t = \sum_{i=1}^{4} |(\dot{\tilde{x}}_i - \acute{\tilde{x}}_i)|^2 + 2Re[e^{j(\phi_1-\phi_2)} \{(\dot{x}_1 - \acute{x}_1)(\dot{x}_3 - \acute{x}_3)^* + (\dot{x}_2 - \acute{x}_2)(\dot{x}_4 - \acute{x}_4)^*\}] \tag{3.12}$$

and

$$G_1^t + G_2^t = \sum_{i=1}^{4} |(\dot{\tilde{x}}_i - \acute{\tilde{x}}_i)|^2 - 2Re[e^{j(\phi_1-\phi_2)} \{(\dot{x}_1 - \acute{x}_1)(\dot{x}_3 - \acute{x}_3)^* + (\dot{x}_2 - \acute{x}_2)(\dot{x}_4 - \acute{x}_4)^*\}]. \tag{3.13}$$

Let

$$\mathcal{A}_t = \sum_{i=1}^{4} |(\dot{\tilde{x}}_i - \acute{\tilde{x}}_i)|^2 \tag{3.14}$$

and

$$\mathcal{B}_t = 2Re[e^{j(\phi_1-\phi_2)} \{(\dot{x}_1 - \acute{x}_1)(\dot{x}_3 - \acute{x}_3)^* + (\dot{x}_2 - \acute{x}_2)(\dot{x}_4 - \acute{x}_4)^*\}], \tag{3.15}$$

then $E_1^t + E_2^t = \mathcal{A}_t + \mathcal{B}_t$ and $G_1^t + G_2^t = \mathcal{A}_t - \mathcal{B}_t$. Hence (3.11) can be rewritten as

$$\mathbf{D}_t^H \mathbf{D}_t = \begin{bmatrix} \mathcal{A}_t + \mathcal{B}_t & 0 & 0 & 0 \\ 0 & \mathcal{A}_t + \mathcal{B}_t & 0 & 0 \\ 0 & 0 & \mathcal{A}_t - \mathcal{B}_t & 0 \\ 0 & 0 & 0 & \mathcal{A}_t - \mathcal{B}_t \end{bmatrix}. \tag{3.16}$$

For parallel paths the minimum length of the error event is T=1. Then for the parallel

path, T=1 error event, $\alpha_1 = \alpha_2 = 0$ and $\beta_1 = \beta_2 = 0$, and we can write

$$\mathcal{A} = \sum_{i=1}^{4} |(\dot{x}_i - \acute{x}_i)|^2 = \sum_{i=1}^{4} |(x_i - \acute{x}_i)|^2 \tag{3.17}$$

$$\begin{aligned}\mathcal{B} = 2Re[e^{j(\phi_1-\phi_2)} \\ \{(x_1 - \acute{x_1})(x_3 - \acute{x_3})^* + (x_2 - \acute{x_2})(x_4 - \acute{x_4})^*\}].\end{aligned} \tag{3.18}$$

3.6.1 4 TS STSTC BPSK - 2 branch trellis

Using Craig's formula [138] for the Gaussian Q function, the moment generating function (MGF) based techniques in [139], and applying the Turin result [140] to evaluate MGF, the worst case PEP for quasi-static Rayleigh fading channel, considering a length T error event and the block diagonal structure of the difference matrix, is given as

$$P(\mathbf{C} \to \acute{\mathbf{C}}) = \frac{1}{\pi} \int_0^{\pi/2} \left\{ \det(\mathbf{I}_{N_t \times S} + \sum_{t=1}^{T} \mathbf{F}_t) \right\}^{-N_r} d\Omega \tag{3.19}$$

where

$$\mathbf{F}_t = \frac{\gamma}{4 \sin^2 \Omega} \mathbf{D}_t^H \mathbf{D}_t \tag{3.20}$$

is a $N_t S \times N_t S$ matrix whose properties depends on the θ and ϕ assigned to the STSTC transmission matrix in (3.9) and $\mathbf{D}_t^H \mathbf{D}_t$ equals (3.16). Let $\mathcal{A}_t + \mathcal{B}_t = \mu_t$ and $\mathcal{A}_t - \mathcal{B}_t = \kappa_t$, then (3.23) can be written as

$$\begin{aligned}P(\mathbf{C} \to \acute{\mathbf{C}}) = \frac{1}{\pi} \int_0^{\pi/2} \left\{ [1 + \frac{\gamma}{4 \sin^2 \Omega} \sum_{i=1}^{T} (\mu_i)]^2 \right\}^{-N_r} \\ \left\{ [1 + \frac{\gamma}{4 \sin^2 \Omega} \sum_{i=1}^{T} (\kappa_i)]^2 \right\}^{-N_r} d\Omega.\end{aligned} \tag{3.21}$$

Hence, for the MRP of the 4 TS 2 branch trellis STSTC shown in Fig. 3.7, with T=3, we have

$$P(\mathbf{C} \to \acute{\mathbf{C}}) = \frac{1}{\pi}\int_0^{\pi/2} \left\{[1 + \frac{\gamma}{4\sin^2\Omega}(\mu_1 + \mu_2 + \mu_3)]^2\right\}^{-N_r} \left\{[1 + \frac{\gamma}{4\sin^2\Omega}(\kappa_1 + \kappa_2 + \kappa_3)]^2\right\}^{-N_r} d\Omega. \tag{3.22}$$

For the MRP, the length of error event for this particular trellis structure is T=3 as shown in Fig. 3.23 and the worst case PEP is given as

$$P(\mathbf{C} \to \acute{\mathbf{C}}) = \frac{1}{\pi}\int_0^{\pi/2} \left\{det(\mathbf{I}_{N_t \times S} + \sum_{t=1}^{T} \mathbf{F}_t)\right\}^{-N_r} d\Omega, \tag{3.23}$$

where

$$\begin{aligned}\mathbf{F}_t &= \frac{\gamma}{4sin^2\Omega}\mathbf{D}_t^H\mathbf{D}_t \\ &= \frac{\gamma}{4sin^2\Omega}\begin{bmatrix} \mathcal{A}_t + \mathcal{B}_t & 0 & 0 & 0 \\ 0 & \mathcal{A}_t + \mathcal{B}_t & 0 & 0 \\ 0 & 0 & \mathcal{A}_t - \mathcal{B}_t & 0 \\ 0 & 0 & 0 & \mathcal{A}_t - \mathcal{B}_t \end{bmatrix}\end{aligned} \tag{3.24}$$

is a $N_tS \times N_tS$ matrix whose properties depends on the θ and ϕ assigned to the STSTC transmission matrix in (3.9) and and $\mathbf{D}_t^H\mathbf{D}_t$ equals (3.16). Let $\mathcal{A}_t + \mathcal{B}_t = \mu_t$ and $\mathcal{A}_t - \mathcal{B}_t = \kappa_t$, then (3.23) can be written as

$$P(\mathbf{C} \to \acute{\mathbf{C}}) = \frac{1}{\pi}\int_0^{\pi/2} \left\{[1 + \frac{\gamma}{4sin^2\Omega}\sum_{i=1}^{T}(\mu_i)]^2\right\}^{-N_r} \left\{[1 + \frac{\gamma}{4sin^2\Omega}\sum_{i=1}^{T}(\kappa_i)]^2\right\}^{-N_r} d\Omega. \tag{3.25}$$

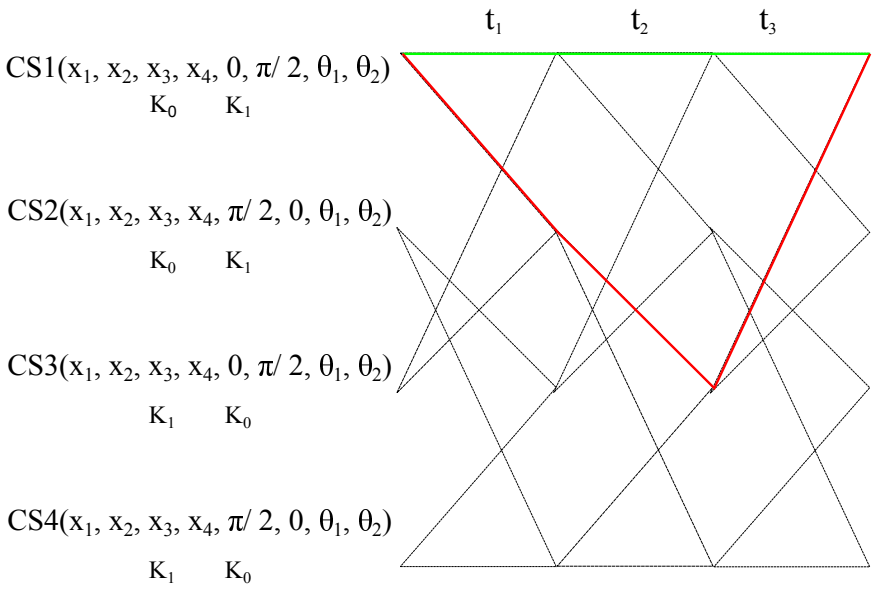

Figure 3.23 A 4 TS STSTC with error event path of T=3.

Hence, for the MRP of the 4 TS 2branch trellis given in Fig. 3.23, with T=3, we have

$$P(\mathbf{C} \to \acute{\mathbf{C}}) = \frac{1}{\pi}\int_0^{\pi/2} \left\{[1+\frac{\gamma}{4sin^2\Omega}(\mu_1+\mu_2+\mu_3)]^2\right\}^{-N_r} \left\{[1+\frac{\gamma}{4sin^2\Omega}(\kappa_1+\kappa_2+\kappa_3)]^2\right\}^{-N_r} d\Omega. \tag{3.26}$$

For the code A given in Table 3.3, consider an error event as shown in Fig. 3.23 in which the correct path for all transitions $t = 1, 2, 3$ is always $\mathbf{X}_t = \{x_1, x_2, x_3, x_4\} = 0000$ from TS_1 to TS_1 and the incorrect path is from TS_1 to TS_2 for $t = 1$, symbols of which are given as $\acute{\mathbf{X}}_1 = \{\acute{x_1}, \acute{x_2}, \acute{x_3}, \acute{x_4}\}$, TS_2 to TS_3 for $t = 2$, symbols of which are given as $\acute{\mathbf{X}}_2 = \{\acute{x_1}, \acute{x_2}, \acute{x_3}, \acute{x_4}\}$ and TS_3 to TS_1 for $t = 3$ symbols of which are given as $\acute{\mathbf{X}}_3 = \{\acute{x_1}, \acute{x_2}, \acute{x_3}, \acute{x_4}\}$. Then for t=1, $\theta_1 = \acute{\theta_1}$, $\theta_2 = \acute{\theta_2}$, $\phi_1 = \acute{\phi_1} = 0$ and $\phi_2 = \acute{\phi_2} = \pi/2$. $\mathbf{X}_1$ belongs to K_0 and $\acute{\mathbf{X}}_1$ belongs to K_1, then according to the set partitioning followed, the worst case would be at most one different symbol in the set of $\{x_1, x_2, x_3, x_4\}$ and $\{\acute{x_1}, \acute{x_2}, \acute{x_3}, \acute{x_4}\}$ for example $\acute{\mathbf{X}}_1 = 0001$. Then from (3.17) and (3.18) $\mathcal{A}_1 = 4$ and $\mathcal{B}_1 = 2Re\{-j(real)\} = 0$ always. Thus for the worst case in code A $\mu_1 = 4, \kappa_1 = 4$. For $t = 2$ in case of code A, $\theta_1 = \acute{\theta_1} = 0$, $\theta_2 = \acute{\theta_2} = 0$, $\phi_1 = \acute{\phi_2} = 0$ and $\phi_2 = \acute{\phi_1} = \pi/2$. $\mathbf{X}_2$ and $\acute{\mathbf{X}}_2$ both belong to K_0, then according to the STSTC structure, the worst case would be

all four different symbols i.e $\acute{\mathbf{X}}_2 = 1111$. Then from (3.17) and (3.18) $\mathcal{A}_2 = 8$ and $\mathcal{B}_2 = 8$ always. Thus for the worst case in code A $\mu_2 = 16, \kappa_2 = 0$ and for $t = 3$, since in the trellis structure given, the codewords for TS_1 and TS_3 are the same. Hence we have $\theta_1 = \acute{\theta_1}$, $\theta_2 = \acute{\theta_2}$, $\phi_1 = \acute{\phi_1} = 0$ and $\phi_2 = \acute{\phi_2} = \pi/2$. $\mathbf{X}_1$ belongs to K_0 and $\acute{\mathbf{X}}_3$ belongs to K_1, then according to the set partitioning employed, the worst case would be at most one different symbol in the set of $\{x_1, x_2, x_3, x_4\}$ and $\{\acute{x_1}, \acute{x_2}, \acute{x_3}, \acute{x_4}\}$ for example $\acute{\mathbf{X}}_3 = 0010$. Then from (3.17) and (3.18) $\mathcal{A}_3 = 4$ and $\mathcal{B}_3 = 2Re\{-j(real)\} = 0$ always and the worst case $\mu_3 = 4, \kappa_3 = 4$. The PEP from (3.26) is given as

$$\begin{aligned} P_A(\mathbf{C} \to \acute{\mathbf{C}}) &= \frac{1}{\pi}\int_0^{\pi/2} \left\{\left[1 + \frac{\gamma}{4sin^2\Omega}(4+16+4)\right]^2\right\}^{-N_r} \\ &\quad \left\{\left[1 + \frac{\gamma}{4sin^2\Omega}(4+0+4)\right]^2\right\}^{-N_r} d\Omega \\ &= \frac{1}{\pi}\int_0^{\pi/2} \left\{\left(\frac{sin^2\Omega + 6\gamma}{sin^2\Omega}\right)\right\}^{-2N_r} \\ &\quad \left\{\left(\frac{sin^2\Omega + 2\gamma}{sin^2\Omega}\right)\right\}^{-2N_r} d\Omega. \end{aligned} \tag{3.27}$$

For the code B given in Table 3.3, consider the same error event as shown in Fig. 3.23 in which the correct path for all transitions $t = 1, 2, 3$ is always $\mathbf{X}_t = \{x_1, x_2, x_3, x_4\} = 0000$ from TS_1 to TS_1 and the incorrect path is from TS_1 to TS_2 for $t = 1$, for which the symbols are given as $\acute{\mathbf{X}}_1 = \{\acute{x_1}, \acute{x_2}, \acute{x_3}, \acute{x_4}\}$, TS_2 to TS_3 for $t = 2$, symbols of which are given as $\acute{\mathbf{X}}_2 = \{\acute{x_1}, \acute{x_2}, \acute{x_3}, \acute{x_4}\}$ and TS_3 to TS_1 for $t = 3$ for which the symbols are given as $\acute{\mathbf{X}}_3 = \{\acute{x_1}, \acute{x_2}, \acute{x_3}, \acute{x_4}\}$. Then for t=1, since both the branches originate from the same state, $\theta_1 = \acute{\theta_1}$, $\theta_2 = \acute{\theta_2}$, $\phi_1 = \acute{\phi_1} = 0$ and $\phi_2 = \acute{\phi_2} = \pi/2$. $\mathbf{X}_1$ belongs to K_0 and $\acute{\mathbf{X}}_1$ belongs to K_1, then according to the set partitioning followed, the worst case would be at most one different symbol in the set of $\{x_1, x_2, x_3, x_4\}$ and $\{\acute{x_1}, \acute{x_2}, \acute{x_3}, \acute{x_4}\}$ for example $\acute{\mathbf{X}}_1 = 0001$. Then from (3.17) and (3.18) $\mathcal{A}_1 = 4$ and $\mathcal{B}_1 = 2Re\{-j(real)\} = 0$ always. Thus for the worst case in code B $\mu_1 = 4, \kappa_1 = 4$. For $t = 2$ in case of code B, $\theta_1 = \acute{\theta_1}$, $\theta_2 \neq \acute{\theta_2}$, $\phi_1 = \acute{\phi_2} = 0$ and $\phi_2 = \acute{\phi_1} = \pi/2$. $\mathbf{X}_2$ and $\acute{\mathbf{X}}_2$ both belong to K_0, then according to the STSTC structure, there are two worst cases possible, first would be all four different

symbols i.e $\acute{\mathbf{X}}_2 = 1111$, in which case, from (3.17) and (3.18) $\mathcal{A}_2 = 4$ and $\mathcal{B}_2 = 4$ always and $\mu_2 = 8, \kappa_2 = 0$. The other worst case would be two similar symbols i.e $\acute{\mathbf{X}}_2 = 0101$, in which case, from (3.17) and (3.18) $\mathcal{A}_2 = 4$ and $\mathcal{B}_2 = -4$ always and $\mu_2 = 0, \kappa_2 = 8$. (Both these cases will end up in same PEP so we will show only the first one). For $t = 3$, since in the trellis structure given, the codewords for TS_1 and TS_3 are same, we have $\theta_1 = \acute{\theta_1}$, $\theta_2 = \acute{\theta_2}$, $\phi_1 = \acute{\phi_1} = 0$ and $\phi_2 = \acute{\phi_2} = \pi/2$. $\mathbf{X}_3$ belongs to K_0 and $\acute{\mathbf{X}}_3$ belongs to K_1, then according to the set partitioning followed, the worst case would be at most one different symbol in the set of $\{x_1, x_2, x_3, x_4\}$ and $\{\acute{x_1}, \acute{x_2}, \acute{x_3}, \acute{x_4}\}$ for example $\acute{\mathbf{X}}_3 = 0010$. Then from (3.17) and (3.18) $\mathcal{A}_3 = 4$ and $\mathcal{B}_3 = 2Re\{-j(real)\} = 0$ always and the worst case $\mu_3 = 4, \kappa_3 = 4$. Then the PEP from (3.26) is given as

$$\begin{aligned} P_B(\mathbf{C} \to \acute{\mathbf{C}}) &= \frac{1}{\pi}\int_0^{\pi/2} \left\{ \left[1 + \frac{\gamma}{4sin^2\Omega}(4+0+4)\right]^2 \right. \\ &\quad \left. \left[1 + \frac{\gamma}{4sin^2\Omega}(4+8+4)\right]^2 \right\}^{-N_r} d\Omega \\ &= \frac{1}{\pi}\int_0^{\pi/2} \left\{ \left(\frac{sin^2\Omega + 2\gamma}{sin^2\Omega}\right) \right. \\ &\quad \left. \left(\frac{sin^2\Omega + 4\gamma}{sin^2\Omega}\right) \right\}^{-2N_r} d\Omega. \end{aligned} \tag{3.28}$$

The closed form for (3.27) and (3.28) can be given using 5A.58 from [141] according to which

$$\begin{aligned} &\frac{1}{\pi}\int_0^{\pi/2} (\frac{\sin^2\theta}{\sin^2\theta + c_1})^{m_1} (\frac{\sin^2\theta}{\sin^2\theta + c_2})^{m_2} \mathrm{d}\theta \\ &= \frac{(c_1/c_2)^{m_2-1}}{2(1-c_1/c_2)^{m_1+m_2-1}} \\ &\left[\sum_{k=0}^{m_2-1} (\frac{c_2}{c_1} - 1)^k B_k I_k(c_2) - \frac{c_1}{c_2} \sum_{k=0}^{m_1-1} (1 - \frac{c_1}{c_2})^k C_k I_k(c_1) \right], \end{aligned} \tag{3.29}$$

where

$$B_k \triangleq \frac{A_k}{\begin{pmatrix} m_1 + m_2 - 1 \\ k \end{pmatrix}} \tag{3.30}$$

$$C_k \triangleq \sum_{n=0}^{m_2-1} \frac{\binom{k}{n}}{\binom{m_1+m_2-1}{n}} A_n \tag{3.31}$$

$$A_k \triangleq (-1)^{m_2-1+k} \frac{\binom{m_2-1}{k}}{(m_2-1)!} \prod_{n=1, n\neq k+1}^{m_2} (m_1+m_2-n) \tag{3.32}$$

$$I_k(c) = 1 - \sqrt{\frac{c}{1+c}} \left[1 + \sum_{n=1}^{k} \frac{(2n-1)!!}{n! 2^n (1+c)^n} \right] \tag{3.33}$$

Then using $c_1 = 2\gamma, c_2 = 6\gamma$ and $m_1 = m_2 = 2N_r$ we can write

$$\begin{aligned} &P_A(\mathbf{C} \to \acute{\mathbf{C}}) = \frac{(2\gamma/6\gamma)^{2N_r-1}}{2(1-2\gamma/6\gamma)^{4N_r-1}} \\ &\left[\sum_{k=0}^{2N_r-1} (\frac{6\gamma}{2\gamma} - 1)^k B_k I_k(6\gamma) - \frac{2\gamma}{6\gamma} \sum_{k=0}^{2N_r-1} (1 - \frac{2\gamma}{6\gamma})^k C_k I_k(2\gamma) \right] \\ &= 3^{2N_r} 2^{-4N_r} \left[\sum_{k=0}^{2N_r-1} 2^k B_k I_k(6\gamma) - \sum_{k=0}^{2N_r-1} (\frac{1}{3})^{k+1} 2^k C_k I_k(2\gamma) \right]. \end{aligned} \tag{3.34}$$

For $N_r = 1$ this simplifies to

$$\begin{aligned} P_A(\mathbf{C} \to \acute{\mathbf{C}}) &= 3^2 2^{-4} \left[\sum_{k=0}^{1} 2^k B_k I_k(6\gamma) - \sum_{k=0}^{1} (\frac{1}{3})^{k+1} 2^k C_k I_k(2\gamma) \right] \\ &= \frac{9}{16}\gamma \left[I_0(6B_0 - \frac{2}{3}C_0) + I_1(12B_1 - \frac{4}{9}C_1) \right]. \end{aligned} \tag{3.35}$$

Similarly, using $c_1 = 2\gamma, c_2 = 4\gamma$ and $m_1 = m_2 = 2N_r$ we can write

$$\begin{aligned} &P_B(\mathbf{C} \to \acute{\mathbf{C}}) = \frac{(2\gamma/4\gamma)^{2N_r-1}}{2(1-2\gamma/4\gamma)^{4N_r-1}} \\ &\left[\sum_{k=0}^{2N_r-1} (\frac{4\gamma}{2\gamma} - 1)^k B_k I_k(4\gamma) - \frac{2\gamma}{4\gamma} \sum_{k=0}^{2N_r-1} (1 - \frac{2\gamma}{4\gamma})^k C_k I_k(2\gamma) \right] \\ &= 2^{2N_r-1} \left[\sum_{k=0}^{2N_r-1} B_k I_k(4\gamma) - \sum_{k=0}^{2N_r-1} (\frac{1}{2})^{k+1} C_k I_k(2\gamma) \right]. \end{aligned} \tag{3.36}$$

For $N_r = 1$ this simplifies to

$$P_B(\mathbf{C} \rightarrow \acute{\mathbf{C}}) = \gamma \left[I_0(8B_0 - 2C_0) + I_1(8B_1 - C_1) \right], \tag{3.37}$$

where

$$B_k \triangleq \frac{A_k}{\begin{pmatrix} 4N_r - 1 \\ k \end{pmatrix}} \tag{3.38}$$

$$C_k \triangleq \sum_{n=0}^{2N_r-1} \frac{\begin{pmatrix} k \\ n \end{pmatrix}}{\begin{pmatrix} 4N_r - 1 \\ n \end{pmatrix}} A_n \tag{3.39}$$

$$A_k \triangleq (-1)^{2N_r-1+k} \frac{\begin{pmatrix} 2N_r - 1 \\ k \end{pmatrix}}{(2N_r - 1)!} \prod_{n=1, n \neq k+1}^{2N_r} (4N_r - n). \tag{3.40}$$

For the code C given in Table 3.3, consider an error event as shown in Fig. 3.24 in which the correct path for all transitions $t = 1, 2, 3$ is $\mathbf{X}_t = \{x_1, x_2, x_3, x_4\} = 0000$ from TS_1 to TS_1 and the incorrect path is from TS_1 to TS_2 for $t = 1$, symbols of which are given as $\acute{\mathbf{X}}_1 = \{\acute{x_1}, \acute{x_2}, \acute{x_3}, \acute{x_4}\}$, TS_2 to TS_3 for $t = 2$, symbols of which are given as $\acute{\mathbf{X}}_2 = \{\acute{x_1}, \acute{x_2}, \acute{x_3}, \acute{x_4}\}$ and TS_3 to TS_1 for $t = 3$ symbols of which are given as $\acute{\mathbf{X}}_3 = \{\acute{x_1}, \acute{x_2}, \acute{x_3}, \acute{x_4}\}$. Then for t=1, $\theta_1 = \acute{\theta_1}$, $\theta_2 = \acute{\theta_2}$, $\phi_1 = \acute{\phi_1} = 0$ and $\phi_2 = \acute{\phi_2} = \pi/2$. $\mathbf{X}_1$ belongs to K_0 and $\acute{\mathbf{X}}_1$ belongs to K_1, then according to the set partitioning followed, the worst case would be at most one different symbol in the set of $\{x_1, x_2, x_3, x_4\}$ and $\{\acute{x_1}, \acute{x_2}, \acute{x_3}, \acute{x_4}\}$ for example $\acute{\mathbf{X}}_1 = 0001$. Then from (3.17) and (3.18) $\mathcal{A} = 4$ and $\mathcal{B} = 2Re\{-j(real)\} = 0$. Thus for the worst case in code C $\mu_1 = 4, \kappa_1 = 4$. For $t = 2$ in case of code C, $\theta_1 = \theta_2 = 0$, $\acute{\theta_1} = \acute{\theta_2} = \pi$, $\phi_1 = \acute{\phi_2} = 0$ and $\phi_2 = \acute{\phi_1} = \pi/2$. $\mathbf{X}_2$ and $\acute{\mathbf{X}}_2$ both belong to K_0, then according to the STSTC structure, the worst case would be all four different symbols i.e $\acute{\mathbf{X}}_2 = 1111$. Then from (3.17) and (3.18) $\mathcal{A} = 0$ and $\mathcal{B}$ is always equal to 0. Thus for the worst case in code

C $\mu_2 = 0, \kappa_2 = 0$. For $t = 3$, since in the trellis structure given, the codewords for TS_1 and TS_3 are same, we have $\theta_1 = \acute{\theta_1}$, $\theta_2 = \acute{\theta_2}$, $\phi_1 = \acute{\phi_1} = 0$ and $\phi_2 = \acute{\phi_2} = \pi/2$. $\mathbf{X}_3$ belongs to K_0 and $\acute{\mathbf{X}}_3$ belongs to K_1, then according to the set partitioning followed, the worst case would be at most one symbol different in the set of $\{x_1, x_2, x_3, x_4\}$ and $\{\acute{x_1}, \acute{x_2}, \acute{x_3}, \acute{x_4}\}$ for example $\acute{\mathbf{X}}_3 = 0010$. Then from (3.17) and (3.18) $\mathcal{A} = 4$ and $\mathcal{B} = 2Re\{-j(real)\} = 0$ always and the worst case $\mu_3 = 4, \kappa_3 = 4$. The PEP from (3.26) is given as

$$\begin{aligned} P_C(\mathbf{C} \to \acute{\mathbf{C}}) &= \frac{1}{\pi} \int_0^{\pi/2} \left\{ [1 + \frac{\gamma}{4sin^2\Omega}(4 + 0 + 4)]^4 \right\}^{-N_r} d\Omega \\ &= \frac{1}{\pi} \int_0^{\pi/2} \left\{ \left(\frac{sin^2\Omega + 2\gamma}{sin^2\Omega} \right)^2 \right\}^{-2N_r} d\Omega. \end{aligned} \tag{3.41}$$

For the error events of T=1, i.e parallel paths, in the code A, B and C, PEP is identical since they follow the same set partitioning. Also, since they all originate from the same TS, $\theta_1 = \acute{\theta_1}$ and $\theta_2 = \acute{\theta_2}$ always. For TS_1 $\phi_1 = \acute{\phi_1} = 0$ and $\phi_2 = \acute{\phi_2} = \pi/2$. According to the set partitioning in the parallel paths, the worst case would be at least two different symbols in the set of $\{x_1, x_2, x_3, x_4\}$ and $\{\acute{x_1}, \acute{x_2}, \acute{x_3}, \acute{x_4}\}$. From (3.17) and (3.18) $\mathcal{A} = 8$ and $\mathcal{B} = 2Re\{-j(realvalue)\} = 0$. Thus, the worst case $\mu_3 = 8, \kappa_3 = 8$ The same results would be obtained for parallel paths in other branches merging into TS_2, TS_3, TS_4, where TS_n represents the n^{th} TS. The worst case PEP for parallel paths is thus given as

$$\begin{aligned} P(\mathbf{C} \to \acute{\mathbf{C}}) &= \frac{1}{\pi} \int_0^{\pi/2} \left\{ [1 + \frac{\gamma}{4sin^2\Omega}(8)]^4 \right\}^{-N_r} d\Omega \\ &= \frac{1}{\pi} \int_0^{\pi/2} \left\{ \left(\frac{sin^2\Omega + 2\gamma}{sin^2\Omega} \right)^4 \right\}^{-N_r} d\Omega \\ &= \frac{1}{\pi} \int_0^{\pi/2} \left\{ \left(\frac{sin^2\Omega}{sin^2\Omega + 2\gamma} \right)^4 \right\}^{N_r} d\Omega, \end{aligned} \tag{3.42}$$

which is also the same as that of the 2TS code. All the above PEP clearly shows a full diversity of $4N_r = N_t S R N_r$ (recall $S = 2, R = 1, N_t = 2$). The closed form of the above

can be given by using 5A.4a from [30], according to which

$$\frac{1}{\pi}\int_0^{\pi/2}\left\{\left(\frac{sin^2\theta}{sin^2\theta+c}\right)\right\}^m d\theta$$
$$=\frac{1}{2}\left[1-\mu(c)\sum_{k=0}^{m-1}\binom{2k}{k}\left(\frac{1-\mu^2(c)}{4}\right)^k\right], \tag{3.43}$$

where

$$\mu(c)\triangleq\sqrt{\frac{c}{c+1}}. \tag{3.44}$$

Then using $c=2\gamma$ and $m=4N_r$ in (3.44) we can have

$$P(\mathbf{C}\rightarrow\acute{\mathbf{C}})=\frac{1}{2}\left[1-\sqrt{\frac{2\gamma}{1+2\gamma}}\sum_{k=0}^{4N_r-1}\binom{2k}{k}\left(\frac{1}{4(1+2\gamma)}\right)^k\right] \tag{3.45}$$

The results from (3.27), (3.28), (3.41) and (3.42) follow in Section 3.7 and Fig. 3.24.

3.7 SIMULATION RESULTS FOR PEP ANALYSIS OF STSTCS

The results from the PEP analysis in Section 3.6 are shown in Fig. 3.24 for 4 TS STSTCs using BPSK and two transmit antennas. All plots are based on considering the MRP error event = 3. It is obvious that PEP for parallel paths is the same for all STSTC A, B and C as expected because they have the same set partitioning. It can also be seen that the result from (3.27) for PEP STSTC A has the best PEP which also gives the best FER in Fig. 3.17.

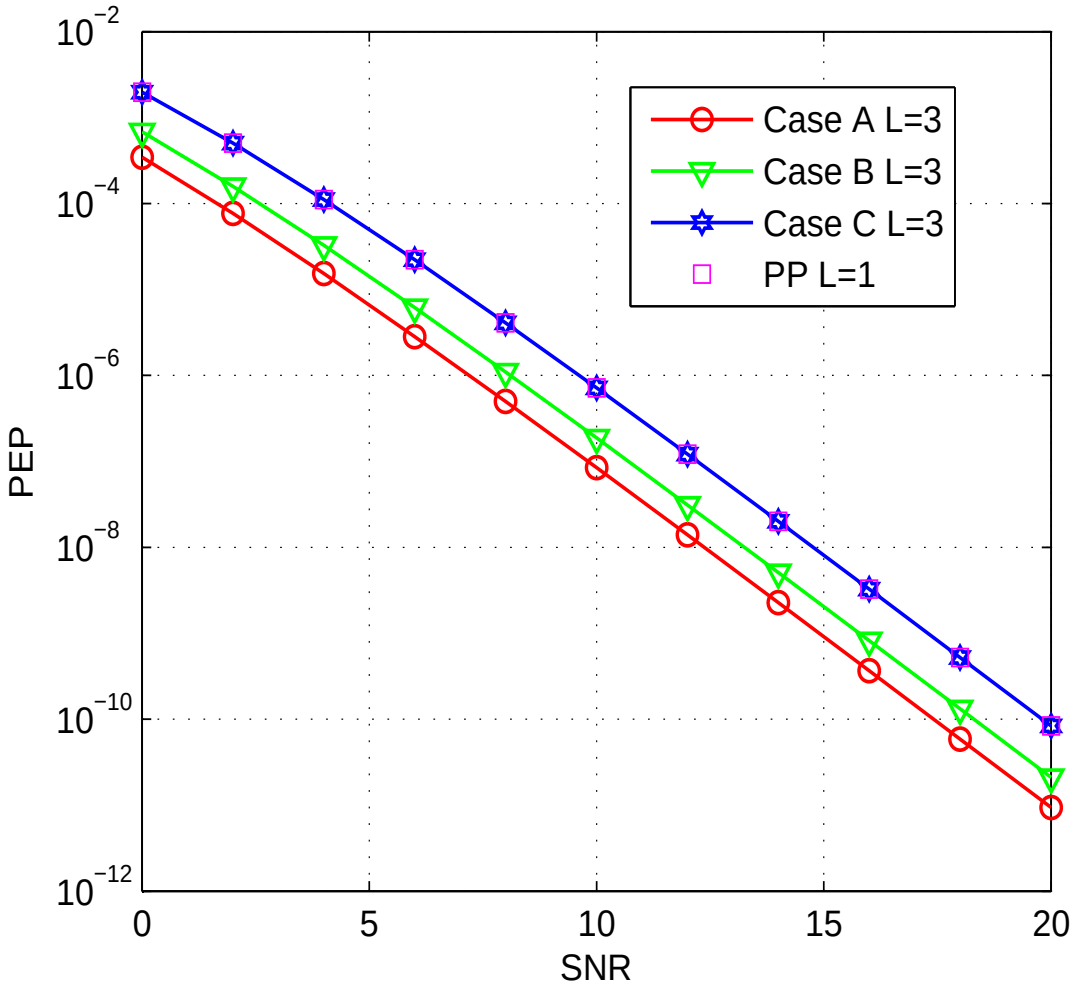

Figure 3.24 Analytical PEP of PP and MRP for 4 TS 2 branch STSTCs given in Fig. 3.8 and Table 3.3 for r=1 bit/s/Hz using BPSK for two transmit antennas.

3.8 CONCLUSION

In this chapter, the concept of concatenating Block Diagonal QOSTBC in a space time trellis is given to achieve full diversity in a reconfigurable antenna system. A novel STSTC with full rate, full diversity and high coding gain is proposed for reconfigurable transmit antenna system for $r = 1$ bits/s/Hz using BPSK and $r = 2$ bits/s/Hz using QPSK. Simulation results confirm that the proposed code offers good performance in a reconfigurable antenna system with more than one channel propagation state. Various four state STSTCs are given using different trellis structures with two and four branches.

It has been shown using the PEP analysis that min CGD is not a sufficient criteria for code design. Further gains can be achieved by selecting a code with maximum min CGD MRP The validity of this criteria is also shown by the FER performance curves. The codes with the higher min CGD MRP inspite of same CGDPP perform better. This criteria is equally valid for BPSK and QPSK and is proved using 4 TS 2 branch trellis structure.

For the 4 TS four branch trellis STSTCs with $r = 1$ bits/s/Hz BPSK, performance factor, CGD MRP criteria are used to select the best codes, which is much simpler and quicker than the complete distance spectrum. These criteria are valid only when the rank of the difference matrix for partial valid path is non zero.

Chapter 4

SELECTION AND SWITCHING

4.1 INTRODUCTION

This chapter is focused on the application of our proposed STSTCs, with various switching and selection techniques presented, on a fully reconfigurable open loop and closed loop MIMO communication system. The purpose of this chapter is to explore whether the proposed STSTCs provide benefits in both open loop and closed loop systems. A comparative assessment of diversity and SNR gains are presented and discussed for different scenarios. We use the system model described in Section 3.2 and different cases considered are summarized in Table 4.1.

4.2 FULLY RECONFIGURABLE MIMO

4.2.1 Antenna State Switching

First we consider antenna switching at the transmitter and receiver in a fixed pattern. We refer to the case of antenna switching in Chapter 3 as Case X, in which both transmit antennas switch state in a fixed pattern every two time slots simultaneously and the receiver has a fixed state and is non reconfigurable $R = 1$. We now introduce Case B in which both transmit antennas switch state at the same time and the receive antenna is reconfigurable and also switches its state every two time slots.

4.2.2 Antenna State Selection

Now we consider selecting the antenna state rather than only switching it in a predefined pattern. This allows us to achieve significant SNR gains. For each case the antenna state selection is made at the start of each 132 symbols transmission and is fixed for the entire frame. The selection is made on the basis of the channel matrix with maximum power. Here we have considered four cases in an open and closed loop systems

Case A: Both the transmit antennas change state at the same time and after two time slots in a fixed pattern, giving two possible transmitter states $S = 2$ and the receiver selects between its two states. This gives two possible channel matrices to select from for time 1 and time 2, and another two possible channel matrices to select from for time 3 and time 4. Thus giving a total of 4 channel propagation states to choose from.

Case AU: This selection criteria gives 8 possible channel matrices to select from for time 1 and time 2 and then again 7 for time 3 and time 4. Thus giving a total of 56 possible channel propagation states for one code word.

Case AUU: Both the transmit antennas and the receiver can change their states independently, giving four possible transmitter states, and the receiver can also change state independently, thus giving a total of eight channel matrices.However, the sub channels used to transmit in time 1 and time 2 cannot be repeated for time 3 and time 4. Thus this selection criteria gives 8 possible channel matrices to select from for time 1 and time 2, and then 5 possible channel matrices to select from for time 3 and time 4, thus giving a total of 40 possible channel propagation states for one code word.

Case AUUU: Now we give a case of reconfigurable transmit antennas without state switching within the STSTC at the transmitter. This selection criteria gives 8 possible channel matrices to select from for time 1 and time 2 and then again 8 for time 3 and time 4. Thus giving a total of 64 possible channel propagation states for one code word. Since selection is based on maximum power, it is similar to no switching case as after two time slots same channel matrix will again be selected as all eight are again available.

Table 4.1 Different cases of selection and switching in a fully reconfigurable MIMO system using STSTCs. (D refers to the comparitive diversity).

CASE	N_t	N_r	S	R	Selection at Rx	Switching at Tx	Switching at Rx	D
X	2	1	2	1	*no*	*yes*	*no*	4
B	2	1	2	2	no	yes	yes	4
A	2	1	2	2	yes	yes	no	8
AU	2	1	2	2	yes	yes	no	8
AUU	2	1	2	2	yes	yes	no	8
AUUU	2	1	2	2	yes	no	no	8
U	2	2	2	1	no	yes	no	8

The result for case AUUU comes out to be the same as if state selection is used at the receiver without state switching within the code word after every two time slots. That is the transmitters and the receiver use the best state to transmit and receive respectively for all 4 time slots in a codeword and it remains constant for the whole frame. The transmitter and the receiver states are fixed at the beginning of each frame based on maximum power of the channel matrix.

Diversity analysis of reconfigurable MIMO: The results show that if selection gain is very high it overcomes the loss due to diversity (because there is no switching within the STSTC codeword, so effectively there are only 2 sub channels instead of 4 available for 4 information symbols (x_1, x_2, x_3, x_4)).

Relationship of selection gain with diversity: If no selection is used at the receiver we do not get the full diversity offered by a reconfigurable antenna system. If selection is used at the receiver, and the two best sub-channels are allowed to transmit for all 4 time slots, we get full diversity along with the gain in SNR.

4.3 SIMULATION RESULTS FOR STSTCS IN A FULLY RECONFIGURABLE MIMO SYSTEM

We present simulation results for a fully reconfigurable MIMO/ MISO system with $N_t = 2, S = 2$ and $N_r = 1, R = 2$. Proposed STSTCs with 2TS given in Chapter 3 and rate r=2 bits/s/Hz using QPSK is considered for all simulations. Now we consider the switching cases, B and X. Fig. 4.1 shows the performance of case B for r=2 bits/s/Hz using QPSK in a reconfigurable transmit and receive antenna MIMO system. For comparison reconfigurable transmit and non reconfigurable receive antenna Case X is also shown in the same figure. It is obvious that there is no performance improvement from receive antenna state switching in Case B. It can be seen from Fig. 4.1 that the performance curves of case B with reconfigurable receive antenna and switching only and of case X with non reconfigurable receive antenna, overlap. Thus there is no additional gain observed with reconfigurable receive antenna using switching only.

Now lets see if selection can provide the gains, switching alone cannot. The performance of Case A with $N_t = 2, N_r = 1, S = 2$ and $R = 2$ is also shown in Fig. 4.1 which shows an improvement of about 5 dB at a FER of 10^{-3} over Case B with $N_t = 2, N_r = 1, S = 2$ and $R = 2$, when antenna state selection is used at the receiver along with switching in an open loop reconfigurable MIMO system. The performance of Case A is also compared with the STSTC using $N_t = 2, N_r = 2, S = 2$ and $R = 1$ (non reconfigurable receive antennas), Case U in Fig. 4.1. Note that both the curves follow the same slope and have same diversity of 8.

Simulation results for Case AU, Case AUU and Case A are presented in Fig. 4.2. Case AU outperforms case AUU and Case A for all SNRs. It can be seen from Fig. 4.2 that all the cases using the proposed STSTCs with antenna state switching along with antenna state selection at the receiver achieve full diversity. It can be noted that the slopes of all the cases using antenna state selection in Fig. 4.2 are equal to that of the performance results of STSTCs without antenna state selection, with $N_t = 2, N_r = 2, S = 2$ and non

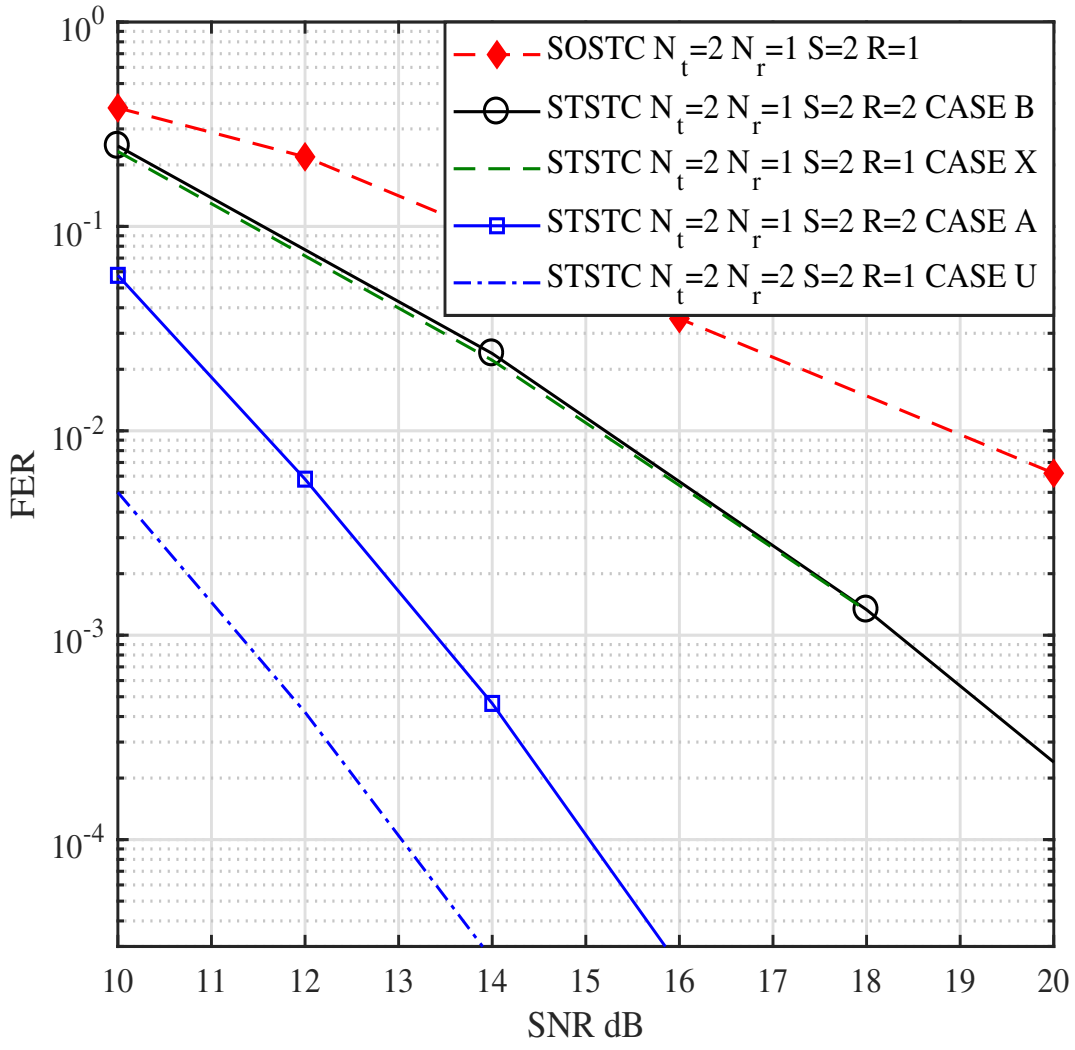

Figure 4.1 Performance of reconfigurable transmit/receive MIMO system with and without selection for $r = 2$ bits/s/Hz using QPSK and 2TS STSTC.

reconfigurable receive antenna, Case U. This has been added here to demonstrate the standard diversity 8 slope for comparision purpose. At a FER of 10^{-3} Case AU is 0.7 dB better than Case AUU and 1.4 dB better than Case A. Also the performance of Case AU is only 0.6 dB away from the case of $N_t = 2$ $S = 2$ and $N_r = 2$ non reconfigurable receive antennas.

Next we present the result of reconfigurable transmit antennas without state switching within the STSTC at the transmitter (Case AUUU). In Fig. 4.2 it can be seen that at

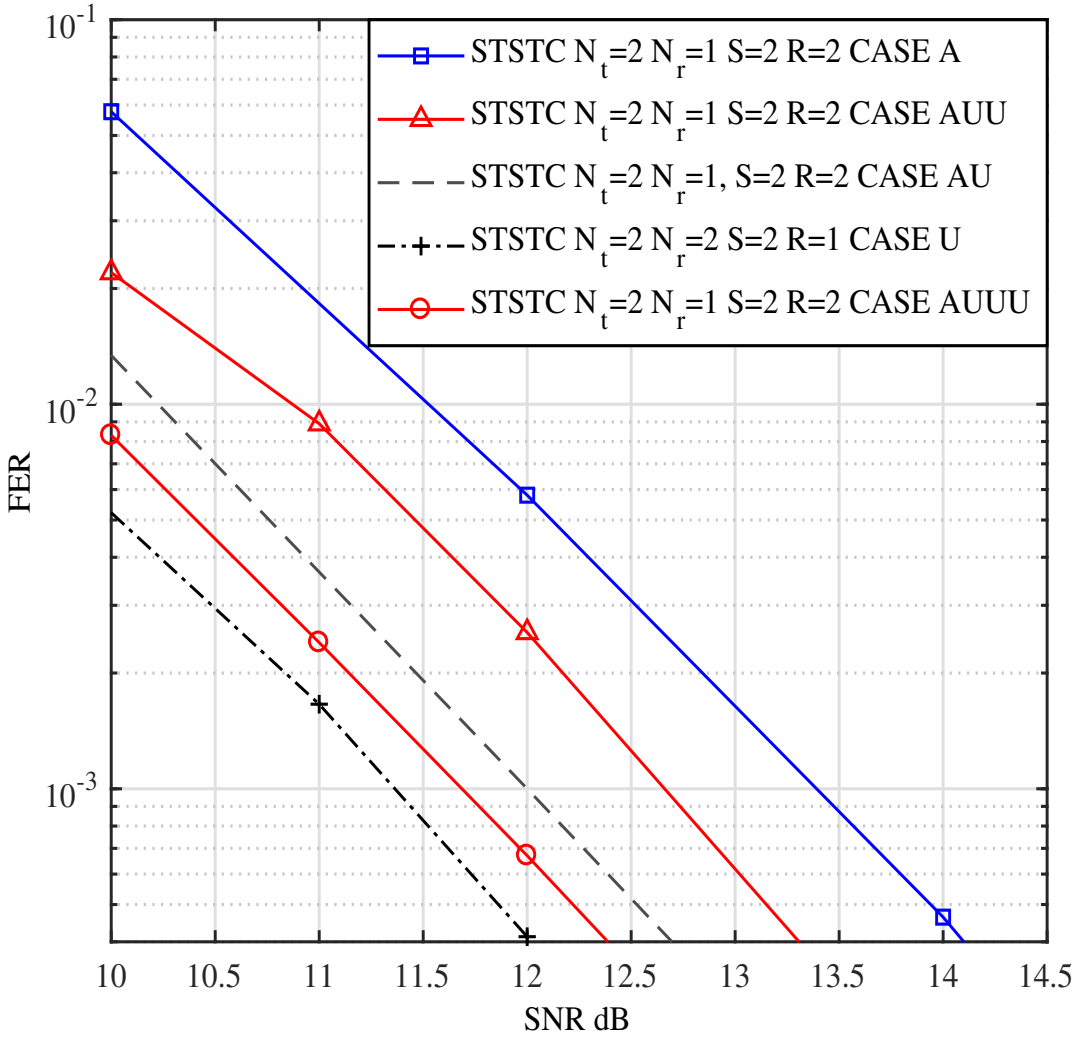

Figure 4.2 Performance of reconfigurable transmit/receive MIMO system with various selection cases for r=2 bits/s/Hz using QPSK and 2TS STSTC.

FER 10^{-3} it is about 0.2 dB better than Case AU at all SNR and about 0.4 dB away from the case of $N_t = 2$, $S = 2$ and $N_r = 2$ non reconfigurable receive antennas and with equal diversity of 8 from comparative analysis.

Case AUUU performs best. The selection gain is so high that it overcomes the loss due to diversity. So Case AUUU in terms of diversity is effectively a $N_t = 2$, $N_r = 1$ system with $S = 1$ and $R = 4$. And with the proposed selection scheme gives full diversity of 8.

4.4 CONCLUSION

Various antenna state switching and selection schemes are considered for open loop and closed loop fully reconfigurable transmit/ receive MIMO system. It is shown that the diversity increase due to a reconfigurable receive antenna states is only possible if selection is used at the receiver. It is also interesting to note that if one of the state is optimally selected we get full diversity even if the other selected state is not optimal or with maximum energy. Also we get full diversity if the state selection is used with no switching within the codeword (Case AUUU). From this analysis it is also concluded that the proposed STSTC is only suitable for an open loop system where the transmitter does not know the channel and the transmit antennas switch states in a predefined pattern to provide full diversity. For a fully reconfigurable open loop MIMO system selection at the receiver along with preset switching at the transmitter adds selection gain along with full diversity. However, it has been observed that in case of closed loop reconfigurable transmit/receive MIMO, where the feedback for the best transmitter state is possible after selection processing at the receiver, keeping the transmitter state switched to a best state and fixed for the entire frame while using selection at the receiver provides higher SNR gain.

Chapter 5

RECONFIGURABLE ANTENNA CODEBOOK FEEDBACK

5.1 INTRODUCTION AND BACKGROUND

Reconfigurable antennas [3, 4, 142] are attractive due to their ability to change radiation pattern, frequency of operation or polarization. This allows the propagation channel to be altered deliberately and dynamically, so that diverse channel conditions can be experienced. Diversity gains in a MIMO/MISO system can be obtained by using space time codes or through intuitive use of channel state information (CSI) at the transmitter employing transmit beamforming. The trade-off between the amount of feedback and performance has been researched extensively [24], [25]. The performance of a quantized beamforming system is naturally impacted by the size of the codebook. The codebook size is also associated with the diversity of the system [10]. It has been shown in [10] that in order to achieve full diversity the codebook size (N_C) should be greater than or equal to the number of transmit antennas. We have shown through simulations that full diversity is still achievable with smaller size codebook (hence less number of feed back bits) as long as the product $N_C S$ is equal to or greater than the number of transmit antennas. Codebook transmit beamforming is now a part of LTE standards [26] and is of great interest in next generation systems due to its well researched benefits [25]. It is desirable to choose N_C large to obtain a good approximation of the channel. On the other hand, minimizing the number of feedback bits motivates choosing a small N_C.

Hence, we propose a limited feedback precoding system employing reconfigurable receive

antennas. The reconfigurable antenna codebook feedback system proposed aims to achieve the performance of large N_C with the benefits of small N_C, i.e fewer feedback bits. We assume that the receiver has correct channel state information (CSI), but instead of feeding back the entire CSI to the transmitter, it compares the normalized reconfigurable channel with the entries in a codebook and feeds back just the index of the nearest codebook entry. With limited codebook cardinality, it is impossible to find a codebook entry at zero distance from the corresponding channel values and a loss is incurred [27]. Increasing the number of possible channel conditions instead of increasing the codebook size and hence the number of feedback bits, is the basis of our underlying approach towards minimizing the loss due to codebook mismatch. Increasing the number of possible channel conditions while having limited codebook cardinality, gives new degrees of freedom, such as reduced codebook or quantization loss and overall improvement in SNR due to increased channel power if the channel states are carefully selected. The optimal approach (OA) proposed here maximizes both the channel power and the direction by carefully selecting the channel state and the codeword. We also consider two more selection approaches called Channel Direction (CD) and Channel Power (CP), to investigate the source of the gains achieved in OA.

The chapter is organized as follows. First we introduce the reconfigurable antenna codebook feedback MISO system and give the three codebook selection techniques. Later we extend it to reconfigurable antenna MIMO limited feedback precoding system and give the basics of the receiver structures used along with the codeword and reconfiguarble antenna selection techniques. Next we give the analytical forms of the expected SNRs for the selection approaches. Simulation results follow for both the reconfigurable antenna codebook feedback MISO with perfect and imperfect CSI, and the reconfigurable antenna codebook feedback MIMO systems. Finally conclusions are drawn.

5.2 SYSTEM MODEL

First we consider a single user MISO feedback system employing single stream transmission using fixed LTE [26], Grassmanian [10] and Random Vector Quantization (RVQ) codebooks [143]. We then consider a single user MIMO feedback system employing single or multiple stream transmission using fixed LTE [26] and Grassmannian [10] codebooks, with different receiver types. The receiver and transmitter share a common codebook and an error free, zero delay feedback link is assumed. CSI information input to codebook selection is perfect.

5.2.1 Reconfigurable MISO Codebook Feedback System Model

Let there be N_t transmit antennas in a $1 \times N_t$ MISO system, where the receive antenna is equipped with a RA that has S uncorrelated channel propagation states (CPSs). This results in S possible channel vectors. The channel vector corresponding to the s^{th} CPS is defined as

$$\mathbf{H}_s = \begin{bmatrix} h_1^s & h_2^s & \cdots & h_{N_t}^s \end{bmatrix}, \tag{5.1}$$

where h_k^s denotes the channel coefficient between the k^{th} transmit and the receive antenna. The overall set of possible channel vectors can be given as $\{\mathbf{H}_1, \mathbf{H}_2, ..., \mathbf{H}_S\}$, where each $\mathbf{H}_s$ is independent. For each transmission, the CPS, s, and hence $\mathbf{H}_s$ is chosen based on the selection techniques discussed later. We assume a frequency flat quasi-static Rayleigh fading channel, where each $h_k^s \sim \mathcal{CN}(0,1)$. First we assume perfect CSI at the receiver. $\mathbf{H}_s = \sqrt{\Lambda_s}\mathbf{v}_s^\dagger$, where $\Lambda_s = \sum_{k=1}^{N_t} |h_k^s|^2$ is the instantaneous channel power, $\mathbf{v}_s^\dagger = \begin{bmatrix} h_1^s & h_2^s & \cdots & h_{N_t}^s \end{bmatrix} / \sqrt{\sum_{k=1}^{N_t} |h_k^s|^2}$ is a row vector representing the normalized channel direction and † denotes the Hermitian transpose. The transmitter encodes the data, d, by a precoding matrix, $\mathbf{C}_p$, which is selected from a codebook, given by $\mathbb{CB}= \{\mathbf{C}_1, \mathbf{C}_2, ..., \mathbf{C}_{N_C}\}$, such that $\mathbf{C}_p^\dagger \mathbf{C}_p = 1$ and each codeword is a $N_t \times 1$ vector. p is the index of the precoding matrix in the codebook. The system input output relationship

can be modelled as

$$r = \mathbf{H}_s \mathbf{C}_p d + n, \tag{5.2}$$

where r is the received scalar signal, $\mathbf{C}_p d$ is the $N_t \times 1$ transmitted signal and n is an i.i.d. $\mathcal{CN}(0, \sigma^2)$ noise term. The codeword index, p, identifying the desired beamforming vector is conveyed from the receiver to the transmitter using $\log_2 N_C$ feedback bits. We assume a total transmit power, $P_t = \mathbf{E}[|d|^2]$, and the noise power is $\mathbf{E}[|n|^2] = \sigma^2$, where $\mathbf{E}[.]$ denotes expectation. Also, we define the mean transmit signal power to mean receive noise power or mean transmit power, $\gamma = \mathbf{E}[|d|^2]/\sigma^2$. Then, the received signal to noise ratio (SNR) is given by

$$\Gamma_{p,s} = \Lambda_s |\mathbf{v}_s^\dagger \mathbf{C}_p|^2 \gamma. \tag{5.3}$$

In (5.3), each state of the receive antenna, s, gives a different channel power, X_s, where $X_s = \Lambda_s$, and we see there is no ceiling on performance as $\Gamma_{p,s}$ increases with γ. However, there is an SNR loss factor due to codebook mismatch given as $Y_{p,s} = |\mathbf{v}_s^\dagger \mathbf{C}_p|^2$. Then, (5.3) can be written as

$$\Gamma_{p,s} = X_s \, Y_{p,s} \gamma. \tag{5.4}$$

For the perfect feedback (PFB) case, the loss factor $Y_{p,s} = 1$, whereas for a codebook feedback system $Y_{p,s} < 1$. The system rate is given as

$$\mathcal{R} = \log_2 \left(1 + \Gamma_{p,s}\right). \tag{5.5}$$

The imperfect CSI is modeled as [144]

$$\hat{h}_k^s = \eta h_k^s + \sqrt{1 - \eta^2}\epsilon, \tag{5.6}$$

where $\hat{h}_k^s$ is imperfect CSI, ϵ is an independent zero mean complex Gaussian variable with variance 0.5 per dimension and η is the correlation between $\hat{h}_k^s$ and h_k^s.

5.2.2 Codeword and State Selection Methods for RA MISO System

5.2.2.1 Maximizing Channel Direction (CD)

This approach uses the channel with the best direction. In this approach, the direction is maximized over all CPSs and codewords $\mathbf{C}_p$. The index of the best codeword, p^*, is fed back to the transmitter, and the receiver is set to CPS = s^*, where

$$(p^*, s^*) = \underset{\substack{p\in\{1,2,..,N_C\}\\ s\in\{1,2,..,S\}}}{\arg\max} \left\{ |\mathbf{v}_s^\dagger \mathbf{C}_p|^2 \right\}. \tag{5.7}$$

5.2.2.2 Maximizing Channel Power (CP)

This approach maximizes the channel power resulting in channel $\mathbf{H}_{s^*}$ being used for transmission, where

$$s^* = \underset{s\in\{1,2,..,S\}}{\arg\max} \left\{ \|\mathbf{H}_s\|^2 \right\}. \tag{5.8}$$

Given s^*, the best codeword, $\mathbf{C}_{p^*}$, is selected based on the best SNR such that

$$p^* = \underset{p\in\{1,2,..,N_C\}}{\arg\max} \{\Gamma_{p,s^*}\} = \underset{p\in\{1,2,..,N_C\}}{\arg\max} \left\{ X_{s^*} |\mathbf{v}_{s^*}^\dagger \mathbf{C}_p|^2 \right\}. \tag{5.9}$$

This approach maximizes channel power over all CPS and then uses the best codeword index for that CPS.

5.2.2.3 Optimum Approach (OA)

In the OA approach, the codeword, $\mathbf{C}_p$, and CPS are selected such that the codeword index $p = p^*$ and CPS $s = s^*$ satisfy

$$(p^*, s^*) = \underset{\substack{p\in\{1,2,..,N_C\}\\ s\in\{1,2,..,S\}}}{\arg\max} \{\Gamma_{p,s}\}. \tag{5.10}$$

This approach simultaneously maximizes both X_s and $Y_{p,s}$ over all codewords and CPSs.

5.2.3 Reconfigurable MIMO Codebook Feedback System Model

We consider a MIMO system with N_t transmit and N_r receive antennas. Each receive antenna is a reconfigurable antenna (RA) that has R uncorrelated states. This results in $S = R^{N_r}$ possible new channel matrices, where each possible channel matrix is denoted as a channel propagation state (CPS). The channel matrix for the s^{th} CPS is defined as

$$\mathbf{H}_s = \begin{bmatrix} h^s_{11} & \cdots & h^s_{1N_t} \\ \vdots & \ddots & \vdots \\ h^s_{N_r1} & \cdots & h^s_{N_rN_t} \end{bmatrix}, \tag{5.11}$$

where h^s_{kl} denotes the channel coefficient between the k^{th} receive and l^{th} transmit antenna. The set of possible channel matrices $\{\mathbf{H}_1, \mathbf{H}_2, ..., \mathbf{H}_S\}$ consists of both dependent and independent channel matrices. For each transmission, the CPS, s, and hence $\mathbf{H}_s$ is chosen based on the selection techniques.

A frequency flat quasi-static Rayleigh fading channel is considered, where each h^s_{kl} is a zero mean complex Gaussian random variable having a variance of 1. We assume perfect CSI at the receiver. The singular value decomposition (SVD) of $\mathbf{H}_s$ gives $\mathbf{H}_s = \mathbf{U}_s\mathbf{D}_s\mathbf{V}^\dagger_s$, where $\mathbf{U}_s \in \mathbb{C}^{N_r \times N_t}$ and $\mathbf{V}_s \in \mathbb{C}^{N_t \times N_t}$ are unitary and $\mathbf{D}_s$ is a diagonal matrix containing the min (N_r, N_t) singular values of $\mathbf{H}_s$ denoted by $\delta_1 \geq \delta_2 \geq ... \ \delta_{min(N_r,N_t)}$ and $\lambda_i = \delta^2_i$ for $(i = 1, 2, ..., min(N_r, N_t))$ are the eigenvalues of $\mathbf{H}^\dagger_s\mathbf{H}_s$, where † denotes the Hermitian transpose.

The system input output relationship can be modeled as

$$\mathbf{r} = \mathbf{H}_s\mathbf{x}_t + \mathbf{n}, \tag{5.12}$$

where $\mathbf{r}$ is the $N_r \times 1$ received signal vector, $\mathbf{x}_t$ is the $N_t \times 1$ transmitted signal and $\mathbf{n}$

is a $N_r \times 1$ vector comprising of i.i.d. $\mathcal{CN}(0, \sigma^2)$ noise terms. The transmitter encodes the modulated data sequence, $\mathbf{d}$, by a precoding matrix, $\mathbf{C}_p$, which is selected from a codebook given by $\mathbb{CB}= [\mathbf{C}_1, \mathbf{C}_2, ..., \mathbf{C}_{N_C}]$ such that $\mathbf{C}_p^\dagger \mathbf{C}_p = \mathbf{I}_L$, where L represents the number of transmission streams, and each codeword $\mathbf{C}_p$ in $\mathbb{C}$ is a quantized version of the first L columns of $\mathbf{V}_s$. Then, the codewords are used to precode the $L \times 1$ data vector, $\mathbf{d}$, so that $\mathbf{x}_t = \mathbf{C}_p\mathbf{d}$ and (5.12) becomes

$$\mathbf{r} = \mathbf{H}_s\mathbf{C}_p\mathbf{d} + \mathbf{n}. \tag{5.13}$$

The codeword index, $p \in \{1, 2, ..., N_C\}$, is conveyed from the receiver to the transmitter using $\log_2 N_C$ bits of feedback. We assume a total transmit power, $P_t = \mathbf{E}[\mathbf{d}^\dagger\mathbf{d}] = \mathbf{E}[\mathbf{x}_t^\dagger\mathbf{x}_t] = 1$ such that $\mathbf{E}[|d_i|^2] = \frac{P_t}{L}$, where $\mathbf{E}[.]$ denotes expectation. We assume the noise power for the i^{th} stream is $\mathbf{E}[|n_i|^2] = \sigma^2 = 1$. Also we define the the mean transmit signal power to mean receive noise power or mean transmit power as $\gamma = \mathbf{E}[|d_i|^2]/\sigma^2$.

5.2.4 Receiver Structures

The received vector, $\mathbf{r}$, is decoded by a linear combiner, $\mathbf{W}$, to produce $\tilde{\mathbf{r}} = \mathbf{W}^\dagger\mathbf{r}$. Two types of receivers, the SVD receiver and MMSE receiver, are considered.

5.2.4.1 SVD

The linear combiner for pre-coded transmission with an SVD receiver is given as

$$\mathbf{W}_{SVD} = \mathbf{U}_s. \tag{5.14}$$

Then, the received signal to interference plus noise ratio (SINR) of the i^{th} stream in the SVD receiver can be written as [145]

$$SINR_i = \frac{\lambda_i |(\mathbf{V}_s)_i^\dagger (\mathbf{C}_p)_i|^2 \mathbf{E}[|d_i|^2]}{\lambda_i \sum_{j=1, j\neq i}^{L} |(\mathbf{V}_s)_i^\dagger (\mathbf{C}_p)_j|^2 \mathbf{E}[|d_j|^2] + \sigma^2}, \tag{5.15}$$

using the notation $(\mathbf{A})_i$ = column i for some matrix $\mathbf{A}$. For $L = 1$ and $i = 1$, (5.15) becomes $SNR = \lambda_1 |(\mathbf{V}_s)_1^\dagger (\mathbf{C}_p)_1|^2 \gamma$ and we see there is no ceiling on the performance. Here, the SNR is scaled by two factors. The first scaling factor is $a_v = \lambda_1$ which represents the strength of the selected channel. The second factor, $b_v = |(\mathbf{V}_s)_1^\dagger (\mathbf{C}_p)_1|^2$, is an SNR loss factor due to a mis-match in the direction of the channel compared to the direction of the codeword. For $L > 1$, the SNR loss in $|(\mathbf{V}_s)_i^\dagger (\mathbf{C}_p)_i|^2$ is often small compared to inter-stream interference which grows with increasing transmit power and λ_i and hence a floor occurs. This can be handled by a massive codebook, which is impractical, or a receiver which handles interference.

5.2.4.2 MMSE

An MMSE receiver can be used to handle interference created by the limited size codebook. The linear combiner for pre-coded transmission is given as [145]

$$\mathbf{W}_{MMSE} = \mathbf{H}_{eq} \left(\frac{L}{\rho} \mathbf{I}_L + \mathbf{H}_{eq}^\dagger \mathbf{H}_{eq} \right)^{-1}, \tag{5.16}$$

where $\mathbf{H}_{eq} = \mathbf{H}_s \mathbf{C}_p = \mathbf{U}_s \mathbf{D}_s \mathbf{V}_s^\dagger \mathbf{C}_p$. The SINR of the i^{th} stream in the MMSE receiver can be written as [145], [27]

$$SINR_i = \frac{|(\mathbf{V})_{ii}^\dagger|^2 \mathbf{E}[|d_i|^2]}{\sum_{j=1, j\neq i}^{L} |(\mathbf{V})_{ij}^\dagger|^2 \mathbf{E}[|d_j|^2] + \sigma^2 (\mathbf{W})_i^\dagger (\mathbf{W})_i}, \tag{5.17}$$

where $\mathbf{V}^\dagger = \mathbf{W}^\dagger \mathbf{H}_{eq}$ and $(\mathbf{B})_{ij}$ refers to the $(i-j)^{th}$ element of some matrix $\mathbf{B}$. For $L = 1$, (5.17) becomes $SNR = |\mathbf{H}_{eq}^\dagger \mathbf{H}_{eq}|^2 \gamma = |\mathbf{C}_p^\dagger \mathbf{V}_s \mathbf{D}_s^\dagger \mathbf{D}_s \mathbf{V}_s^\dagger \mathbf{C}_p|^2 \gamma$. Here there is no performance floor. As for the SVD receiver, the SNR is affected by both the channel power (via $\mathbf{D}_s^\dagger \mathbf{D}_s$) and, the codebook-channel direction mismatch (via $\mathbf{C}_p^\dagger \ \mathbf{V}_s$).

The sum rate ($\mathcal{SR}$) for both the above receiving techniques under inter-stream interference is given as [27]

$$\mathcal{SR} = \sum_{i=1}^{L} \log_2 (1 + SINR_i) \,. \tag{5.18}$$

5.2.5 Codeword and State Selection Methods

The following three approaches have been investigated to minimize the codebook loss.

5.2.5.1 Maximizing Channel Direction (CD)

This approach uses the channel with the best direction. It is further divided into two: CD1 and CD2. In the first approach, CD1, the direction is maximized over all CPSs and codewords $\mathbf{C}_p$. The index of the best codeword, p^*, is fed back to the transmitter, and the receiver is set to CPS = s^*, where

$$(p^*, s^*) = \underset{\substack{p\in\{1,2,..,N_C\}\\ s\in\{1,2,..,S\}}}{\arg\max} \left\{ \sum_{i=1}^{L} |(\mathbf{V}_s)_i^{\dagger} (\mathbf{C}_p)_i|^2 \right\}. \tag{5.19}$$

In the second approach, CD2, for each codeword $\mathbf{C}_p$, $p = 1, 2, .., N_C$, we choose CPS, s^*, using

$$s^* = \underset{s\in 1,2,...,S}{\arg\max} \left\{ \sum_{i=1}^{L} |(\mathbf{V}_s)_i^{\dagger} (\mathbf{C}_p)_i|^2 \right\}. \tag{5.20}$$

This results in N_C pairs of (p, s^*). Then the best codeword out of the N_C pairs of (p, s^*) is selected based on the best sum rate as follows

$$p^* = \underset{p\in\{1,2,..,N_C\}}{\arg\max} \left\{ \sum_{i=1}^{L} \log_2(1 + SINR_i)_{(p,s^*)} \right\}. \tag{5.21}$$

In (5.21) the subscript (p, s^*) denotes the fact that the SINR is computed using codeword p and CPS s^*. Hence, the index of the best codeword is p^* which is fed back to the transmitter and the receiver is set to CPS = s^*.

5.2.5.2 Maximizing Channel Power (CP)

This approach maximizes the channel power resulting in channel $\mathbf{H}_{s^*}$ being used for transmission, where

$$s^* = \underset{s\in\{1,2,..,S\}}{\arg\max} \left\{ \|\mathbf{H}_s\|^2 \right\}. \tag{5.22}$$

Then, the best codeword, $\mathbf{C}_{p^*}$, is selected, where

$$p^* = \underset{p\in\{1,2,..,N_C\}}{\arg\max} \left\{ \sum_{i=1}^{L} \log_2(1+SINR_i)_{(p,s^*)} \right\}. \tag{5.23}$$

In the SVD case, for $L = 1$, this approach maximizes a_v over all CPS and uses the codeword index from the best corresponding b_v, i.e $\arg\max_p \left\{ |(\mathbf{V}_{s^*})_1^\dagger (\mathbf{C}_p)_1|^2 \right\}$.

5.2.5.3 Optimum Approach (OA)

In the case of the OA approach, the codeword, $\mathbf{C}_p$, and CPS are selected such that the codeword index, $p = p^*$, and CPS, $s = s^*$, satisfy

$$(p^*, s^*) = \underset{\substack{p\in\{1,2,..,N_C\}\\ s\in\{1,2,..,S\}}}{\arg\max} \left\{ \sum_{i=1}^{L} \log_2(1+SINR_i)_{(p,s)} \right\}, \tag{5.24}$$

where $SINR_i$ in (5.24) is from (5.15) and (5.17) for an SVD and MMSE receiver, respectively. This approach globally maximizes the sum rate.

5.3 ANALYSIS

In order to understand the different selection methods, and quantify the gains obtained from CD and CP, we now derive the expectation of the received SNR by looking at the distributions of the CD and CP approaches. In order to make analytical progress, RVQ

codebooks are assumed here. We consider the special case of a reconfigurable MISO system where the channel matrices $\mathbf{H}_s(s \in 1, 2, ..S)$ in $\mathbf{H}$ are all independent and $S = R$. Then the SNR can be given as follows:

5.3.1 Maximizing Channel Direction

When maximizing $\Gamma_{p,s}$ for CD we maximize only over the loss factor term $Y_{p,s}$ and X_s is ignored in (5.4). Since X_s and $Y_{p,s}$ are independent, we can write

$$SNR_{CD} = X \max\{ Y_{p,s}\}\gamma, \tag{5.25}$$

where X is an arbitrary channel power and

$$\mathbf{E}[SNR_{CD}] = \mathbf{E}[X]\mathbf{E}[\max\{ Y_{p,s}\}]\gamma. \tag{5.26}$$

Assuming RVQ codebooks of size N_C, the cummulative distribution function (cdf), probability density function (pdf) and expectation of an arbitrary Y are given by [143],

$$F_Y(y) = (1 - (1 - y)^{N_t - 1})^{N_C}, \tag{5.27}$$

$$f_Y(y) = N_C(1 - (1 - y)^{N_t - 1})^{N_C - 1} \times (N_t - 1)(1 - y)^{N_t - 2}, \tag{5.28}$$

$$\mathbf{E}[Y] = 1 - N_C B\left(N_C, \frac{N_t}{N_t - 1}\right), \tag{5.29}$$

respectively, where $B(.,.)$ is the Beta function. Then, using (5.27), it is straightforward to show that the cdf of $\max\{Y_{p,s}\}$ for $s = 1, 2, .., S$ is equal to

$$(F_Y(y))^S = (1 - (1 - y)^{N_t - 1})^{N_C S}. \tag{5.30}$$

Note that the cdf in (5.30) is the same as that for a non-reconfigurable antenna (NRA) codebook feedback system with a codebook size of $N_C S$. From (5.29) it follows that

$$\mathbf{E}[\max\{Y_{p,s}\}] = \left(1 - N_C SB\left(N_C S, \frac{N_t}{N_t - 1}\right)\right). \tag{5.31}$$

Also, $X = \sum_{k=1}^{N_t} |h_k|^2$ has a χ^2 distribution[1], assuming an i.i.d. Rayleigh fading channel, so that $\mathbf{E}[X] = N_t$ and

$$\mathbf{E}[SNR_{CD}] = N_t\left(1 - N_C SB\left(N_C S, \frac{N_t}{N_t - 1}\right)\right)\gamma. \tag{5.32}$$

5.3.2 Maximizing Channel Power

In the case of maximizing CP, we maximize only over X_s and $Y_{p,s}$ is ignored. Since X and Y are independent we have

$$SNR_{CP} = \max\{X_s\}\, Y\gamma, \tag{5.33}$$

where Y is an arbitrary SNR loss factor,

$$\mathbf{E}[SNR_{CP}] = \mathbf{E}[\max\{X_s\}]\mathbf{E}[Y]\gamma, \tag{5.34}$$

and $\mathbf{E}[Y]$ is given by (5.29).

The cdf of $\max\{X_s\}$ is the cdf of the maximum of S χ^2 variables having pdf and cdf equal to

$$f_X(x) = \frac{x^{N_t-1}e^{-x}}{(N_t-1)!}, \;\; F_X(x) = 1 - \sum_{m=0}^{Nt-1}\frac{x^m}{m!}e^{-x} = 1 - T. \tag{5.35}$$

The cdf of $\max\{X_s\}$ with $s = 1, 2, ...S$, is $(F_X(x))^S$ and the pdf is $SF_X(x)^{S-1}f_X(x)$. Hence, using the above equations,

$$\mathbf{E}[\max\{X_s\}] = \int_0^\infty xS(F_X(x))^{S-1}f_X(x)dx. \tag{5.36}$$

[1]As X is an arbitrary channel power, the superscript in h_k^s has been dropped.

Also, from (5.35) we can write

$$(F_X(x))^{S-1} = (1-T)^{S-1} = \sum_{\alpha=0}^{S-1} \binom{S-1}{\alpha} (-1)^{\alpha} T^{\alpha}, \tag{5.37}$$

$$T^{\alpha} = \sum_{m_1=0}^{N_t-1} ... \sum_{m_\alpha=0}^{N_t-1} \frac{x^{\sum_{g=1}^{\alpha}(m_g)} e^{-\alpha x}}{\prod_{g=1}^{\alpha}(m_g!)}. \tag{5.38}$$

Substituting (5.35), (5.37) and (5.38) in (5.36) gives

$$\begin{aligned}
\mathbf{E}[\max\{X_s\}] = S \int_0^{\infty} & \frac{x^{N_t} e^{-x}}{(N_t-1)!} \sum_{\alpha=0}^{S-1} \binom{S-1}{\alpha} \\
& (-1)^{\alpha} \sum_{m_1} ... \sum_{m_\alpha} \frac{x^{\sum_{g=1}^{\alpha} m_g} e^{-\alpha x}}{\prod_{g=1}^{\alpha} m_g!} dx \\
& = \frac{S}{(N_t-1)!} \left[N_t! + \sum_{\alpha=1}^{S-1} \binom{S-1}{\alpha} (-1)^{\alpha} \sum_{m_1=0}^{N_t-1} .. \right. \\
& \left. .. \sum_{m_\alpha=0}^{N_t-1} \frac{(N_t + \sum_{g=1}^{\alpha} m_g)!}{\prod_{g=1}^{\alpha}(m_g!)(\alpha+1)^{N_t+\sum_{g=1}^{\alpha} m_g+1}} \right].
\end{aligned} \tag{5.39}$$

Hence,

$$\begin{aligned}
\mathbf{E}[SNR_{CP}] = & \left(1 - N_C B\left(N_C, \frac{N_t}{N_t-1}\right)\right) \frac{S}{(N_t-1)!} \\
& \left[N_t! + \sum_{\alpha=1}^{S-1} \binom{S-1}{\alpha} (-1)^{\alpha} \sum_{m_1=0}^{N_t-1} ..... \sum_{m_\alpha=0}^{N_t-1} \right. \\
& \left. \frac{(N_t + \sum_{g=1}^{\alpha} m_g)!}{\prod_{g=1}^{\alpha}(m_g!)(\alpha+1)^{N_t+\sum_{g=1}^{\alpha} m_g+1}} \right] \gamma.
\end{aligned} \tag{5.40}$$

5.4 SIMULATION RESULTS FOR A RA CODEBOOK FEEDBACK MISO SYSTEM

Three types of codebooks are used in the simulations. We use RVQ codebooks to compare the simulated and analytical results. Grassmanian codebooks are used to explore the codebook expansion effect due to their availability in different sizes. Standard LTE codebooks

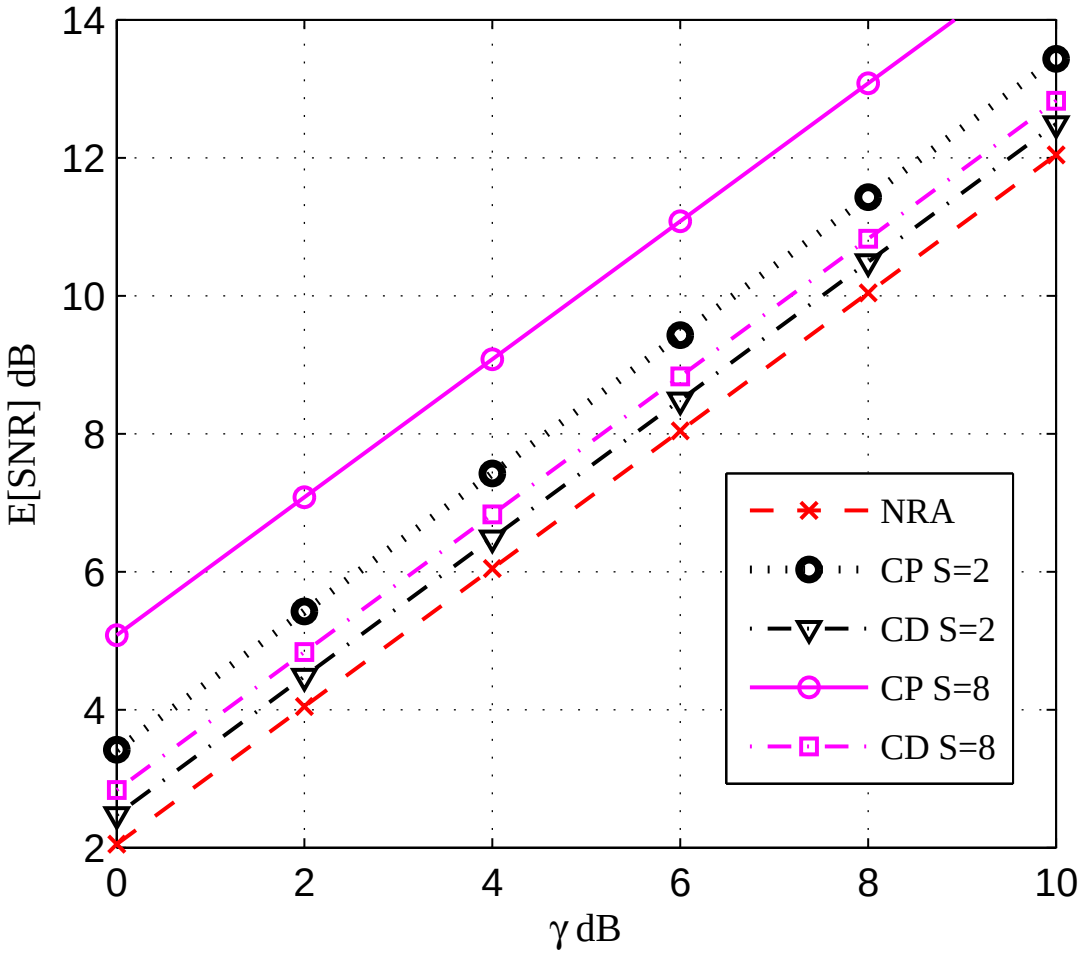

Figure 5.1 Analytical (represented by lines) and simulated (represented by points) results of E[SNR] for a 1×2 MISO RA codebook feedback system using RVQ codebooks with $S = 2, 8$ and using CP and CD selection.

are then used to demonstrate the improvements offered by RAs over NRA systems.

Fig. 5.1 presents the CD and CP results derived in the previous section for a 1×2 MISO system using RA with $S = 2, 8$, and RVQ codebooks. Note that the analytical results in (5.32) and (5.40) are given by the lines and simulations are plotted using points and it can be seen that they follow each other almost exactly. Also, the average SNR using CP always significantly outperforms CD and NRA codebook feedback.

The SNR improvements due to reconfiguration are summarized in Table 5.1. The percentage improvement values are calculated as $(\mathbf{E}[SNR_{S=2,4,8}] - \mathbf{E}[SNR_{S=1}])/\mathbf{E}[SNR_{S=1}]$.

Table 5.1 Average SNR % improvement over NRA, using different selection methods in a RA 1x2 MISO system with an LTE codebook.

S	**E**[SNR] CP %gain	**E**[SNR] CD % gain	**E**[SNR] OA % gain
1	0	0	0
2	7	38	39
4	11	77.5	79
8	14	118	121

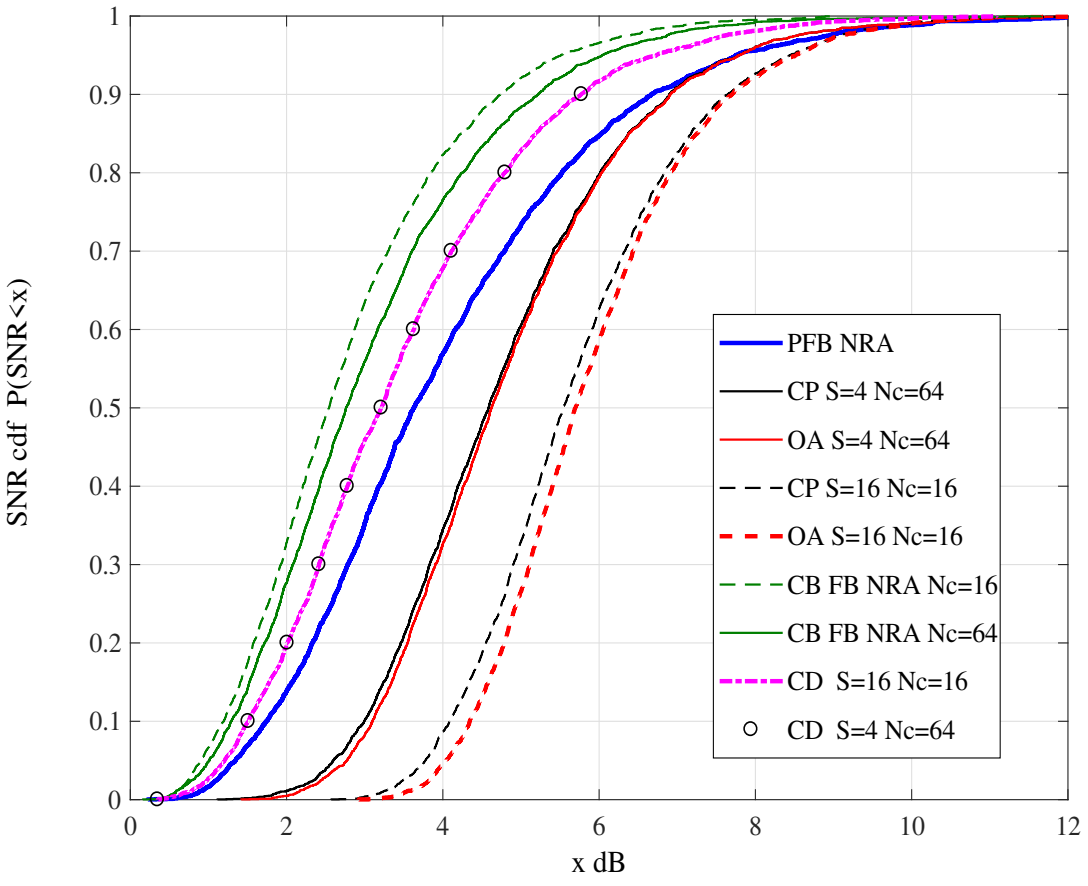

Figure 5.2 SNR cdf for 1×4 MISO RA FB system using Grassmanian codebooks [1] with $N_C = 64$, S=4 (solid lines) and $N_C = 16$, S=16 (dotted lines).

Note that the % gains going from S=1 to S=2 for CP and OA are approximately half the gains observed in going from S=1 to S=4 and one third of the gains in going from S=1 to S=8.

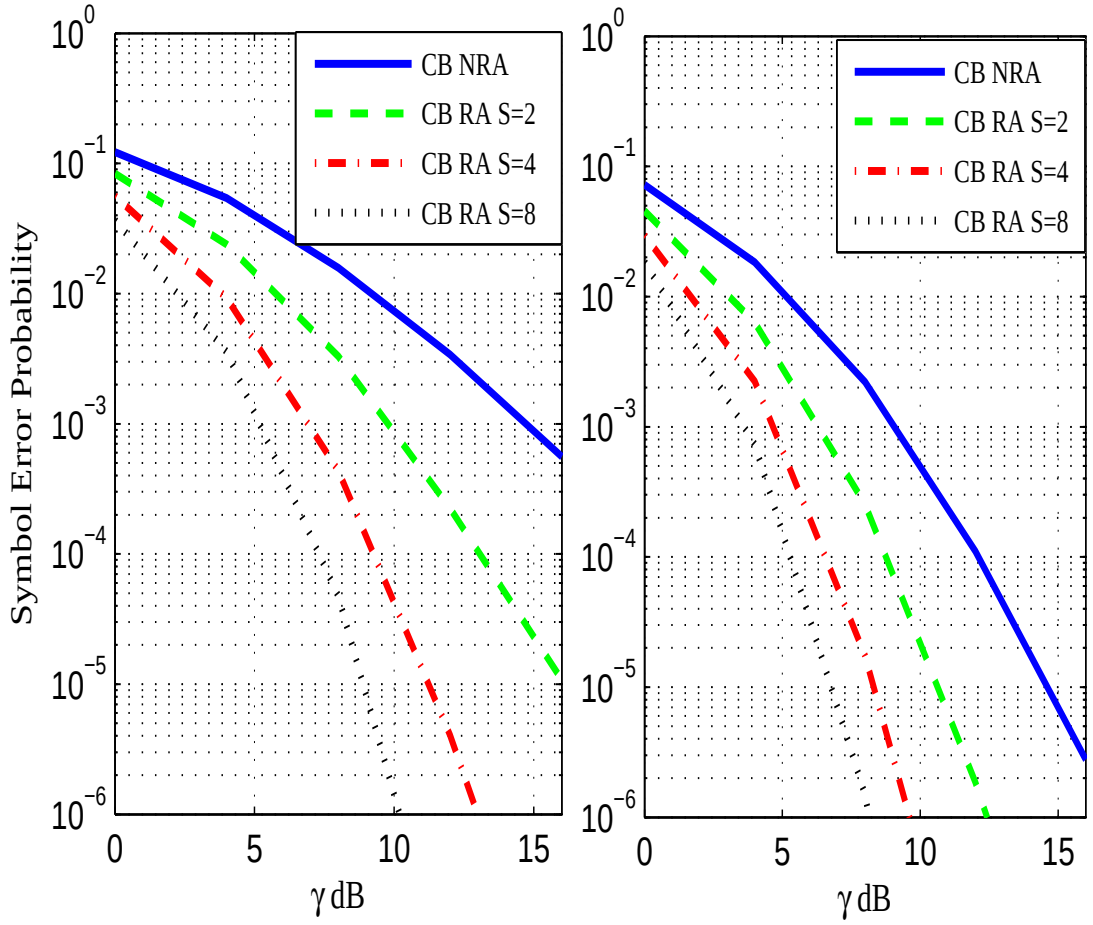

Figure 5.3 SER performance results of 1×2 (left) and 1×4 (right) MISO system using LTE codebooks with $N_C = 4$ and $N_C = 16$, $S = 1, 2, 4, 8$.

Fig. 5.2 presents the SNR cdfs for a 1×4 MISO systems with $N_C = 16$, $S = 16$ (dotted lines) and $N_C = 64$, $S = 4$ (solid lines). It clearly shows that OA has the best performance compared to CD and CP and that CD method improves over NRA codebook feedback, but never exceeds PFB unlike the CP and OAs. Moreover, the gains of OA over CP are marginal. Note here that the expanded codebook size, $\tilde{N_C}$ is $N_C S = 256$ for both cases and as also shown by the superimposed curves for CD in Fig. 5.2 and in (5.30), the SNR_{CD} cdfs are equal. However, there is a higher selection gain for OA and CP for $S = 16$ while using a smaller codebook (4 bits), compared with $S = 4$ and a 4 times larger codebook (6 bits).

Fig. 5.3 shows the QPSK SER comparison for NRA (solid line) and $S = 2, 4, 8$ (dotted

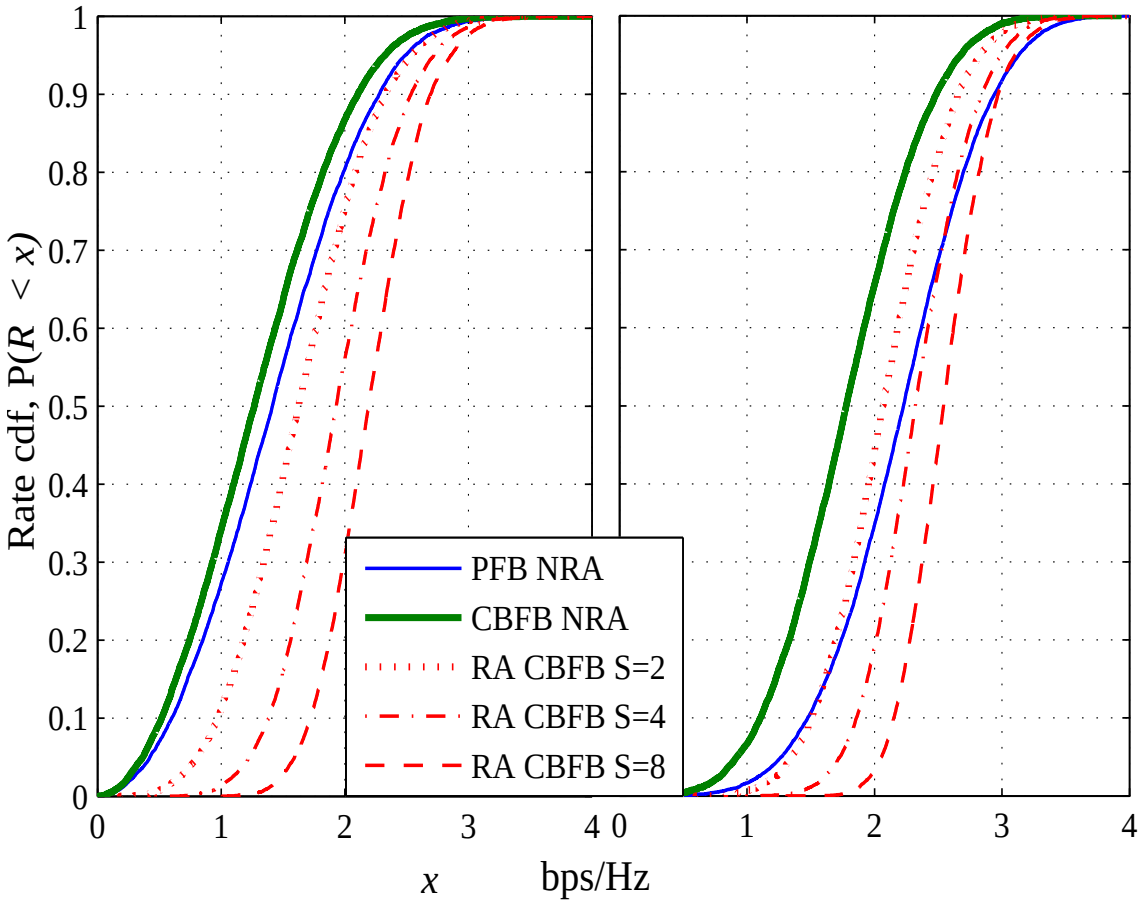

Figure 5.4 Rate $\mathcal{R}$ cdfs for 1×2 (left) and 1×4 (right) MISO systems using OA selection, with S=2, 4, 8 and LTE codebooks.

lines) for codebook feedback MISO systems using OA selection. For the 1×2 system at SER of 10^{-3}, the gain in γ for $S = 2$ is about 5.2 dB over NRA codebook feedback and it is 3 dB more for $S = 4$ and a further 2 dB for $S = 8$. For the 1×4 system at a SER of 10^{-3}, the gain in γ for $S = 2$ is about 3 dB over NRA codebook feedback. It is about 1.7 dB for $S = 4$ over $S = 2$ and about 1 dB for $S = 8$ over $S = 4$. We see that the SER gains diminish with increasing S. Also, comparing a smaller 1×2 system with $N_C = 4$ and a larger 1×4 system, with $N_C = 16$, we notice that the smaller system with $S = 2$ and the larger system with NRA ($S = 1$) have almost the same SER slopes at high γ, suggesting similar diversity.

Fig. 5.4 shows the rate cdfs for the MISO systems using OA selection for $S = 2, 4, 8$

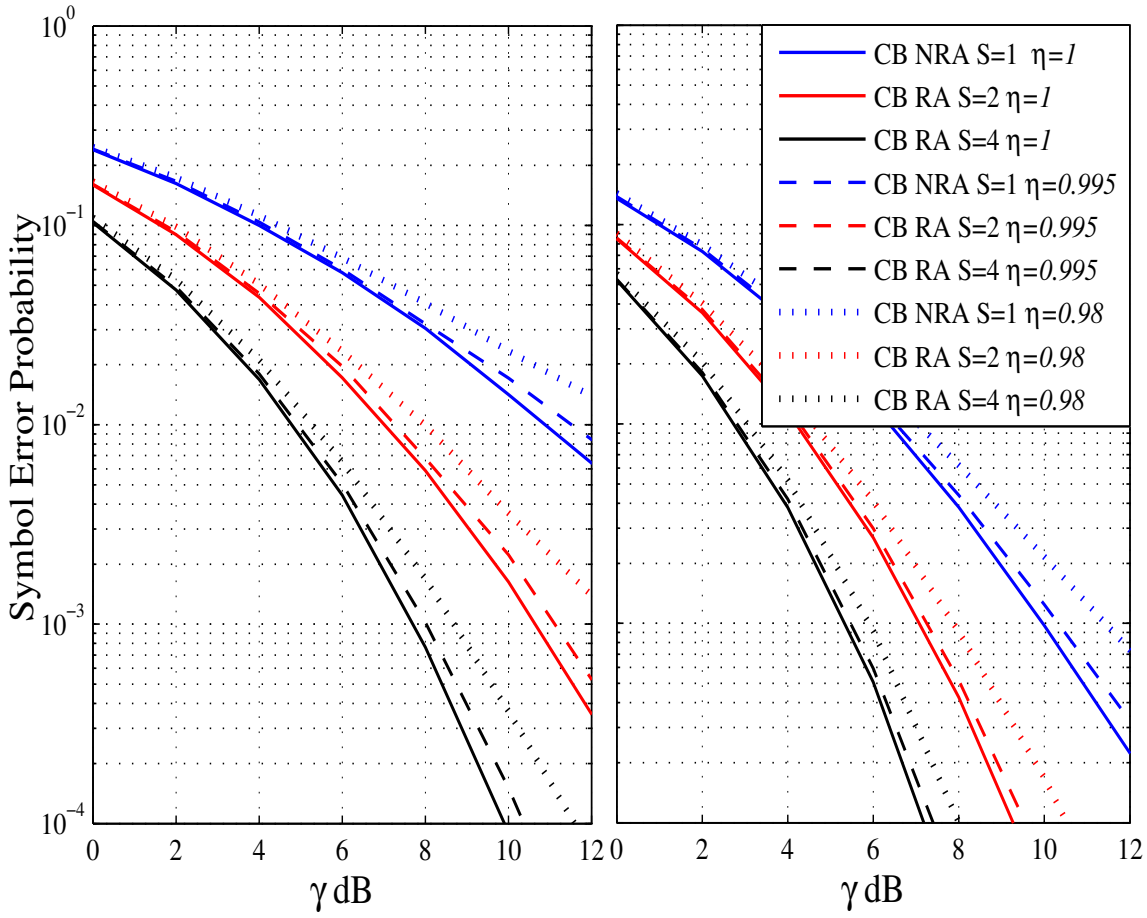

Figure 5.5 SER performance results of 1×2 (left) and 1×4 (right) MISO systems using LTE codebooks with $N_C = 4$ and $N_C = 16$, $S = 1, 2, 4$ and perfect and imperfect CSI. (η is the correlation between $\hat{h}_k^s$ and h_k^s.)

and LTE codebooks. We see that for the $N_t = 2$ system (left) with just $S = 2$, the rate performance achieved, not only overcomes the quantization/codebook loss, but is always better than the rate achieved from the PFB NRA case. As S increases, this gain over PFB NRA increases. However, in a $N_t = 4$ system (right), reconfiguration with $S = 2$ achieves better rate than PFB NRA for 13% of the time, $S = 4$ for 70% of the time and $S = 8$ for 93% of the time. In this system, even by just using $S = 2$, the performance always exceeds that achieved by the PFB NRA case at low rates, however, it does not exceed the PFB NRA case for high rates.

Fig. 5.5 shows the simulation results of QPSK SER comparison for NRA (blue line) and

RA with $S = 2$ (red lines) and $S = 4$ (black lines) codebook feedback MISO systems using OA selection. First we consider the perfect CSI case (solid lines). For the 1×2 system at a SER of 10^{-2}, the gain in γ for $S = 2$ is about 4 dB over NRA CB feedback and is 2 dB more for $S = 4$. For the 1×4 system at a SER of 10^{-3}, the gain in γ for $S = 2$ is about 3 dB over NRA CB feedback. It is about 1.7 dB for $S = 4$ over $S = 2$. We see that the SER gains diminish with increasing S. Also, comparing a smaller 1×2 system with $N_C = 4$ and a larger 1×4 system, with $N_C = 16$, we notice that the smaller system with $S = 4$ and the larger system with $S = 2$ have similar SER slopes at high γ, suggesting similar diversity. The curves with imperfect CSI in Fig. 5.5, for $\eta = 0.995$ (dashed lines) and $\eta = 0.98$ (dotted lines), show the RAs can still provide diversity gains with imperfect CSI.

5.5 SIMULATION RESULTS FOR RA CODEBOOK FEEDBACK MIMO SYSTEM

In all simulations, the transmission power is fixed at the transmitter for all multi-stream transmissions. The MIMO CSI is assumed to be perfectly known by the receiver and only the index of the codeword is fed back to the transmitter. Grassmannian codebooks and standard LTE codebooks are used to demonstrate the improvements offered by RAs over NRA codebook feedback systems. First, we present expected SNR results of a single layer MIMO system. Fig. 5.6 shows the average SNR in dB of different codeword selection techniques for a $N_r \times N_t = 4 \times 2$ MIMO RA codebook feedback system with $L = 1$ using Grassmannian codebooks and an MMSE receiver. We see that the OA selection approach always outperforms the others at all SNRs. We also see that CD2 is better than CD1. This is because the former is directly based on the best $\mathcal{SR}$ selection whereas CD1 is solely based on the channel direction. Note that CD2 has been introduced to be fair in CP and CD selection comparisons for $L = 2$.

The SNR improvement for a single layer 2×2 MIMO RA codebook feedback system due to reconfiguration while using MMSE and SVD receivers and LTE codebook is shown in Table

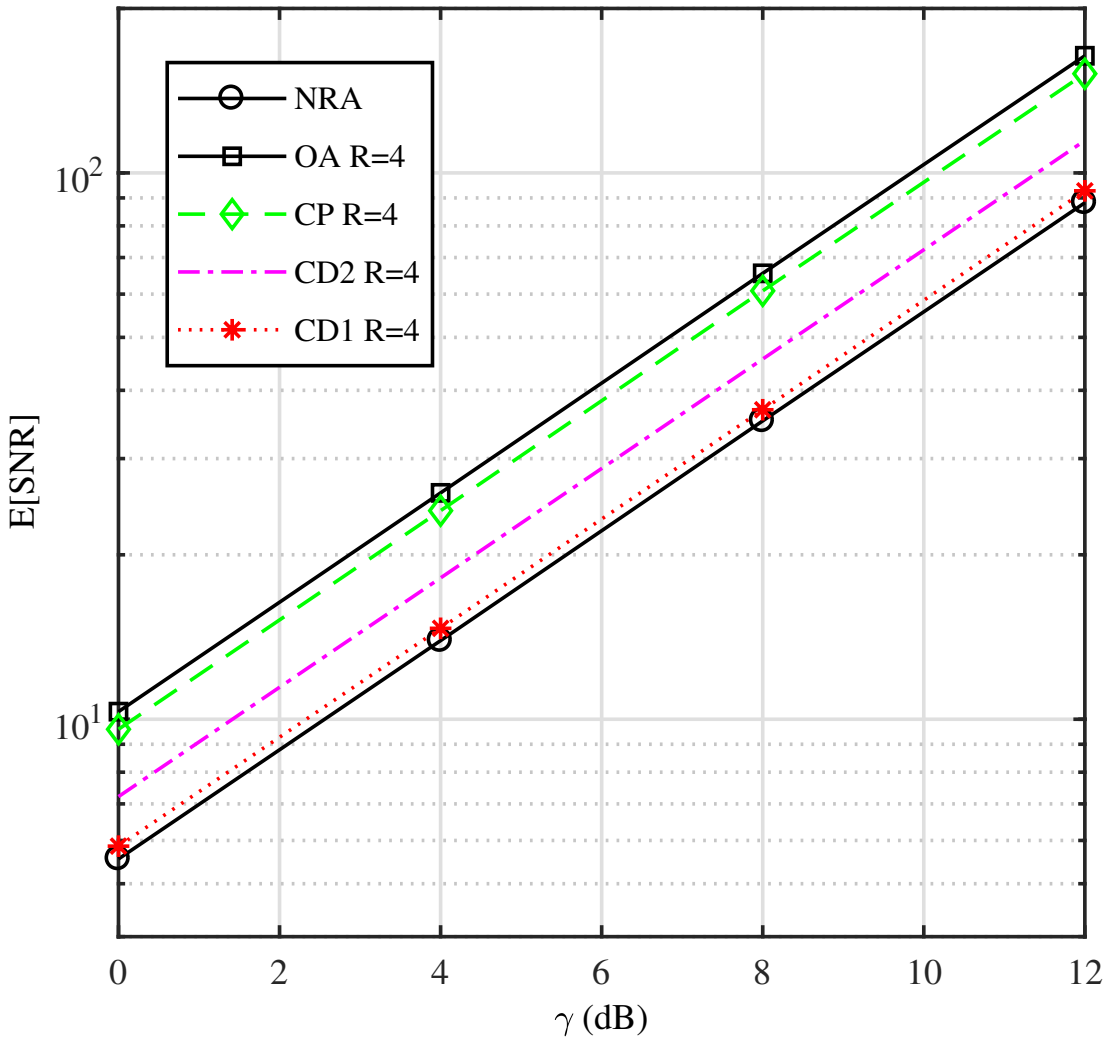

Figure 5.6 Simulation results for E[SNR] of an $L = 1$, 4×2 MIMO codebook feedback system with a Grassmannian codebook and an MMSE receiver using various selection methods for $R = 4$ reconfiguration.

5.2. The percentage gain values are given by $(\mathbf{E}[SNR_{R=1,2,4,8}] - \mathbf{E}[SNR_{R=1}])/\mathbf{E}[SNR_{R=1}]$ and the table shows the improvement in the % gain values, by doubling R each time, i.e $R = 1$ to $R = 2$ (2-1), $R = 2$ to $R = 4$ (4-2) and $R = 4$ to $R = 8$ (8-4). It is seen that using SVD receiver, the %gain improvement is higher than that for the MMSE receiver. It is also observed from Table 5.2 that, as the value of R increases, the %gain improvement, from CP and OA keeps increasing while that from direction (CD1 and CD2), increases for $R = 1$ to $R = 2$ and then decreases for $R = 2$ to $R = 4$ and so on.

Table 5.2 Average SNR percentage improvement using different selection methods in a reconfigurable 2×2 MIMO system with $L = 1$ using the LTE codebook for various values of R and using SVD(SV)/MMSE(MM) receivers.

R	**E**[SNR] CD2 %gain improvements		**E**[SNR] CP %gain improvements		**E**[SNR] OA %gain improvements		**E**[SNR] CD1 %gain improvements	
	SV	MM	SV	MM	SV	MM	SV	MM
1-1	0	0	0	0	0	0	0	0
2-1	28	27	38	35	40	39	7	5
4-2	20	19	42	38	44.5	43	3	2.6
8-4	12	11	43	38.17	46	45	1.8	1.5

From Fig. 5.7, it can be seen that the MMSE receiver's expected SNR is always better than that of an SVD receiver for all reconfigurations and at all SNRs in the case of a single layer 4×2 MIMO codebook feedback system using a Grassmannian codebook and OA selection. Fig. 5.8 gives the QPSK symbol error rate (SER) results for an $L = 1$, 4×2 codebook feedback MIMO system using an MMSE receiver with OA selection and an LTE codebook of size $N_C = 4$ and various reconfigurations, $R = 1$, 2, 4, 8. It can be seen that as R increases, the SER performance improves.

Next, we present results for multi layer MIMO codebook feedback systems. Fig. 5.9 gives the QPSK SER comparison of $L = 1$ and $L = 2$ transmission for a 4×4 reconfigurable antenna codebook feedback MIMO system using an MMSE receiver and OA selection. Even with $R = 8$, the SER of $L = 2$ is not better than that of $L = 1$ with $R = 1$ NRA codebook feedback because of the multi-layer interference loss. Both the above figures are simulated to conclude on whether SER improves with increasing R and the overall conclusions remain same even with less simulation points, hence the SER curves are not refined for more SNR points.

In Fig. 5.10 it can be seen that a critically loaded, 2×2 RA codebook feedback MIMO system, using MMSE receiver and proposed OA selection, with $R = 4$, gives almost equal QPSK SER performance as an underloaded 4×2 NRA codebook feedback MIMO system. Thus, using the RA codebook feedback system allows the use of fewer receive antennas and

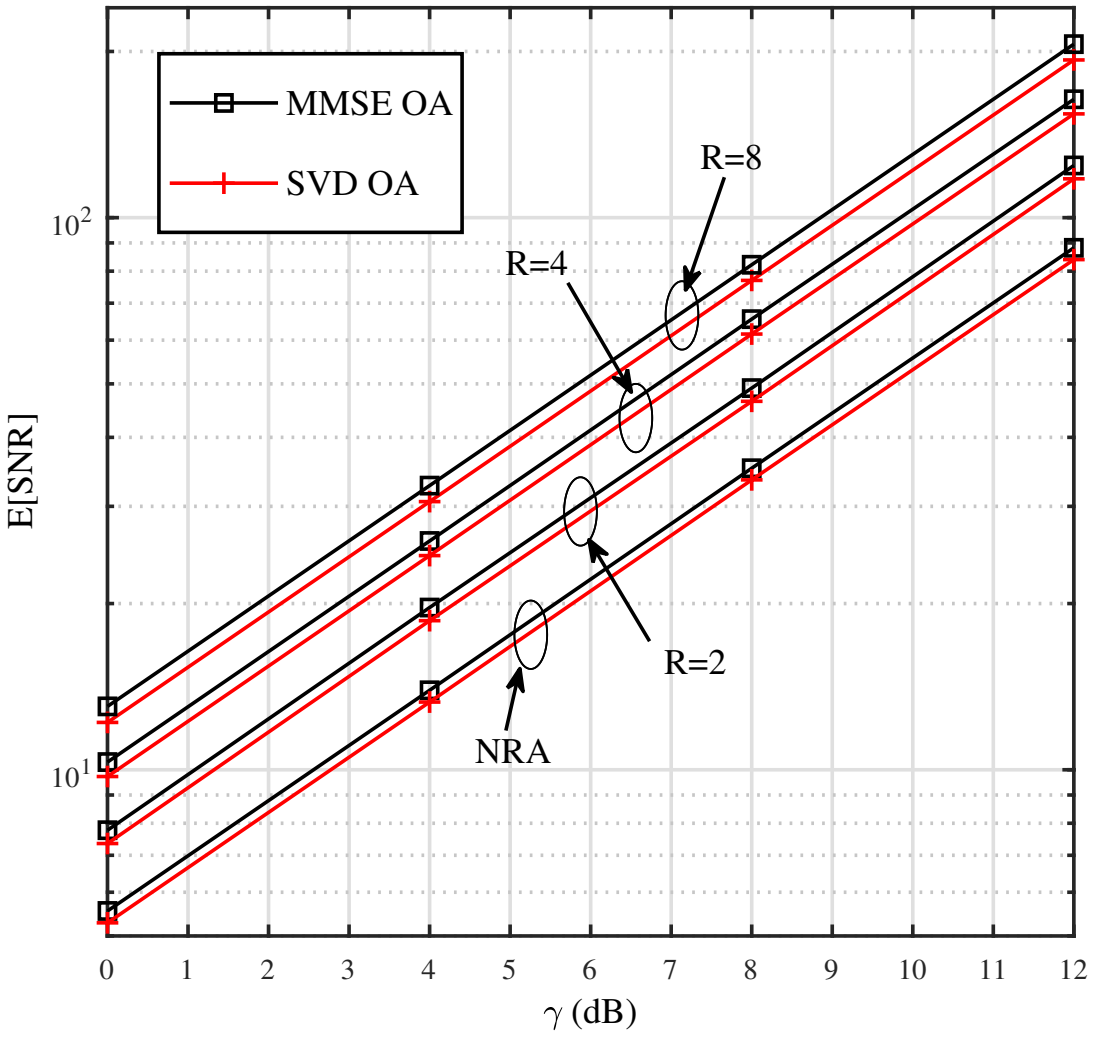

Figure 5.7 Simulation results for E[SNR] of an $L = 1$, 4×2 MIMO codebook feedback system using a Grassmannian codebook and OA selection with varying R and SVD/MMSE receivers.

RF chains, to achieve the same improved SER performance. Also, the SER performance of the 2×2 RA codebook feedback MIMO system with $R = 8$, exceeds that of the 4×2 NRA codebook feedback MIMO system.

Fig. 5.11 shows the QPSK SER comparison for NRA (solid lines) and $R = 2$ (dotted lines) for an $L = 2$ MIMO codebook feedback system with different sizes using an MMSE receiver with OA selection. It is observed that for smaller system, $N_r = 2, N_t = 2, R = 2$, the gains are higher over corresponding NRA CB. Also by doubling the number of transmit

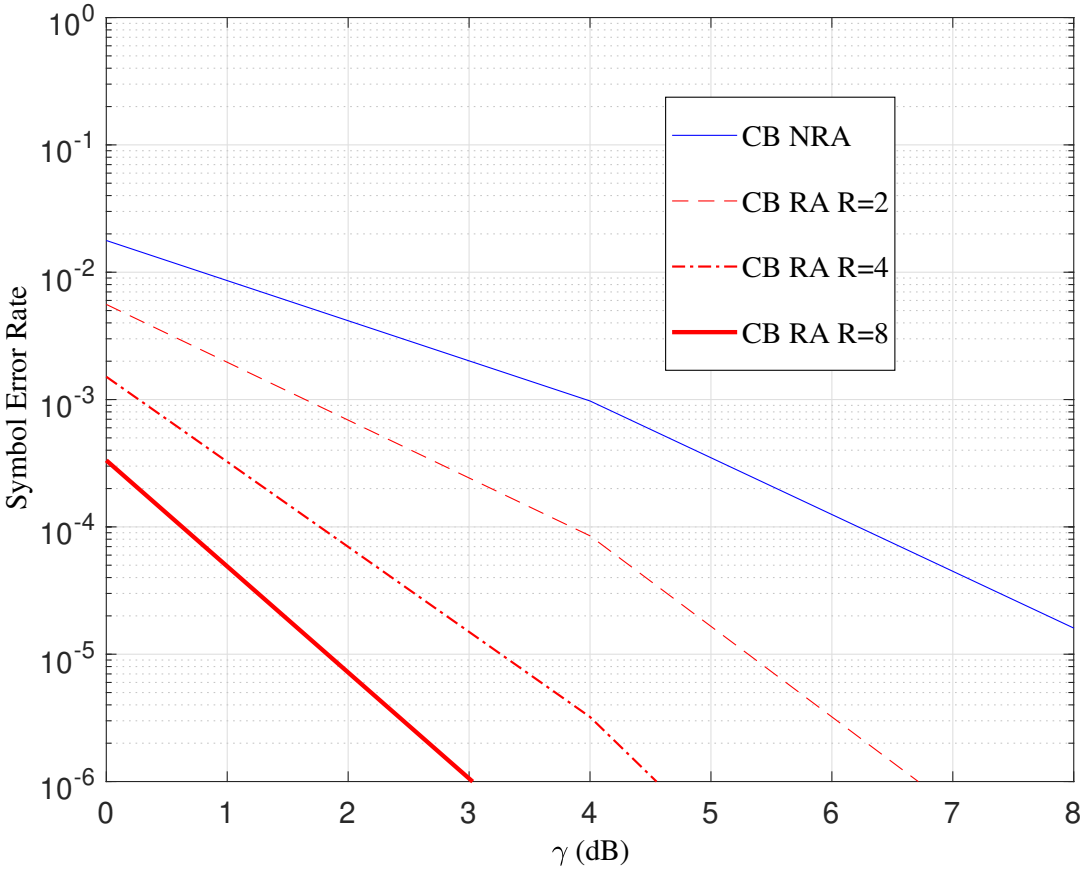

Figure 5.8 QPSK SER performance of an $L = 1$, 4×2 MIMO system using an MMSE receiver and an LTE codebook with size $N_C = 4$, $R = 1$, 2, 4, 8 reconfigurations and OA selection.

antennas versus doubling the number of receive antennas, the gains are higher in the case of increasing transmit antennas. At an error rate of 10^{-2} , the gain in SNR for an $R = 2$ RA CB over an NRA CB, is about 9 dB for a 2×2 system ($S = 4$), about 4 dB for a 2×4 system ($S = 4$), about 1.8 dB for a 4×4 system ($S = 16$) and about 3.6 dB for a 4×2 system ($S = 16$).

Figs. 5.12 and 5.13 give the comparison of the cumulative distribution function (cdf) of the $\mathcal{SR}$ for an $L = 1$ critically loaded 2×2 MIMO system. It can be seen in Fig. 5.13 that the $\mathcal{SR}$ for an SVD receiver (dotted lines) always follows that of an MMSE receiver (solid lines), for all different selection techniques, such that the former always has slightly lesser values. Also, as reconfiguration increases from $R = 2$ (Fig. 5.13) to $R = 4$ (Fig. 5.12),

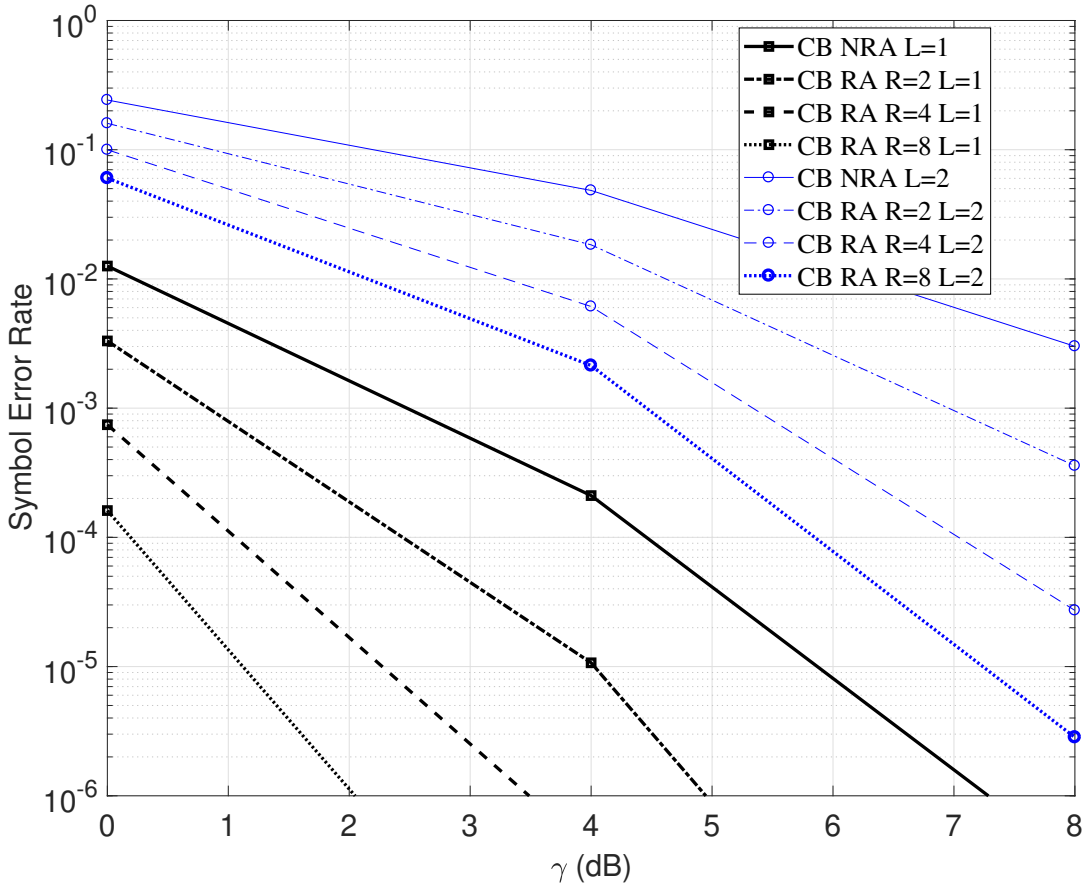

Figure 5.9 QPSK SER performance results for $L = 1$ and $L = 2$, 4×4 MIMO RA codebook feedback systems using various reconfigurations and an MMSE receiver with OA selection and an LTE codebook with size $N_C = 16$.

the difference between the $\mathcal{SR}$ achieved using OA and CD2 increases. This is due to the fact that as the number of CPSs increases, the CP selection gain increases and hence OA increases. However, in both cases they exceed the perfect NRA FB (PFB) (black solid line) $\mathcal{SR}$. Also the cdfs follow the same order with the OA approach being the best.

Fig. 5.14 gives the cdf of the $\mathcal{SR}$ for an overloaded 2×4 MIMO FB system for $L = 1$ transmission with an LTE codebook and MMSE detection. It can be seen from Fig. 5.12 and 5.13 that for $N_t = 2$ system with just $R = 2$, the $\mathcal{SR}$ performance achieved not only overcomes the quantization loss but also adds a gain to it and is better than that of the PFB NRA case. As R increases, this gain over PFB NRA increases. However, in the

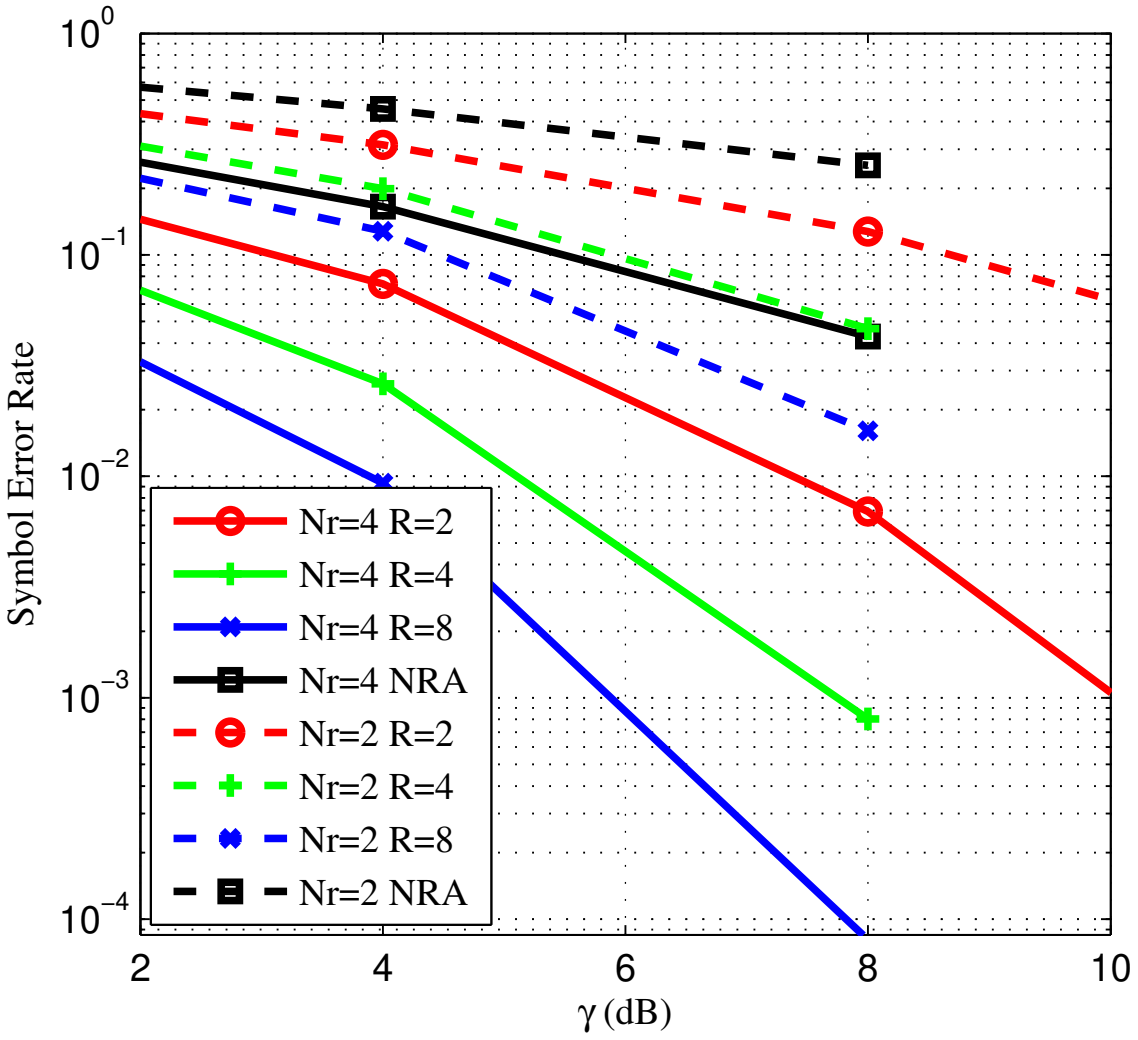

Figure 5.10 QPSK SER comparison for various reconfigurations using an $N_t = 2$ $N_r = 2/4$, codebook FB MIMO system with an $L = 2$ and $N_C = 3$ LTE codebook, using an MMSE receiver with OA selection.

$N_t = 4$ system shown in Fig. 5.14, OA reconfiguration of $R = 4$ achieves a better $\mathcal{SR}$ compared to PFB NRA 90% of the time. Using $R = 2$ means that performance exceeds that of the PFB NRA case at low $\mathcal{SR}$ about 15 % of the time, however, it does not exceed the NRA PFB case for high sum rates. The quantization loss and gain over PFB NRA for different scenarios is indicated by red arrows.

Fig. 5.15 gives the cdf of $\mathcal{SR}$ using (5.18) for a 2×2 MIMO FB system with $L = 2$ transmission and an LTE codebook. It can be seen that SVD receiver performs very

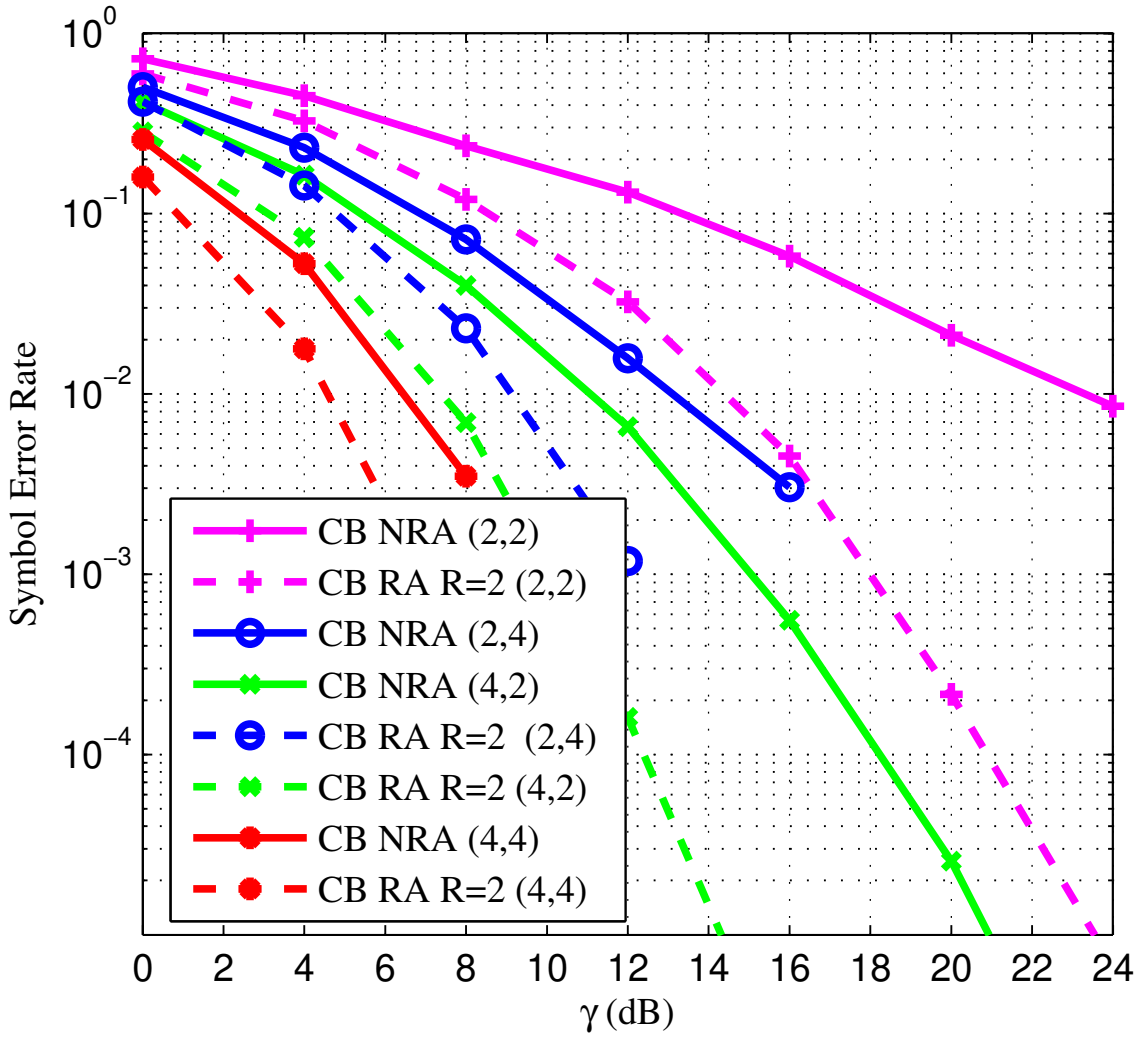

Figure 5.11 QPSK SER comparison for NRA (solid lines) and $R = 2$ (dotted lines) using an $L = 2$ MIMO codebook FB system with different sizes (N_r, N_t) using an MMSE receiver with OA selection.

poorly due to interference and its $\mathcal{SR}$ is far from that of the MMSE receiver. Even with the gain from using a RA codebook with $R = 4$, SVD only achieves a 20% better SNR compared to NRA codebook FB using an MMSE receiver. As an upperbound for the $\mathcal{SR}$ of this system, the PFB from RA system is also plotted (golden line). As R increases, the $\mathcal{SR}$ performance can reach the upper bound. It can be seen that the $\mathcal{SR}$ loss due to quantization in a NRA codebook feedback (cyan dotted line) is highly reduced with only $R = 2$ RA codebook feedback (cyan solid line), and with $R = 4$ RA codebook feedback (cyan solid line) $\mathcal{SR}$ improves 70% of the time over the PFB NRA case. The quantization

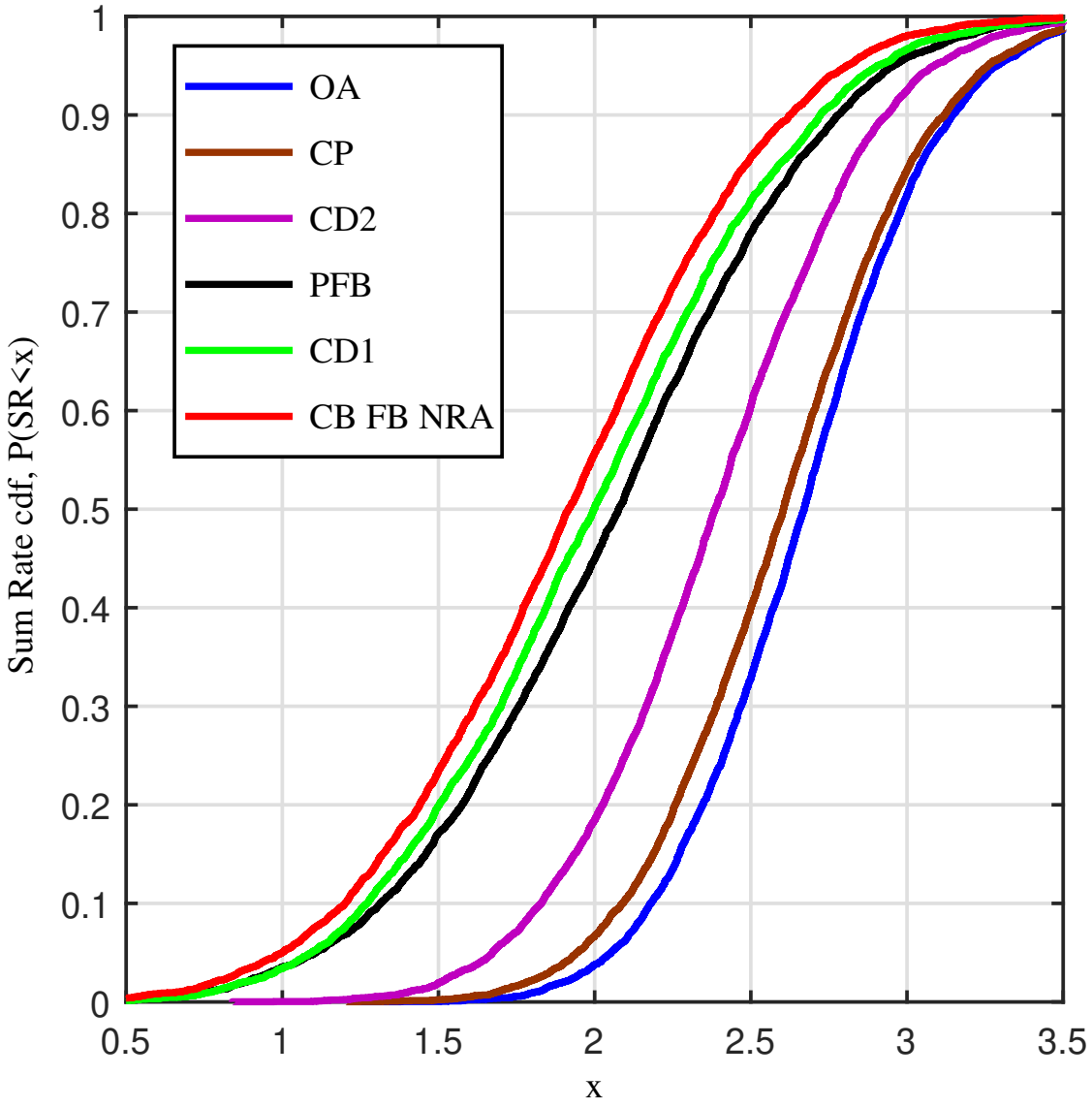

Figure 5.12 $\mathcal{SR}$ cdf comparison at $\gamma = 0$ dB for NRA and $R = 4$ using $L = 1$, 2×2 MIMO system with different selection methods and MMSE receiver.

loss is indicated by red arrows.

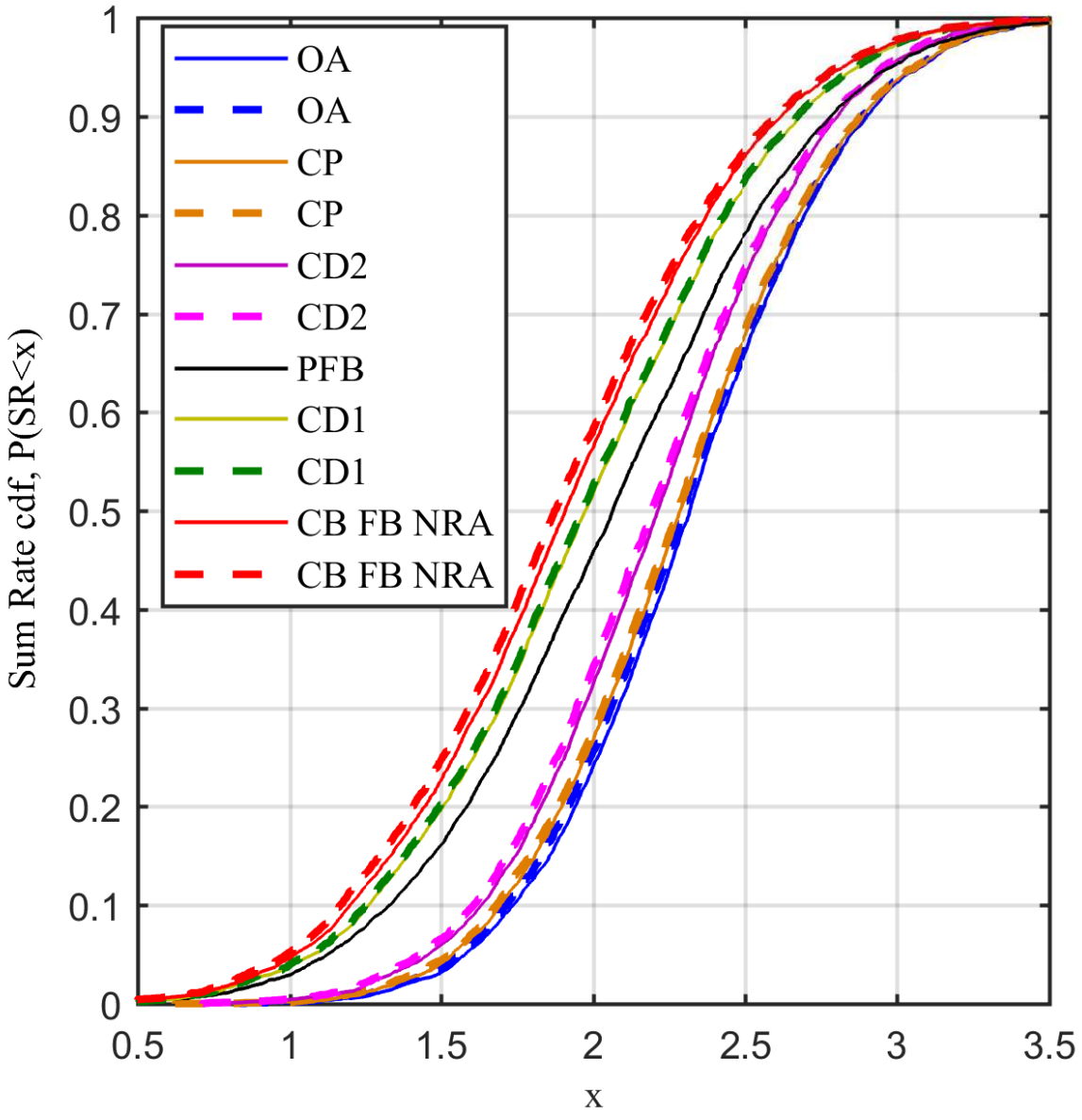

Figure 5.13 $\mathcal{SR}$ cdf comparison at $\gamma = 0$ dB for NRA and $R = 2$ using $L = 1$, 2×2 MIMO system with different selection methods and MMSE (solid lines)/SVD (dotted lines) receivers.

5.6 CONCLUSION

The RA codebook feedback system proposed significantly improves the SINR/SNR, SER and the rate of the codebook feedback MISO/MIMO system. Our analytical and simulation results show that using CD selection in a codebook feedback MISO/MIMO system

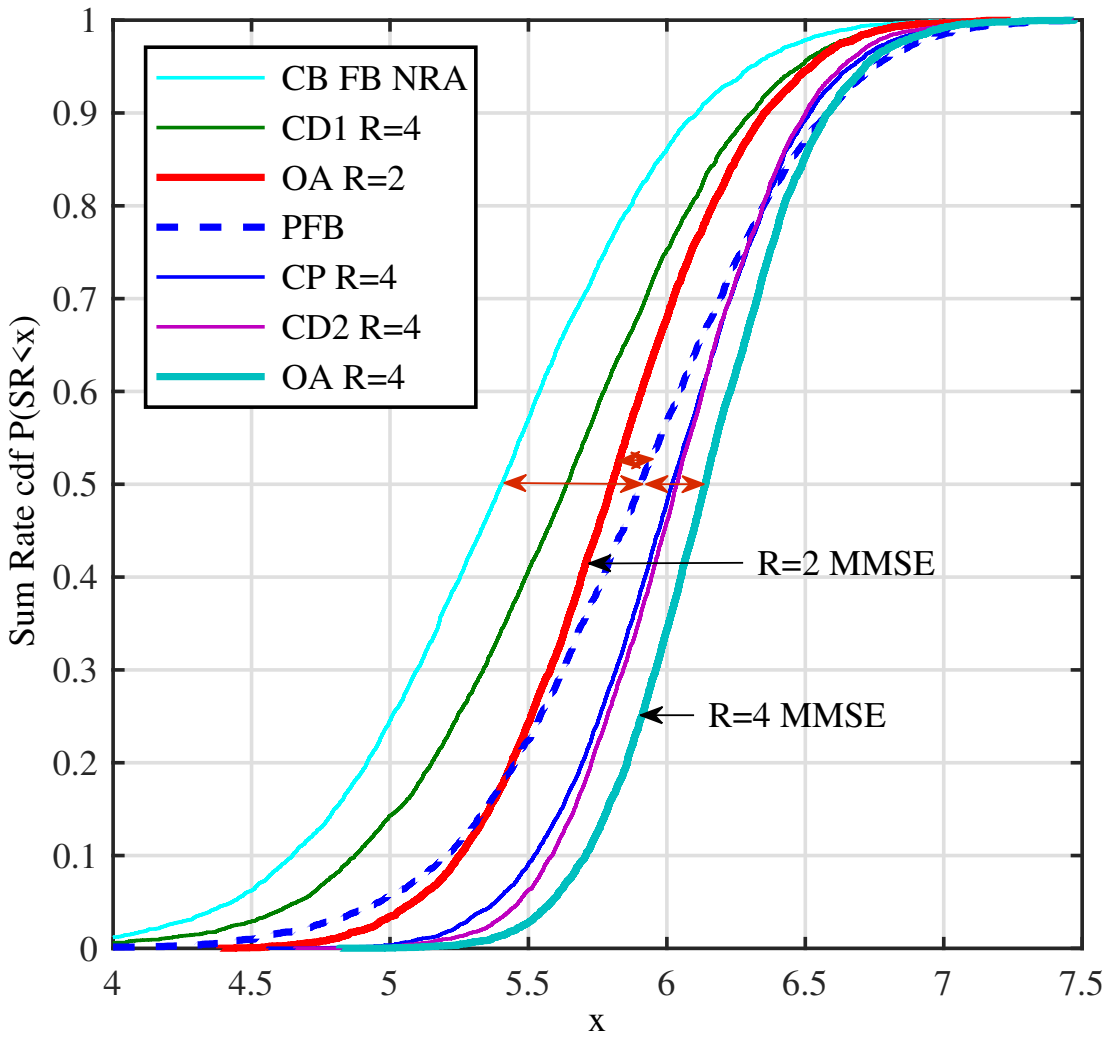

Figure 5.14 Sum rate cdf comparison at $\gamma = 10$ dB for NRA and $R = 2$ and 4 using an $L = 1$, 2×4 MIMO FB system using LTE codebooks and MMSE receivers.

equipped with an $S = R^{N_r}$ state RA at the receiver, is the same as using an expanded codebook with size $\tilde{N_C} = N_C S$. Thus smaller codebook can be used to achieve the same SNR performance as with a larger codebook and hence lessens the number of feedback bits.

We give three RA codebook selection techniques and have demonstrated that in terms of SNR and rate performance, CD is far less than CP and that CP is almost equal to OA. The SNR expectation expressions for CD and CP for the RA codebook feedback system are

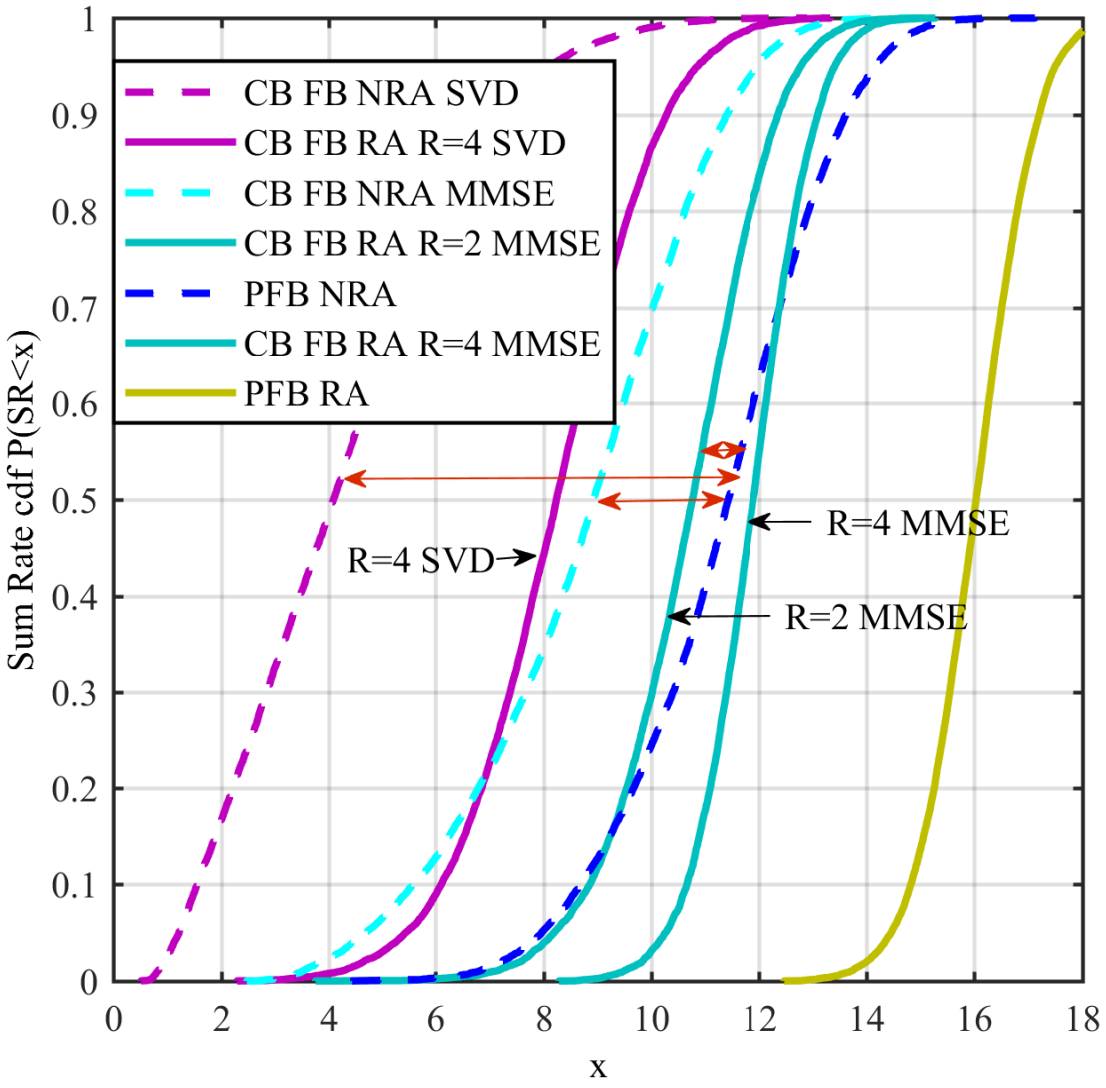

Figure 5.15 Sum rate cdf comparison at $\gamma = 20$ dB for NRA and an $R = 2, 4$, $L = 2$, 2×2 MIMO precoding system using an LTE codebook with different selection methods and MMSE and SVD receivers.

also given from which we conclude that the traditional CD approach provides only a very small part of the gains offered by OA. We also show that as the number of CPSs increase, the gain in SNR, SER and the rate of the system using RA codebook feedback with OA selection, increases, and their cdfs show that they not only overcome the codebook loss, but the gain exceeds that achieved by a NRA perfect feedback. SER curves show that the SER slope of the system improves as S increases. Also a larger 1×4 system with $N_C = 16$,

$S = 2$ and a smaller 1×2 system with $N_C = 4$ and $S = 4$ have similar SER slopes at high γ. By doubling S the gain in SNR is approximately 40% as compared to $S = 1$. The overall SER conclusions remain the same for the imperfect CSI cases considered ($\eta = 0.995, 0.98$), which are more realistic scenarios and require less training overhead.

For both $L = 1$ and $L = 2$, RA codebook feedback MIMO systems, the expected SINR and $\mathcal{SR}$, from using an MMSE receiver is better than that of an SVD receiver for all reconfigurations and transmit SNRs. We have shown for under loaded and critically loaded RA codebook feedback MIMO systems, the SNR and rate performance for CD1 is much less than CD2, and that for CD2 is less than CP which in turn is less than OA which performs the best. For overloaded systems, CD2 and CP, both contribute almost equally to OA in terms of rate performance and SNR. It is also observed that SER gains from using RA codebook feedback over NRA codebook feedback are higher for smaller MIMO systems and as R increases, SER performance improves with diminishing returns. Doubling the number of transmit antennas rather than doubling the number of receive antennas in a RA codebook feedback MIMO system, gives higher SER gains over the corresponding NRA codebook feedback MIMO system. Using the proposed RA codebook feedback, it is possible to remove the codebook/quantization loss completely in smaller single layer MIMO systems with only $R = 2$, and the $\mathcal{SR}$s performance achieved always exceeds that achieved from a perfect FB NRA MIMO system. However, when using $L = 2$, reconfiguration of only $R = 2$, improves the codebook/quantization loss significantly, but the $\mathcal{SR}$s achieved do not always exceed that from a perfect feedback NRA MIMO system and higher reconfiguration of at least $R = 4$ is required to exceed the PFB NRA MIMO system $\mathcal{SR}$s, most of the time.

Thus, using proposed RA codebook feedback system with OA selection, the codebook loss due to quantization can be significantly reduced with only $S = 2$ and the improvement has no floor, therefore, SNR and rate achieved can exceed the perfect feedback traditional NRA system SNR and rates in a RA codebook feedback MISO system.

Chapter 6

CONCLUSIONS AND FUTURE WORK

6.1 INTRODUCTION

This chapter summarizes the novel contributions of this thesis and highlights several potential extensions and open problems for future work.

6.2 CONCLUSIONS

6.2.1 Conclusions from STSTC

We have shown that full diversity is not possible in a reconfigurable transmit antenna MIMO system, while using existing trellis codes. We used SOSTTC in a MIMO system with $N_t = 2$ and $S = 2$, to demonstrate this. Hence we proposed 2TS STSTC. In this thesis, the concept of concatenating Block Diagonal QOSTBC in a space time trellis is given. This is to achieve full diversity in a reconfigurable antenna system which other exixting trellis codes failed to achieve. A novel STSTC with full rate, full diversity and high coding gain has been proposed for reconfigurable transmit antenna system for $r = 1$ bits/s/Hz using BPSK and $r = 2$ bits/s/Hz using QPSK. Simulation results confirm that the proposed code offers good performance in a reconfigurable antenna system with more than one channel propagation state.

The research initially provided two trellis state STSTC, which is further extended to also

provide various four trellis state STSTCs, for BPSK and QPSK, using different trellis structures with two and four branches.

We also give PEP performance analysis for the proposed STSTC in a quasi-static Rayleigh fading channel to emphasize the importance of minimum CGD MRP. It is shown through analysis that traditional min CGD of parallel path, is not enough criteria for code design. Additional gains can be achieved by selecting a code with maximum min CGD MRP. The validity of this criteria is also shown by the FER performance curves. The codes with the higher minimum CGD MRP inspite of same minimum CGD PP perform better. This criteria is equally valid for BPSK and QPSK and is proved using 4 TS 2 branch trellis structure. We also give new design criteria which is based not only on minimum CGD of PP alone but also on the minimum CGD MRP, rank of the partial valid path, and the performance factor. For the 4 TS four branch trellis STSTCs, performance factor, min CGD MRP criteria given are much simpler and quicker than the complete distance spectrum to pick the best codes. The computer simulations demostrate the performance of the proposed code and shows its superiority in comparision to STSBC and all other existing trellis codes, to the best of our knowledge, in a reconfigurable antenna MIMO system.

The STSTC proposed, are also studied in a fully reconfigurable MIMO system. From the simulation results of various switching and selection schemes considered, it is concluded that the proposed STSTC is only useful for an open loop system where the channel is not known to the transmitter and the reconfigurable transmit antennas switch states in a predefined pattern to provide full diversity. It is also observed that unless selection is used at the receiver no additional diversity gain is realized due to receive antenna reconfiguration of $R \geq 2$. A comparative assessment of diversity increase is presented and it is shown through simulations that the diversity increase due to a reconfigurable receive antenna states is only possible if selection is used at the receiver. For a fully reconfigurable open loop MIMO system, using selection at the receiver along with preset switching at the transmitter adds selection gain along with full diversity. In case of closed

loop reconfigurable transmit/receive MIMO, where the feedback for the best transmitter state is possible after selection processing at the receiver, it is seen that keeping the transmitter state switched to a best state and fixed for the entire frame while using selection at the receiver provides higher SNR gain. Hence, if selection is used at the receiver, and the two best sub-channels are allowed to transmit for all 4 time slots, we get full diversity along with the gain in SNR. We have also shown that if selection gain is very high it overcomes the loss due to diversity.

6.2.2 Conclusions from RA Codebook Feedback system

The RA codebook feedback system proposed aims to improve the SINR, SER and $\mathcal{SR}$ of the single user MIMO system. We have shown through simulations that using RA at the receiver in a codebook feedback system allows the use of a smaller codebook to achieve the same SINR and $\mathcal{SR}$ performance expected of a larger codebook and hence requires fewer feedback bits. Two types of receivers are explored for the proposed system and it is found that for $L = 1$ and $L = 2$, proposed RA codebook feedback MIMO systems, the expected SINR and $\mathcal{SR}$, from using an MMSE receiver is better than that of an SVD receiver for all reconfigurations and transmit SNRs. Then various configurations of $N_r \times N_t$ are explored and it is found that for under loaded and critically loaded systems, CD1 $<<$ CD2 $<$ CP $<$ OA. And for overloaded systems, CD2 and CP, both contribute almost equally to OP.

Different configurations of the proposed RA codebook feedback systems are compared with their traditional NRA codebook feedback systems and it is found that the SER gains from using proposed RA codebook feedback over NRA codebook feedback are higher for smaller MIMO systems and as the number of reconfigurable receive antenna states, R, increases, SER performance improves, for both $L = 1$ and $L = 2$, with diminishing returns. Doubling the number of transmit antennas rather than doubling the number of receive antennas in a RA codebook feedback system proposed, gives higher SER gains over the corresponding NRA codebook feedback system. For $L = 2$ MIMO systems using standard LTE codebooks, the SER gains from using RA codebook feedback are higher for

smaller systems than the larger systems, such that the gains for 2×2, 2×4, 4×2 and 4×4 MIMO systems are in decreasing order. As R increases, the incremental gains in SINR and $\mathcal{SR}$, from CP keep increasing whereas it decreases from matching the channel direction, CD1 and CD2. It is interesting to see that a critically loaded, 2×2 RA codebook feedback MIMO system, using MMSE receiver and proposed OA selection, with $R = 4$, gives almost equal SER performance as an underloaded 4×2 NRA codebook feedback MIMO system. Thus, using the RA codebook feedback system permits the use of fewer receive antennas and RF chains, to achieve the same improved SER performance. This is specially attractive for small hand held devices.

We have also demonstrated that by using the proposed RA codebook feedback system, it is possible to remove the codebook/quantization loss completely in smaller single layer MIMO systems with only $R = 2$, and the $\mathcal{SR}$s performance achieved always exceeds that achieved from a perfect feedback NRA MIMO system. However, when using $L = 2$, reconfiguration of only $R = 2$, improves the codebook/quantization loss significantly, but the $\mathcal{SR}$s achieved do not always exceed that from a PFB NRA MIMO system and higher reconfiguration of at least $R = 4$ is required to exceed the PFB NRA MIMO system $\mathcal{SR}$s, most of the time.

The performance of the proposed system is also investigated for MISO systems and it is shown that the proposed RA codebook feedback system improves the SNR, SER and the rate of the codebook feedback MISO system, significantly. Our analytical and simulation results exhibit that using CD selection in a codebook feedback MISO system equipped with an S states RA ($S = R^{N_r}$) at the receiver, is the same as using an expanded codebook with size $\tilde{N_C} = N_C S$. Thus smaller codebook can be used to achieve the same SNR performance as with a larger codebook and hence lessens the number of feedback bits. We give three RA codebook selection techniques for the RA codebook feedback MISO system, and have demonstrated that CD $\ll$ CP $\approx$ OA in terms of SNR and rate performance. The expected SNR expressions for CD and CP for RA codebook feedback system are also given. We also show that as the CPSs increase, the gain in SNR, SER and the rate of the

system using RA codebook feedback with proposed OA selection, increases, and their cdfs show that they not only overcome the codebook loss, but the gain exceeds that achieved by a traditional NRA perfect feedback system. SER curves show that the SER slope of the system improves as S increases. Also a larger NRA 1×4 system with $N_C = 16$ and a smaller 1×2 system with $N_C = 4$ and $S = 2$ has same SER slopes at high γ. By doubling S the gain in SNR is approximately 40% as compared to $S = 1$. Thus, using proposed RA codebook feedback system with OA selection, the codebook loss due to quantization can be significantly reduced with only $S = 2$ and the improvement has no floor, therefore, SNR and rate achieved can exceed the PFB traditional NRA system SNR and rates.

6.3 FUTURE WORK

This section gives the directions of future extensions. The following ideas could be explored as potential areas for future work.

1. Performance of our proposed STSTCs in other channel environments:

Current work is done using quasi-static flat Rayleigh fading channels. It could be interesting to observe the performance of our proposed codes in other types of channels and optimizing it according to the environment.

2. Design of 3D STSTCs using generator matrix approach:

Our proposed code could be designed using generator matrix approach. In this, trellis codes are described in terms of closed analytical forms leading to a more tractable generator matrix description. It follows the systematic search for best codes. The generator matrix once formed, it is very easy to expand the trellis states thus increasing the coding gain further. However the gains are diminishing with increasing trellis states.

3. Validation of the simulation results analytically for RPVP and PF:

Currently, the additional gains achieved by using RPVP and PF are demonstrated using

simulations only. Analytical expressions could be derived.

4. Extention of the proposed 3D STSTCs to more RA states and more transmit antennas:

Another potential area for future work includes extention of the proposed STSTCs to more reconfigurable antenna states and more transmit antennas. Up to date it is designed for $N_tS = 4$, the goal could be to extend it to $N_tS = 8$ for larger systems. Higher reconfigurable antenna states will give more gains if all other parameters in the code are carefully selected. Set partitioning will also have to be redefined for $N_tS = 8$.

5. Extention of the proposed STSTCs from four trellis states to higher trellis states:

Up to date, the proposed STSTC are designed for two branch and four branch, two trellis states and four trellis states. It can be extended to higher TSs using the trellis or the generator matrix approach.

6. Extention of the proposed 3D STSTCs to 4D STFSTCs for fast fading channels:

The goal of this stage is that the 3D STSTCs developed will be further extended to 4D codes incorporting the frequency dimension to increase the available degrees of freedom, which are inherently present in the system without compromising any other resource. Adding the fourth dimension of frequency will give increased diversity along with the high coding gain acheived using trellis coding. To the best of my knowledge, no literature to date has used all four resourses (time, frequency, space and state/polarization) together in a trellis code, which are present in a reconfigurable frequency selective MIMO system. These codes could be called Space Time Frequency State trellis Codes having a diversity of $N_tN_rKT\Psi$, where K is the no of propagation paths, T is the rank of the channel temporal correlation matrix and Ψ represents the total number of reconfigurable states of the transmit and receive antennas' combination. It will involve generating a novel coding structure in four dimensions. One proposed way is that the 3D STSTCs will be replicated for each channel frequency using OFDM thus giving a novel 4D STFSTC with increased diversity and gain. [146] gives a block code for RA MIMO OFDM system but the trellis

code having high coding gain is not found in the literature.

The focus is not hardware complexity reduction, as I believe that over time hardware will evolve to handle much more complex systems/algorithms. The main focus of this thesis is the reliable data transmission with full diversity and rate.

7. Diversity analysis of the proposed RA codebook FB system:

The goal of this project will be to quantify the diversity improvement/advantage due to RA codebook FB system proposed over traditional codebook FB systems (using LTE, Grassmanian and random codebooks) for a single user, single layer MISO System.

REFERENCES

[1] D. Love, "Grassmannian subspace packing," https://engineering.purdue.edu/∼djlove/grass.html, 2014.

[2] D. Anagnostou, G. Zheng, M. Chryssomallis, J. Lyke, G. Ponchak, J. Papapolymerou, and C. Christodoulou, "Design, fabrication, and measurements of an RF-MEMS-based self-similar reconfigurable antenna," *Antennas and Propagations, IEEE Transactions on*, vol. 54, no. 2, pp. 422 – 432, Feb. 2006.

[3] C. Jung, M. Lee, G. Li, and F. De Flaviis, "Monolithic integrated re-configurable antenna with RF-MEMS switches fabricated on printed circuit board," in *Proc. IECON*, Nov. 2005, pp. 1–6.

[4] A. Grau, J. Romeu, L. Jofre, and F. De Flaviis, "On the polarization diversity gain using the ORIOL antenna in fading environments," in *Proc. AP-S Intl. Symp.*, Jul. 2005, pp. 14–17.

[5] N. Haridas, A. Erdogan, T. Arslan, A. J. Walton, S. Smith, T. Stevenson, C. Dunare, A. Gundlach, J. Terry, P. Argyrakis, K. Tierney, A. Ross, and T. O'Hara, "Reconfigurable MEMS Antennas," in *Proc. Adaptive Hardware and Systems, NASA/ESA*, Jun. 2008, pp. 147–154.

[6] M. Shafi, A. F. Molisch, P. J. Smith, T. Haustein, P. Zhu, P. De Silva, F. Tufvesson, A. Benjebbour, and G. Wunder, "5g: A tutorial overview of standards, trials, challenges, deployment, and practice," *IEEE Journal on Selected Areas in Communications*, vol. 35, no. 6, pp. 1201–1221, June 2017.

[7] S. N. M. Zainarry, N. Nguyen-Trong, and C. Fumeaux, "A frequency- and pattern-reconfigurable two-element array antenna," *IEEE Antennas and Wireless Propagation Letters*, vol. 17, no. 4, pp. 617–620, April 2018.

[8] N. Nguyen-Trong, A. Piotrowski, L. Hall, and C. Fumeaux, "A frequency- and polarization-reconfigurable circular cavity antenna," *IEEE Antennas and Wireless Propagation Letters*, vol. 16, pp. 999–1002, 2017.

[9] Z. Nie, H. Zhai, L. Liu, J. Li, D. Hu, and J. Shi, "A dual-polarized frequency-reconfigurable low-profile antenna with harmonic suppression for 5g application," *IEEE Antennas and Wireless Propagation Letters*, vol. 18, no. 6, pp. 1228–1232, June 2019.

[10] D. Love, R. Heath, and T. Strohmer, "Grassmannian beamforming for multiple-input multiple-output wireless systems," *Information Theory, IEEE Transactions on*, vol. 49, no. 10, pp. 2735–2747, Oct. 2003.

[11] V. Tarokh, N. Seshadri, and A. Calderbank, "Space-time codes for high data rate wireless communication: performance criterion and code construction," *Information Theory, IEEE Transactions on*, vol. 44, no. 2, pp. 744 –765, mar 1998.

[12] S. Alamouti, "A simple transmit diversity technique for wireless communications," *Selected Areas in Communications, IEEE Transactions on*, vol. 16, no. 8, pp. 1451 –1458, oct 1998.

[13] H. Jafarkhani and N. Seshadri, "Super-orthogonal space-time trellis codes," *Information Theory, IEEE Transactions on*, vol. 49, no. 4, pp. 937 – 950, april 2003.

[14] G. Ungerboeck, "Channel coding with multilevel/phase signals," *Information Theory, IEEE Transactions on*, vol. 28, no. 1, pp. 55 – 67, jan 1982.

[15] S. Sandhu, R. Heath, and A. Paulraj, "Space-time block codes versus space-time trellis codes," in *Communications, 2001. ICC 2001. IEEE International Conference on*, vol. 4, 2001, pp. 1132 –1136 vol.4.

[16] H. Jafarkhani, "A quasi-orthogonal space-time block code," *"Communications, IEEE Transactions on"*, vol. 49, no. 1, pp. 1 –4, jan 2001.

[17] O. Tirkkonen, A. Boariu, and A. Hottinen, "Minimal non-orthogonality rate 1 space-time block code for 3+ tx antennas," in *Spread Spectrum Techniques and Applications, 2000 IEEE Sixth International Symposium on*, vol. 2, 2000, pp. 429 –432 vol.2.

[18] W. Su and X.-G. Xia, "Quasi-orthogonal space-time block codes with full diversity," in *Proc. GLOBECOM*, vol. 2, nov. 2002, pp. 1098 – 1102.

[19] D. Wang and X.-G. Xia, "Optimal diversity product rotations for quasiorthogonal stbc with mpsk symbols," *Communications, IEEE Transactions on*, vol. 9, no. 5, pp. 420 – 422, may 2005.

[20] H. Jafarkhani and N. Hassanpour, "Super-quasi-orthogonal space-time trellis codes for four transmit antennas," *Wireless Communications, IEEE Transactions on*, vol. 4, no. 1, pp. 215 – 227, jan. 2005.

[21] N. Hassanpour and H. Jafarkhani, "Super-quasi-orthogonal space-time trellis codes," in *Proc. ICC*, vol. 4, may 2003, pp. 2613 – 2617 vol.4.

[22] U. Afsheen, P. A. Martin, and P. J. Smith, "Space time state trellis codes for reconfigurable antenna systems," in *2013 IEEE 78th Vehicular Technology Conference (VTC Fall)*, Sep. 2013, pp. 1–5.

[23] F. Fazel, A. Grau, H. Jafarkhani, and F. Flaviis, "Space-time-state block coded mimo communication systems using reconfigurable antennas," *Wireless Communications, IEEE Transactions on*, vol. 8, no. 12, pp. 6019 –6029, december 2009.

[24] D. Love, R. Heath, W. Santipach, and M. Honig, "What is the value of limited feedback for MIMO channels?" *"IEEE Wireless Communications Magazine"*, vol. 42, no. 10, pp. 54–59, 2004.

[25] D. Love, R. Heath, V. Lau, D. Gesbert, B. Rao, and M. Andrews, "An overview of limited feedback in wireless communication systems," *Selected Areas in Communications, IEEE Journal on*, vol. 26, no. 8, pp. 1341–1365, Oct. 2008.

[26] 3GPP TS 36.211, "Evolved universal terrestrial radio access (E-UTRA), physical channels and modulation," vol. V10.0.0, Jan. 2011.

[27] J. Mirza, P. Dmochowski, P. Smith, and M. Shafi, "Capacity loss for multilayer codebook precoding in mimo systems," in *Proc. PIMRC Intl. Symp.*, Sept. 2012, pp. 1890–1895.

[28] J. Roh and B. Rao, "Transmit beamforming in multiple-antenna systems with finite rate feedback: a VQ-based approach," *Information Theory, IEEE Transactions on*, vol. 52, no. 3, pp. 1101–1112, 2006.

[29] T. Rappaport, *Wireless communications: Principles and practice*, 2nd ed., ser. Prentice Hall communications engineering and emerging technologies series. Prentice Hall, 2002.

[30] H. Jafarkhani, *Space-Time Coding Theory and Practice*. Cambridge, U.K: Cambridge University Press, 2005.

[31] Y. S. Cho, J. Kim, W. Y. Yang, and C. G. Kang, *MIMO-OFDM Wireless Communications with MATLAB*. Singapore: John Wiley & Sons (Asia) Pte, 2010.

[32] A. F. Molish, *Wireless Communications*. UK: John Wiley & Sons Ltd, 2012.

[33] E. Biglieri, J. Proakis, and S. Shamai, "Fading channels: information-theoretic and communications aspects," *IEEE Transactions on Information Theory*, vol. 44, no. 6, pp. 2619–2692, Oct 1998.

[34] G. J. Foschini and M. J. Gans, "On limits of wireless communications in a fading environment when using multiple antennas," *Wireless Personal Communications*, vol. 6, no. 3, pp. 311 – 335, March 1998.

[35] A. Paulraj, R. Nabar, and D. Gore, *Introduction to Space-Time Wireless Communications*. Cambridge University Press, 2003.

[36] G. Foschini, "Layered space-time architecture for wireless communication in a fading environment when using multi-element antennas," *Bell Labs Technical Journal*, vol. 1, no. 2, pp. 41–59, 1996.

[37] B. Ezio, C. Robert, C.Anthony, g.Andrea, P. Arogyaswami, and P. Vincent, *MIMO Wireless Communications*. Cambridge,UK: Cambridge University Press, 2007.

[38] J. D. Boerman and J. T. Bernhard, "Performance Study of Pattern Reconfigurable Antennas in MIMO Communication Systems," *IEEE Transactions on Antennas and Propagation*, vol. 56, no. 1, pp. 231 – 236, January 2008.

[39] A. B. Gershman and N. D. Sidiropoulos, *Space-Time Processing for MIMO Communications*. Eds. West Sussex, U.K: Wiley, 2005.

[40] A. L. Moustakas, H. U. Baranger, L. Balents, A. M. Sengupta, and S. H. Simon, "Communication through a diffusive medium: Coherence and capacity," *Science*, vol. 287, no. 5451, pp. 287 – 290, January 2000.

[41] A. Grau, S. Liu, B. Cetiner, and F. De Flaviis, "Investigation of the influence of antenna array parameters on adaptive MIMO performance," in *Proc. IEEE Antennas and Propagation Society International Symposium*, vol. 2, June 2004, pp. 1704 – 1707.

[42] M. R. Andrews, P. P. Mitra, and R. DeCarvalho, "Tripling the capacity of wireless communications using electromagnetic polarization," *Nature*, vol. 409, no. 6818, pp. 316 – 318, January 2001.

[43] C. Waldschmidt, T. Fugen, and W. Wiesbeck, "Spiral and dipole antennas for indoor MIMO-systems," *IEEE Antennas and Wireless Propagation Letters*, vol. 1, no. 1, pp. 176 – 178, 2002.

[44] L. Dong, H. Ling, and R. Heath, "Multiple-input multiple-output wireless communication systems using antenna pattern diversity," in *Proc. IEEE Global Telecommunications Conference, GLOBECOM '02.*, vol. 1, November 2002, pp. 997 – 1001.

[45] T. Svantesson and A. Ranheim, "Mutual coupling effects on the capacity of multielement antenna systems," in *Proc. IEEE International Conference on Acoustics, Speech and Signal Processing*, vol. 4, May 2001, pp. 2485 – 2488.

[46] D. Piazza and K. R. Dandekar, "Reconfigurable antenna solution for MIMO-OFDM systems," *Electronics Letters*, vol. 42, no. 8, pp. 446 – 447, April 2006.

[47] R. Nabar, H. Bolcskei, V. Erceg, D. Gesbert, and A. Paulraj, "Performance of multiantenna signaling techniques in the presence of polarization diversity," *IEEE Transactions on Signal Processing*, vol. 50, no. 10, pp. 2553 – 2562, October 2002.

[48] R. Heath and A. Paulraj, "Switching between diversity and multiplexing in MIMO systems," *Communications, IEEE Transactions on*, vol. 53, no. 6, pp. 962 – 968, June 2005.

[49] B. Cetiner, E. Akay, E. Sengul, and E. Ayanoglu, "A System With Multifunctional Reconfigurable Antennas," *IEEE Antennas and Wireless Propagation Letters*, vol. 5, no. 1, pp. 463 – 466, 2006.

[50] J. Ventura-Traveset, G. Caire, E. Biglieri, and G. Taricco, "Impact of diversity reception on fading channels with coded modulationPart I: coherent detection," *Communications, IEEE Transactions on*, vol. 45, no. 5, pp. 563 – 572, May 1997.

[51] V. Tarokh, N. Seshadri, and A. Calderbank, "Spacetime codes for high data rate wireless communication: performance criterion and code construction," *IEEE Transactions on Information Theory*, vol. 44, no. 2, pp. 744–765, March 1998.

[52] M. Jankiraman, *Space-Time Codes and MIMO Systems.* Norwood, MA, USA: Artech House, Inc., 2004.

[53] A. Goldsmith, *Wireless Communications.* Cambridge University Press, 2005.

[54] S. N. Diggavi, N. Al-Dhahir, A. Stamoulis, and A. R. Calderbank, "Great expectations: The value of spatial diversity in wireless networks," in *Proc. IEEE*, February 2004, pp. 219 – 270.

[55] G. D. Gray, "The simulcasting technique: An approach to total-area radio coverage," *IEEE Transactions on Vehicular Technology*, vol. VT-28, no. 2, pp. 117–125, May 1979.

[56] D. G. Brennan, "Linear diversity combining techniques," in *Proc. IEEE*, February 2003, pp. 331 – 356.

[57] S. Alamouti, "A simple transmitter diversity scheme for wireless communications," *IEEE Journal on Selected Areas in Communications*, vol. 16, no. 8, pp. 1451–1458, October 1998.

[58] T. Svantesson, "AStudy of PolarizationDiversity using an Electromagnetic Spatio-Temporal ChannelModel," in *Proc. IEEE Vehicular Technology Conference.*

[59] Z. Liu, G. B. Giannakis, B. Muquet, and S. Zhou, "Space-time coding for broadband wireless communications," *Wireless Syst. Mobile Comput.*, vol. 1, no. 1, pp. 33 – 53, January - March 2001.

[60] A. Wittneben, "A new bandwidth efficient transmit antenna modulation diversity scheme for linear digital modulation," in *Proc. IEEE ICC*, May 1993, p. 16301634.

[61] N. Seshadri and J. H. Winters, "Two signaling schemes for improving the error performance of frequency-division-duplex (FDD) transmission systems using transmitter antenna diversity," in *Proc. IEEE Veh. Technol. Conf. (VTC)*, May 1993, p. 508511.

[62] V. DaSilva and E. Sousa, "Fading-resistant modulation using several transmitter antennas," *IEEE Transactions on Communications*, vol. 45, no. 10, pp. 1236 – 1244, October 1997.

[63] V. Tarokh, H. , and A. Calderbank, "Space-time block codes from orthogonal designs," *IEEE Transactions on Information Theory*, vol. 45, no. 5, pp. 1456–1467, July 1999.

[64] G. Ganesan and P. Stoica, "Space-time diversity using orthogonal and amicable orthogonal designs," in *Proc. of the IEEE International Conference on Acoustics, Speech, and Signal Processing, ICASSP*, vol. 5, June 2000, pp. 2561–2564.

[65] H. Jafarkhani, "A quasi-orthogonal space-time block code," *IEEE Transactions on Communications*, vol. 49, no. 1, pp. 1–4, January 2001.

[66] O. Tirkkonen, A. Boariu, and A. Hottinen, "Minimal non-orthogonality rate 1 space-time block code for 3+ tx antennas," in *Proc. ISSSTA*, vol. 2, September 2000, pp. 429 – 432.

[67] O. Tirkkonen, "Optimizing space-time block codes by constellation rotations," in *Finnish Wireless Comm. Workshop*, vol. 1, 2000, pp. 1–6.

[68] W. Su and X.-G. Xia, "Quasi-orthogonal space-time block codes with full diversity," in *IEEE Global Telecommunications Conference, GLOBECOM '02.*, November 2002.

[69] H. Jafarkhani and N. Hassanpour, "Super-quasi-orthogonal space-time trellis codes for four transmit antennas," *IEEE Transactions on Wireless Communications*, vol. 4, no. 1, pp. 215–227, January 2005.

[70] D. Wang and X.-G. Xia, "Optimal diversity product rotations for quasi-orthogonal STBC with MPSK symbols," *Communications Letters, IEEE*, vol. 9, no. 5, pp. 420 – 422, May 2005.

[71] N. Sharma and C. B. Papadias, "Improved quasi-orthogonal codes through constellation rotation," *IEEE Transactions on Communications*, vol. 51, no. 3, pp. 332 – 335, March 2003.

[72] V. Tarokh, A. Naguib, N. Seshadri, and A. Calderbank, "Combined array processing and space-time coding," *Information Theory, IEEE Transactions on*, vol. 45, no. 4, pp. 1121 – 1128, May 1999.

[73] Z. Chen, J. Yuan, and B. Vucetic, "Improved space-time trellis coded modulation scheme on slow Rayleigh fading channels," *Electronics Letters*, vol. 37, no. 7, pp. 440 – 441, March 2001.

[74] W. Firmanto, B. Vucetic, and J. Yuan, "Space-time TCM with improved performance on fast fading channels," *Communications Letters, IEEE*, vol. 5, no. 4, pp. 154 – 156, April 2001.

[75] J.-C. Guey, M. Fitz, M. Bell, and W.-Y. Kuo, "Signal design for transmitter diversity wireless communication systems over Rayleigh fading channels," *IEEE Transactions on Communications*, vol. 47, no. 4, pp. 527–537, April 1999.

[76] J. Grimm, "Transmitter diversity code design for achieving full diversity on Rayleigh fading channels," Ph.D. dissertation, Purdue University, December 1998.

[77] S. Baro, G. Bauch, and A. Hansmann, "Improved codes for space-time trellis-coded modulation," *IEEE Communications Letters*, vol. 4, no. 1, pp. 20–22, January 2000.

[78] A. Hammons and H. E. Gamal, "On the theory of space-time codes for PSK modulation," *IEEE Transactions on Information Theory*, vol. 46, no. 2, pp. 524–542, March 2000.

[79] Q. Yan and R. Blum, "Optimum space-time convolutional codes," in *Proc. of the IEEE Wireless Communications and Networking Confernce, WCNC*, vol. 3, September 2000, pp. 1351–1355.

[80] P. Viland, G. Zaharia, and J. Hlard, "Optimal generation of spacetime trellis codes via coset partitioning," *IEEE Transactions on Vehicular Technology*, vol. 60, no. 3, pp. 937 – 980, March 2011.

[81] H. Jafarkhani and N. Seshadri, "Super-orthogonal space-time trellis codes," *IEEE Transactions on Information Theory*, vol. 49, no. 4, pp. 966 – 950, April 2003.

[82] A. Birol, U. Aygolu, and M. Yucel, "Super-orthogonal space-time PSK trellis codes for fast fading channels," in *IEEE 13th Signal Processing and Communications Applications Conference*, May 2005.

[83] S. Sandhu, R. Heath, and A. Paulraj, "Space-Time Block Codes versus Space-Time Trellis Codes," in *IEEE International Conference on Communications, ICC 2001.*, June 2001.

[84] S. Alamouti, V. Tarokh, and P. Poon, "Trellis-coded modulation and transmit diversity: design criteria and performance evaluation," in *Proc. IEEE International Conference on Universal Personal Communications, ICUPC*, vol. 1, October 1998, pp. 703–707.

[85] J. C. Guey, "Concatenated coding for transmit diversity systems," in *Proc. VTC*, vol. 5, September 1999, pp. 2500–2504.

[86] A. Yongacoglu and M. Siala, "Space-time codes for fading channels," in *Proc. VTC*, vol. 5, September 1999, pp. 2495–2499.

[87] S. Sandhu and A. Paulraj, "Space-time block codes: a capacity perspective," *IEEE Communication Letters*, vol. 4, no. 12, pp. 384 – 386, December 2000.

[88] "Recent results on coding for multiple-antenna transmission systems," in *Proc. IEEE 6th Intl. Symposium on Spread Spectrum Techniques and Applications*, vol. 1, September 2000, pp. 121 – 177.

[89] L. Lihua, T. Xiaofeng, Z. Ping, and H. Haas, "A practical space-frequency block coded OFDM scheme for fast fading broadband channels ," in *The 13th IEEE International Symposium on Personal, Indoor and Mobile Radio Communications*, September 2002.

[90] X. Ma, H. Kobayashi, and S. Schwartz, "An EM-based channel estimation algorithm for space-time and space-frequency block coded OFDM," in *IEEE International Conference on Acoustics, Speech, and Signal Processing proceedings*, vol. 4, April 2003, pp. 389–392.

[91] D. Agrawal, V. Tarokh, A. Naguib, and N. Seshadri, "A Systematic Design of High-rate Full-diversity Space-Frequency Codes for MIMO-OFDM Systems," in *Proc. of the 48th IEEE Vehicular Technology Conference, VTC*, vol. 3, May 1998, pp. 2232–2236.

[92] K. Lee and D. Williams, "A Space-frequency transmitter diversity technique for OFDM systems," in *IEEE GLOBECOM*, November 2000.

[93] R. Blum, Y. G. Li, J. Winters, and Q. Yan, "Improved space-time coding for MIMO-OFDM wireless communications," *Communications, IEEE Transactions on*, vol. 49, no. 11, pp. 1873–1878, November 2001.

[94] Y. Gong and K. Letaief, "An efficient space-frequency coded wideband OFDM system for wireless communications," in *Proc. of the IEEE International Conference on Communications, ICC*, vol. 1, May 2002, pp. 475–479.

[95] B. Lu and X. Wang, "Space-time code design in OFDM systems," in *Proc. of the IEEE Global Telecommunications Conference, GLOBECOM 2000*, vol. 2, November 2000, pp. 1000–1004.

[96] W. Su, Z. Safar, M. Olfat, and K. Liu, "Obtaining full-diversity space-frequency codes from space-time codes via mapping," *IEEE Transactions on Signal Processing*, vol. 51, no. 11, pp. 2905–2916, November 2003.

[97] H. Bolcskei and A. Paulraj, "Space-frequency coded broadband OFDM systems," in *Proc. of the IEEE Wireless Communications and Networking Conference, WCNC 2000*, vol. 1, September 2000, pp. 1–6.

[98] ——, "Space-frequency codes for broadband fading channels," in *Proc. of the IEEE International Symposium on Information Theory*, June 2001, p. 219.

[99] W. Su, Z. Safar, and K. Liu, "Full-Rate Full-Diversity SpaceFrequency Codes With Optimum Coding Advantage," *IEEE Transactions on Information Theory*, vol. 51, no. 1, pp. 229–249, January 2005.

[100] W. Zhang, X.-G. Xia, and P. Ching, "A design of high-rate space-frequency codes for MIMO-OFDM systems," in *IEEE Global Telecommunications Conference, 2004. GLOBECOM '04.*, November 2004.

[101] X. Ma and G. Giannakis, "Full-diversity full-rate complex-field space-time coding," *IEEE Transactions on Signal Processing*, vol. 51, no. 11, pp. 2917–2930, November 2003.

[102] B. Lu and X. Wang, "A space-time trellis code design method for OFDM systems," *Wireless Personal Commun.*, vol. 24, no. 3, pp. 403 – 418, 2003.

[103] Z. Liu, Y. Xin, and G. Giannakis, "Space-time-frequency coded OFDM over frequency-selective fading channels," *IEEE Transactions on Signal Processing*, vol. 50, no. 10, pp. 2465–2476, October 2002.

[104] J. Mietzner, R. Schober, L. Lampe, W. Gerstacker, and P. Hoeher, "Multiple-Antenna Techniques for Wireless Communications A Comprehensive Literature Survey," *IEEE Communications Surveys & Tutorials*, vol. 11, no. 2, pp. 87–105, Second Quarter 2009.

[105] W. Su, Z. Safar, and K. Liu, "Towards Maximum Achievable Diversity in Space, Time, and Frequency: Performance Analysis and Code Design," *Wireless Communications, IEEE Transactions on*, vol. 4, no. 4, pp. 1847–1857, July 2005.

[106] Y. Gong and K. B. Letaief, "Space-frequency-time coded OFDM for broadband wireless communications," in *Proc. IEEE GLOBECOM*, November 2001.

[107] N. K. Noordin, B. M. Ali, and S. S. Jamuar, "CODED SPACE-TIME-FREQUENCY OFDM OVER IEEE 802.11 FADING CHANNELS," *The Institution of Engineers, Malaysia*, vol. 68, no. 1, pp. 10–15, March 2007.

[108] K. Aksoy and U. Aygolu, "Super-orthogonal space-time-frequency trellis coded OFDM," *IET Communications*, vol. 1, no. 3, pp. 317 – 324, June 2007.

[109] D. Agrawal, V. Tarokh, A. Naguib, and N. Seshadri, "Space-time coded OFDM for high data-rate wireless communication over wideband channels," in *48th IEEE Vehicular Technology Conference*, May 1998.

[110] J. Flores, J. Sanchez, and H. Jafarkhani, "Quasi-Orthogonal Space-Time-Frequency Trellis Codes for Two Transmit Antennas," *IEEE Transactions on Wireless Communications*, vol. 9, no. 7, pp. 2125 – 2129, July 2010.

[111] F. Fazel and H. Jafarkhani, "Quasi-Orthogonal Space-Frequency and Space-Time-Frequency Block Codes for MIMO OFDM Channels," *IEEE Transactions on Wireless Communications*, vol. 7, no. 1, pp. 184–192, January 2008.

[112] A. Grau, J. Romeu, L. Jofre, and F. De Flaviis, "On the polarization diversity gain using the ORIOL antenna in fading indoor environments," in *Antennas and Propagation Society International Symposium, IEEE*, July 2005.

[113] C. W. Jung, M. jer Lee, G. Li, and F. De Flaviis, "Monolithic integrated reconfigurable antenna with RF-MEMS switches fabricated on printed circuit board," in *31st Annual Conference of IEEE Industrial Electronics Society, IECON 2005*, November 2005.

[114] D. Anagnostou, G. Zheng, M. Chryssomallis, J. Lyke, G. Ponchak, J. Papapolymerou, and C. Christodoulou, "Design, fabrication, and measurements of an RF-MEMS-based self-similar reconfigurable antenna," *Antennas and Propagation, IEEE Transactions on*, vol. 54, no. 2, pp. 422–432, February 2006.

[115] C. won Jung, M. jer Lee, G. Li, and F. De Flaviis, "Reconfigurable scan-beam single-arm spiral antenna integrated with RF-MEMS switches," *Antennas and Propagation, IEEE Transactions on*, vol. 54, no. 2, pp. 455 – 463, February 2006.

[116] D. Piazza and K. Dandekar, "Reconfigurable antenna solution for MIMO-OFDM systems," *Electronics Letters*, vol. 42, no. 8, pp. 446 – 447, April 2006.

[117] B. Cetiner, E. Akay, E. Sengul, and E. Ayanoglu, "A MIMO system with multifunctional reconfigurable antennas," *Antennas and Wireless Propagation Letters, IEEE*, vol. 5, no. 1, pp. 463 – 466, December 2006.

[118] B. Cetiner, J. Qian, H. Chang, M. Bachman, G. Li, and F. De Flaviis, "Monolithic integration of rf mems switches with a diversity antenna on pcb substrate," *Microwave Theory and Techniques, IEEE Transactions on*, vol. 51, no. 1, pp. 332 – 335, January 2003.

[119] B. Cetiner, L. Jofre, C. Chang, J. Qian, M. Bachman, G. Li, and F. De Flaviis, "Integrated MEM antenna system for wireless communications," in *Proc. IEEE MTT-S International Microwave Symposium Digest*, vol. 2, June 2002, pp. 1333 – 1336.

[120] S. Nikolaou, R. Bairavasubramanian, J. Lugo, C., I. Carrasquillo, D. Thompson, G. Ponchak, J. Papapolymerou, and M. Tentzeris, "Pattern and frequency reconfigurable annular slot antenna using PIN diodes," *Antennas and Propagation, IEEE Transactions on*, vol. 54, no. 2, pp. 439 – 448, February 2006.

[121] A. Grau, M.-J. Lee, J. Romeu, H. , L. Jofre, and F. De Flaviis, "A multifunctional MEMS-reconfigurable PIXEL antenna for narrowband MIMO communications," in *Antennas and Propagation Society International Symposium, IEEE*, June 2007.

[122] C. Jung, M.-J. Lee, G. Li, and F. D. Flaviis, "Monolithic integrated re-configurable antenna with RF-MEMS switches fabricated on printed circuit board," in *IEEE Industrial Electronics Conference*, November 2005.

[123] G. Huff and J. Bernhard, "Integration of packaged RF MEMS switches with radiation pattern reconfigurable square spiral microstrip antennas," *IEEE Transactions on Antennas and Propagation*, vol. 54, no. 2, pp. 464–469, February 2006.

[124] P. Panaia, C. Luxey, G. Jacquemod, R. Staraj, G. Kossiavas, L. Dussopt, F. Vacherand, and C. Billard, "EMS-based reconfigurable antennas," in *Proc. IEEE International Symposium Industrial Electronics*, vol. 1, May 2004.

[125] C. W. Jung and F. De Flaviis, "RF-MEMS capacitive series switches of CPW and MSL configurations for reconfigurable antenna application ," vol. 2A, July 2005, pp. 425 – 428.

[126] H. Deng, T. Xu, and F. Liu, "Broadband pattern-reconfigurable filtering microstrip antenna with quasi-yagi structure," *IEEE Antennas and Wireless Propagation Letters*, vol. 17, no. 7, pp. 1127–1131, July 2018.

[127] R. Simons, D. Chun, and L. Katehi, "Polarization reconfigurable patch antenna using microelectromechanical systems (MEMS) actuators," in *Antennas and Propagation Society International Symposium, IEEE*, 2002.

[128] H. Aissat, L. Cirio, M. Grzeskowiak, J.-M. Laheurte, and O. Picon, "Reconfigurable circularly polarized antenna for short-range communication systems," *Microwave Theory and Techniques, IEEE Transactions on*, vol. 54, no. 6, pp. 2856 – 2863, June 2006.

[129] N. Jin, F. Yang, and Y. Rahmat-Samii, "A novel reconfigurable patch antenna with both frequency and polarization diversities for wireless communications," in *Antennas and Propagation Society International Symposium, IEEE*, June 2004.

[130] Y. Sung, T. Jang, and Y.-S. Kim, "A reconfigurable microstrip antenna for switchable polarization," *Microwave and Wireless Components Letters, IEEE*, vol. 14, no. 11, pp. 534–536, November 2004.

[131] M. Shirazi, T. Li, J. Huang, and X. Gong, "A reconfigurable dual-polarization slot-ring antenna element with wide bandwidth for array applications," *IEEE Transactions on Antennas and Propagation*, vol. 66, no. 11, pp. 5943–5954, Nov 2018.

[132] F. Fazel, A. Grau, H. Jafarkhani, and F. De Flaviis, "State-Selection in a Space-Time-State Block Coded MIMO Communication System Using Reconfigurable PIXEL Antennas," in *Global Telecommunications Conference, IEEE*, November 2008.

[133] F. Fazel, A. Grau, H. Jafarkhani, and F. Flaviis, "Space-Time-State Block Coded MIMO Communication Systems Using Reconfigurable Antennas," *Wireless Communications, IEEE Transactions on*, vol. 8, no. 12, pp. 6019–6029, December 2009.

[134] A. Grau, H. Jafarkhani, and F. De Flaviis, "A reconfigurable multiple-input multiple-output communication system," *Wireless Communications, IEEE Transactions on*, vol. 7, no. 5, pp. 1719 – 1733, May 2008.

[135] F. Fazel, A. Grau, H. Jafarkhani, and F. D. Flaviis, "Space-Time Block Coded Reconfigurable MIMO Communication System Using ORIOL Antennas," in *Proc. IEEE WCNC 2008*, March 2008.

[136] F. Fazel, A. Grau, H. Jafarkhani, and F. De Flaviis, "State-selection in a space-time-state block coded mimo communication system using reconfigurable pixel antennas," in *Proc. GLOBECOM*, 30 2008-dec. 4 2008, pp. 1 –5.

[137] A. Grau, H. Jafarkhani, and F. De Flaviis, "A reconfigurable multiple-input multiple-output communication system," *Wireless Communications, IEEE Transactions on*, vol. 7, no. 5, pp. 1719 –1733, may 2008.

[138] J. Craig, "A new, simple and exact result for calculating the probability of error for two-dimensional signal constellations," in *Proc. MILCOM*, vol. 2, Nov. 1991, pp. 571–575.

[139] M. K. Simon, "Evaluation of average bit error probability for space-time coding based on a simpler exact evaluation of pairwise error probability," *Int. Jour. of Commun. and Networks*, vol. 3, pp. 257–264, Sept. 2001.

[140] G. L. Turin, "The characteristic function of Hermitian quadratic forms in complex normal variables," *Biometrika*, vol. 47, pp. 199–201, Jun. 1960.

[141] M. K. Simon and M. S. Alouini, *Digital Communication over Fading Channels*. John Wiley and Sons, Inc., 2005.

[142] D. Anagnostou, G. Zheng, M. Chryssomallis, J. Lyke, G. Ponchak, J. Papapolymerou, and C. Christodoulou, "Design, fabrication, and measurements of an rf-mems-based self-similar reconfigurable antenna," *Antennas and Propagation, IEEE Transactions on*, vol. 54, no. 2, pp. 422 – 432, feb. 2006.

[143] C. K. A. Yeung and D. Love, "On the performance of random vector quantization limited feedback beamforming in a MISO system," *Wireless Communications, IEEE Transactions on*, vol. 6, no. 2, pp. 458–462, 2007.

[144] S. J. Grant and J. K. Cavers, "Multi-user channel estimation for detection of cochannel signals," *IEEE Trans. Commun.*, vol. 49, no. 10, pp. 1845–1855, 2001.

[145] D. Love and R. Heath, "Limited feedback precoding for spatial multiplexing systems using linear receivers," in *Proc. MILCOM*, vol. 1, 2003, pp. 627–632.

[146] V. Vakilian, J. Frigon, and S. Roy, "On increasing the slow-fading channel diversity using block-coded mimo-ofdm with reconfigurable antennas," *IEEE Transactions on Vehicular Technology*, vol. 65, no. 9, pp. 7207–7218, Sep. 2016.